DISTORTIONAL BUCKLING

OF

COLD-FORMED STEEL Z-SECTIONS

by

PIMARN CHARNVARNICHBORIKARN, M. ENG.

DISSERTATION

Presented to the Faculty of the Graduate School of

The University of Manitoba

in Partial Fulfilment

of the Requirements

for the Degree of

DOCTOR OF PHILOSOPHY

in the Department of Civil Engineering

THE UNIVERSITY OF MANITOBA

April, 1992

ISBN 0-315-78057-6

DISTORTIONAL BUCKLING OF COLD-FORMED STEEL Z-SECTIONS

BY

PIMARN CHARNVARNICHBORIKARN

A Thesis submitted to the Faculty of Graduate Studies of the University of Manitoba in partial fulfillment of the requirements for the degree of

DOCTOR OF PHILOSOPHY

ABSTRACT

Current specifications for the design of cold-formed steel structural members, such as the American Iron and Steel Institute (AISI) Specification (1989) and the Canadian Standard Association (CSA) Standard S136 (1989), consider the web of cold-formed steel Z-sections as a fully stiffened element. This, however, may not be true if the flanges of such sections do not have sufficient stiffness to provide the restraint necessary for the web to reach its buckling load before the flanges reach their buckling load. In this case, distortional failure of the flange-edge stiffener component will cause premature failure of the web and thus limit the load-carrying capacity of the section with very little post-buckling strength being realized.

In the current design guidelines it is also assumed that once the web of a cold-formed Z-section fails by local buckling it will continue to carry additional load until the member fails by lateral buckling or torsional buckling. This is known as post-buckling capacity. If the flanges, however, have insufficient stiffness, they may fail by distortional buckling before the web reaches its post-buckling strength. Thus, the interaction between the web and the flange-edge stiffener component must be considered in the design process.

In this study, the effect of web buckling on the load-carrying capacity of Z-sections is examined both theoretically and experimentally. The investigation was carried out in three phases: The first phase involved the testing of 85 Z-sections loaded under directed compression; the second involved the testing of 20 Z-sections

loaded under pure bending; and the third involved the testing of 18 Z-sections subjected to an eccentrically applied axial load.

The main parametric variations were the lengths of specimens, which varied from 18 to 54 inches, the width-to-thickness ratio of the web, which varied from 68 to 132, the width-to-thickness ratio of the flanges, which varied from 25 to 49, and the width-to-thickness ratio of the edge stiffeners, which varied from 0 to 33.

The theoretical models were developed from the governing differential equations of combined torsion and flexure of an undistorted section supported by a continuous elastic foundation. The solution of these simultaneous differential equations yielded the distortional buckling stress of the section.

Based on the results of this investigation, methods for predicting the load-carrying capacity of cold-formed steel Z-sections are recommended. These methods account for the interactions between the web and the flanges - a behavioral phenomenon which is missing in the design specifications.

Key Words: **Cold-Formed, Steel, Distortional buckling, Edge stiffeners, Z-sections, Web buckling**

ACKNOWLEDGEMENTS

The author wishes to express his sincere gratitude and appreciation to his advisor, Dr. Dimos Polyzois, Associate Professor, Civil Engineering Department, University of Manitoba, for his guidance and encouragement throughout the course of this study. The author would like to express his sincere thanks and appreciation to Dr. Sami H. Rizkalla for giving him the opportunity to join the graduate program in the Civil Engineering Department and for his continuing support and encouragement. The author is also grateful to the members of his examination committee, Drs. R. Laboube, from the University of Missouri-Rolla, G. Morris, R.K.N.D. Rajapakse, and R. Britton, for their valuable and insightful comments.

Special thanks are due also to Professor John Glanville for his inspiration, superior motivating ability and encouragement. Gratitude is also extended to Muriel Innes, Arlene Flatfoot-Beaulieu, Mr. Bill Alcorn and Dr. Luis Magalhaes of the University of Manitoba Engineering Access Program for providing encouragement, unflagging support and for allowing the author to use the office facilities while preparing this dissertation.

The assistance given by the technical staff of the Structural Engineering and Construction Research and Development Facility of the Civil Engineering Department, Messrs. Ed Lemke, Moray McVey, Martin Green, Steve Meyerhoff and Brian Turnbull during the experimental program is gratefully appreciated.

Last but not least, the author expresses his sincere gratitude to the people who have been the key factors in the completion of this work, his parents for their support and patience, and to Miss Piyawadee Srisurapol for her understanding, encouragement, motivation and most of all her love throughout the graduate program.

The research project was financially supported by the Natural Science and Engineering research Council of Canada (NSERC).

TABLE OF CONTENTS

APPENDICES

LIST OF TABLES

LIST OF FIGURES

LIST OF SYMBOLS

A = gross cross sectional area of the member (in.^{2});

A_d = cross sectional area of the flange-edge stiffener component or the equivalent column (in.^{2});

A_e = effective cross sectional area of member (in.^{2});

B = flat width-to-thickness ratio of stiffened element;

b = flat width of plate or flange element (in.);

b_1, b_2 = effective widths illustrated in Figure 2.4 (in.);

b_e = effective width of plate (in.);

b_f = flat width of flange element (in.);

c = flat width of straight edge stiffeners (in.);

C_1, C_2 = coefficients defined in Figure 2.3;

C_b = bending coefficient (C_b = 1.0);

C_{mx}, C_{my} = coefficient of moment gradient (C_{mx}, C_{my} = 1.0);

C_f = axial compressive load in the member due to factored loads (kN), (CSA, 1989);

C_r = the compressive resistance for member in compression (kN), (CSA, 1989);

C_w = torsional warping constant of the flange-edge stiffener component or the equivalent column or torsional warping constant of the cross sectional Z-section (in.^{6});

D, D_s = overall width of edge stiffener (in.);

d = flat width of straight edge stiffeners or distance from neutral axis of beam to the centroid of the equivalent column (in.);

d_c = distance from neutral axis of beam to the extreme compressive fibre of the section (in.);

d_e = effective width of stiffener (CSA, 1989);

d_r = reduced effective width of stiffener illustrated in Figure 2.6, (CSA, 1989), to be used in calculating overall effective section properties (mm);

d_s = reduced effective width of the stiffener (in.), (AISI,1989);

d_s' = effective width of the stiffener (in.), (AISI, 1989);

d_{min} = minimum required overall width of the edge stiffener (in.);

E = elastic modulus of the cold-formed steel (ksi);

e_x, e_y = x- and y-coordinates of the eccentric loading on the equivalent column with respect to the centroid (in.);

(F) = the forcing function;

(F^{el}) = the elastic load vector;

$(F^{el})_{i-1}$ = the elastic force vector based on displacement for iteration (i-1);

f = the critical stress of member according to the AISI Specification (1989) (ksi);

f_1, f_2 = stresses shown in Figure 2.4 (AISI, 1989), calculated on the basis of effective section (ksi), or calculated stresses shown in Figure 2.7 (MPa), (CSA, 1989);

F_n = inelastic critical stress of member caused by its instability (ksi);

F_p = critical elastic buckling stress, being the least of the stresses for Euler-flexural elastic buckling, multiplied by the coefficient 0.833 (MPa), (CSA, 1989);

F_y = yield strength of the cold-formed steel (ksi);

G = elastic shear modulus of the cold-formed steel (ksi), 11,346 ksi;

H = overall width of web element (in.);

h_x, h_y = x- and y-coordinates of the supported edge as defined in Figure 3.3 (in.);

I_a = required stiffness of the edge stiffener (in.^{4});

I_b = moment of inertia of the full, unreduced cross section about the axis of bending (in.^{4});

I_s = moment of inertia of the full stiffener about its own centroidal axis parallel to the element to be stiffened (in.^{4});

I_{cx}, I_{cy} = moments of inertia of the flange-edge stiffener component or the equivalent column with respect to the geometric x- and y-axes, respectively (in.^{4});

I_{cxy} = product moment of inertia of the flange-edge stiffener component or the equivalent column with respect to the geometric x- and y-centroidal axes (in.^{4});

I_{min} = minimum allowable moment of inertia of stiffeners (of any shape) with respect to its own centroidal axis parallel to the stiffened element (in.^{4});

I_{co} = polar second moment of area of the flange-edge stiffener component or the equivalent column with respect to the shear centre (in.^{4});

I_{xx}, I_{yy}, I_{zz} = moments of inertia of the cross sectional Z-sections with respect to the x-, y- and z-axes, respectively (in.^{4});

I_{xy} = product moment of inertia of the cross sectional Z-section with respect to the geometric x- and y-centroidal axes (in.^{4});

I_{xp}, I_{yp} = moment of inertia of the cross sectional Z-sections with respect to the principal x- and y-axes, respectively (in.^{4});

I_{yc} = moment of inertia of the compression portion of a section about the gravity axis of the entire section parallel to the web, using the full unreduced section (in.^{4});

J_c = St. Venant torsional constant of the flange-edge stiffener component or the equivalent column (in.^{4});

J = St. Venant torsional constant of the cross sectional Z-sections ($in.^4$);

k = local buckling coefficient;

$[K]_{i-1}$ = the stiffness matrix based on deformed geometry from the (i-1) iteration;

$[K_T]$ = the tangent stiffness matrix;

$[K]$ = normal stiffness matrix;

K_b = effective length factor in the plane of bending;

K_x, K_y, K_t = effective length factors for bending about the x- and y-axes, and for twisting;

k_x, k_y, k_ϕ = stiffnesses of lateral and rotational restraints (kips/in., kips-in./rads);

L = length of test specimens (in.);

L_b = actual unbraced length (in.);

L_x, L_y, L_t = unbraced length of member for bending about the x- and y-axes, and for twisting (in.);

M_{AISI} = predicted bending capacity obtained through the AISI Specification (1989) (kips-in.);

M_c = inelastic critical moment of Z-section beam (kips-in.);

M_{cr} = critical moment with respect to the major principal axis of cold-formed steel cross section or bending capacity of Z-section members caused by distortional buckling stress (kips-in.);

M_{crx} = critical moment with respect to the geometric x-axis (kips-in.);

M_{CSA} = predicted bending capacity obtained through the CSA Standard (1989) (kips-in.);

M_e = elastic critical moment of Z-section beam (kips-in.);

M_n = smaller of the moment strength calculated according to the AISI Specification (1989) (kips-in.);

M_r = moment resistance of member in bending (kN-m), (CSA, 1989);

M_{Test} = bending capacity obtained from testing (kips-in.);

M_{Theory} = predicted bending capacity obtained through the simplified theoretical model (kips-in.);

M_x, M_y = applied moment with respect to the geometric x- and y-centroidal axes, respectively (kips-in.);

M_{ax}, M_{ay} = allowed moments about the centroidal axes determined according to AISI Specification (1989) (kips-in.);

M_{rx} = moment resistance according to CSA Standard (1989);

M_{fx} = maximum calculated moment due to axial compression load in accordance with CSA Standard (1989);

M_y = yielding moment of Z-section member (kips-in.);

P = applied axial load (kips);

P_a = maximum axial load, considering lateral buckling (kips);

P_n = critical compressive resistance determined according to AISI Specification (1989) (kips);

P_{AISI} = predicted axial load obtained through the AISI Specification (1989) (kips);

P_{ao} = maximum axial load based on yielding failure (kips);

P_c = applied compressive force on the flange-edge stiffener component (kips);

P_e = Euler axial buckling load with respect to the geometric x-axis (kips);

P_{cr} = load-carrying capacity of Z-section which is caused by the distortional buckling stress (kips);

P_{CSA} = predicted axial load obtained through the CSA Standard (1989) (kips);

P_{Test} = load-carrying capacity obtained from testing (kips);

P_{Theory} = predicted axial load obtained through the simplified theoretical model (kips);

Q = a function of stress (termed the plastic potential) determining the direction of plastic strain;

r = centerline bend radius of flange-edge stiffener junction or flange-web junction (in.) or radius of gyration of the fully effective cross sectional area according to CSA Standard (1989) (mm);

r_i = inside bend radius of flange-edge stiffener junction (in.);

r_x = radius of gyration of the principal x-axis (in.);

r_y = radius of gyration of the principal y-axis (in.);

r_o = polar radius of gyration of the cross section about the shear center (in.);

$[S]$ = stiffening stiffness matrix;

S_c = elastic section modulus of the effective section calculated at a critical stress in the extreme compression fibre ($in.^3$);

S_{cf} = compressive section modulus based on the moment of inertia of the fully effective cross sectional area, (CSA, 1989), (mm^3);

S_e = compressive section modulus of the effective cross sectional area with respect to the major axis ($in.^3$);

S_f = elastic section modulus of the full unreduced section for the extreme compression fibre ($in.^3$);

S_t = tensile section modulus based on the moment of inertia of the effective gross cross sectional area, (CSA, 1989), (mm^3);

S_{tn} = tensile section modulus based on the moment of inertia of the effective net cross sectional area, (CSA, 1989), (mm^3);

S_x = elastic section modulus of the gross section with respect to the geometric x-axis ($in.^3$);

S_{xc} = compressive section modulus of the fully effective cross sectional area with respect to the geometric x-axis, I_{xx} divided by the distance from the neutral axis to the extreme compressive fibre ($in.^3$);

t = thickness of the cold-formed section (in.);

u, v, z, ϕ = deflections in the x-, y- and z-coordinates of the shear centre axis and angle of rotation of section with respect to those axes (in.);

$(u)_i$ = the displacement vector at the current iteration;

w = flat width of web element (in.);

W = flat width ratio of element (w/t);

x, y = x- and y-coordinates of flange-edge stiffener component or equivalent column (in.);

x_c, y_c = x- and y-coordinates of flange-web junction of Z-section column with respect to the centroid (in.);

x_o, y_o = distance from the shear centre to the centroid of section along the principal x- and y-axes (in.);

x_{co}, y_{co} = x- and y-coordinates of the flange-edge stiffener component or the equivalent column with respect to the shear centre (in.);

$\overline{x_c}$, $\overline{y_c}$ = x- and y-coordinates of the flange-edge stiffener component or the equivalent column with respect to the centroid (in.);

α = angle of rotation of principal axis (degrees);

α_x, α_y = amplification factors;

ω_x = coefficient = 1.0;

ρ = parameter used to determine effective width;

θ = angle between edge stiffener and flange element (degrees);

λ = the multiplier determining the amount of plastic strain or a slenderness factor used to determine effective width;

ϵ^{pl} = plastic strain;

ν = poisson's ratio;

Ω_c, Ω_f = factor of safety for compression and bending, respectively, (AISI, 1989);

Δ = deflection as defined in Figure 3.4 (in.);

δ = axial deformation of column and beam-column specimens or vertical deflection of beam specimens (in.);

σ_{cr} = inelastic critical stress of the compressive fibre flange which is caused by the distortional buckling stress of the flange-edge stiffener or the equivalent column (ksi);

σ_c = inelastic distortional buckling stress of the equivalent column (ksi);

σ_{dcr} = elastic critical stress of the compressive fibre flange which is caused by the distortional buckling stress of the flange-edge stiffener component or the equivalent column (ksi);

F_{ex}, σ_{ex} = critical elastic flexural buckling stress with respect to the principal x-axis of Z-section member (ksi);

F_{ey}, σ_{ey} = critical elastic flexural buckling stress with respect to the principal y-axis of Z-section member (ksi);

F_t, σ_t = torsional buckling stress of Z-section member (ksi);

σ_{eq} = equivalent stress (ksi);

σ_1, σ_2, $\sigma 3$ = the principal stresses which are calculated from the stress components by the cubic equation;

U_I, U_J, U_k, U_L = u-displacement (in x-direction) of nodes I, J, K, and L;

s, t = element coordinates;

(σ) = stress vector;

(ϵ) = strain vector;

[D] = elasticity matrix;

(u) = nodal displacements vector

[B] = the strain-displacement matrix, which is based on the element shape function, must be evaluated at each integration point;

σ_i = assumed stress variations;

(Δu) = the nodal displacement increment vector;

$(\Delta u)_i$ = the incremental displacement vector,
$(u)_i = (u)_{i-1} + (\Delta u)_i$.

CHAPTER 1

INTRODUCTION

In steel construction, there are two main families of structural members. One is the familiar group of hot-rolled shapes. The other, which is less familiar, but of growing importance, is sections that are cold-formed from steel sheet, plates, or flat bars. Their width-to-thickness ratios are usually much larger than those of hot-rolled sections and thus, they are also referred to as "thin-walled" steel sections.

Common types of cold-formed sections used in the construction of metal buildings, especially as girts and purlins, are Z-shaped sections which are produced with either unstiffened flange, as shown in Figure 1.1(a), or with stiffened flange, as shown in Figure 1.1(b). Their cross sectional configuration, however, gives rise to behavioral phenomena, such as local and distortional buckling, which could affect the overall load-carrying capacity of the member. Edge stiffeners are added to the flanges to enhance the post-buckling strength of the section. Local and distortional buckling are functions of the rigidity of the edge stiffeners. If the rigidity of the edge stiffeners is adequate, local buckling of the individual plate elements will take place, as shown in Figure 1.2(a). In this case, the post-buckling capacity of the elements can be developed. On the other hand, if the rigidity of the edge stiffeners is inadequate, distortional buckling of the flange-edge stiffener components will take place, as shown in Figure 1.2(b). The post-buckling capacity of the elements, in this case, may not be developed and the overall capacity of the member may be

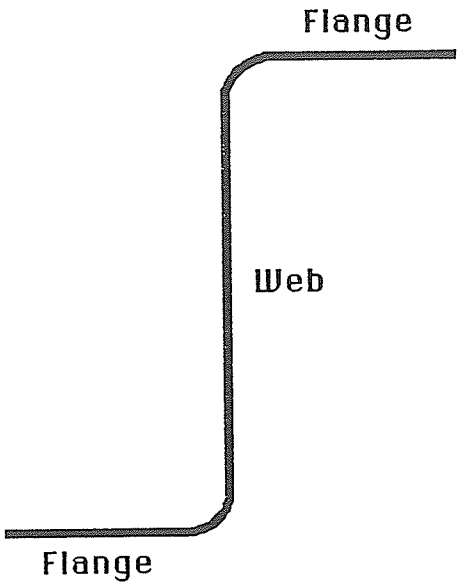

(a) Unstiffened Flange Section

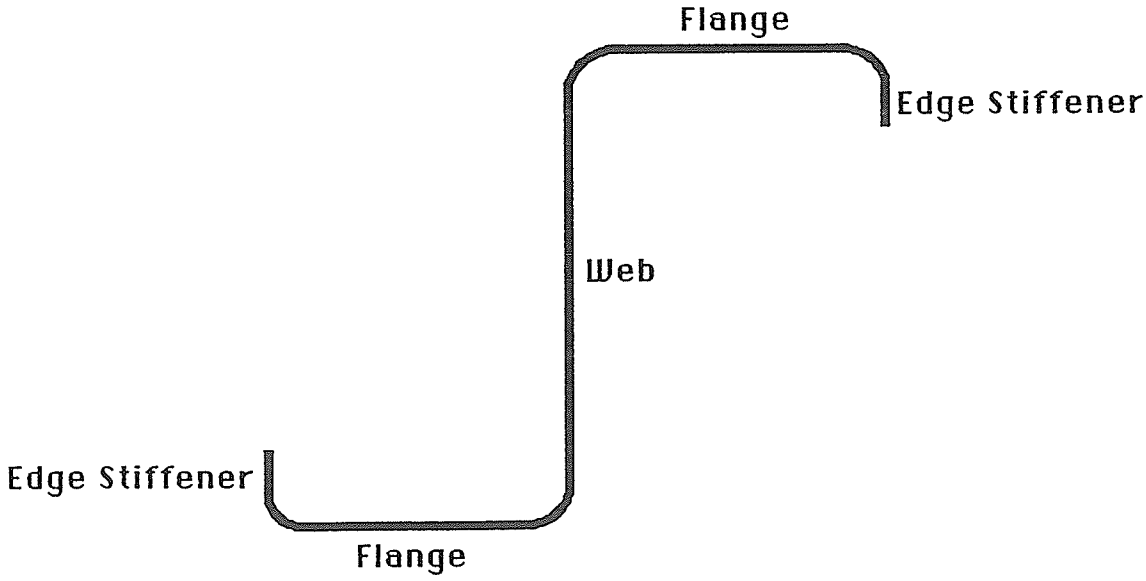

(b) Stiffened Flange Section

Figure 1.1 Typical Cold-Formed Z-Section with Unstiffened and Stiffened Flange Section

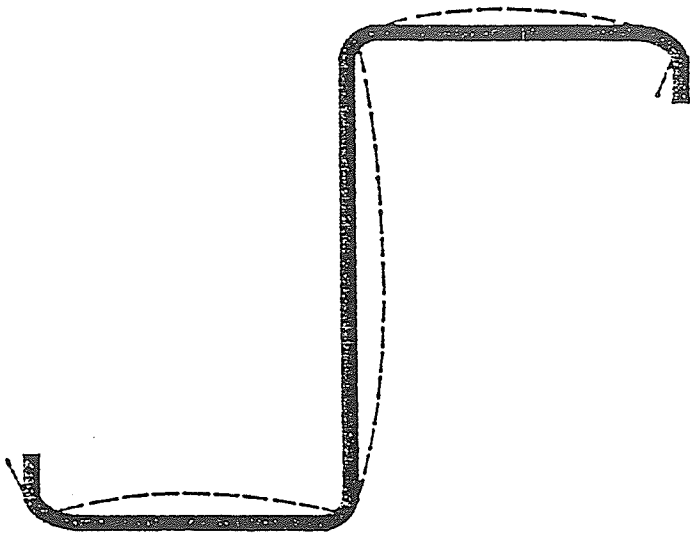

(a) Local Buckling

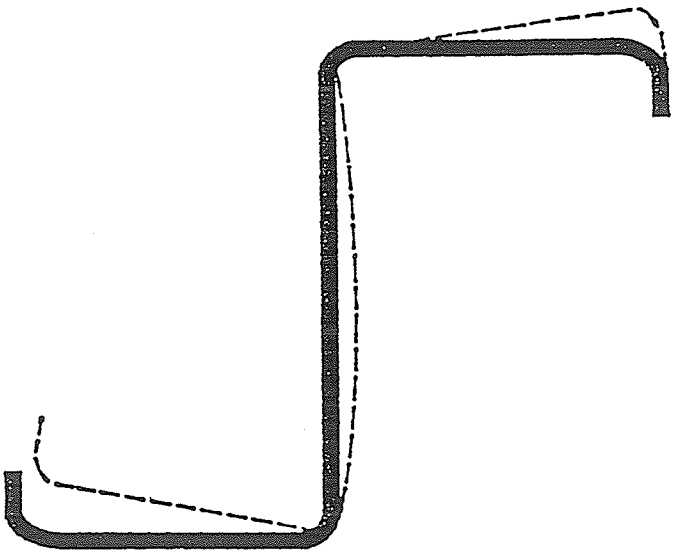

(b) Distortional Buckling

Figure 1.2 Buckling Behaviour of Cold-Formed Steel Z-Sections

drastically reduced. In the North American Specifications for the design of cold-formed steel members, the concept of partially stiffened flanges is used. This recognizes the fact that an edge stiffener may not provide adequate rotational restraint to a compression flange. Expressions are given for computing the buckling coefficient of compression flanges, which ranges from 0.43 for unstiffened flanges, to 4.0 for fully stiffened flanges. It is not clear, however, what the buckling coefficient of the web element should be. The practice has been to consider the web as a fully stiffened element. A buckling coefficient of 4.0 is used if the web is under direct compression, while 24.0 is used if the web is under pure bending. This, however, may not be true if the flanges of the sections cannot provide sufficient restraint to the web. A premature failure of the compression flanges, such as distortional buckling, will cause buckling of the web at a stress well below the local buckling stress. Also if the web element becomes unstable first, distortional failure of the flange-edge stiffener may take place. These phenomena will limit the load-carrying capacity of the section with little post-buckling strength being realized.

An experimental and analytical study was carried out to determine the effect of web buckling on the load-carrying capacity of cold-formed Z-sections with partially stiffened flanges. The objectives of the study were:

a) to determine the effect of local buckling of a web element on the load-carrying capacity of cold-formed steel Z-sections with partially stiffened flanges,

b) to evaluate the design specifications, specifically the American Specification (AISI, 1989) and Canadian Standard (CSA S136, 1989), and

c) to develop appropriate design procedures.

CHAPTER 2

DESIGN SPECIFICATIONS

Cold-formed steel members have been used as major members of metal buildings. The performance of thin cold-formed structural members under load differs in several significant respects from that of hot-rolled steel members. The structural forms, shapes, connections, and fabrication practices which have been developed in cold-formed steel construction, also differ in many ways from those used in conventional steel structures. The need to continuously update the design specification for cold-formed steel structural members is significant. The North American design specifications, the American Specification (AISI, 1980-1989) and the Canadian Standard (CSA, 1980-1989), are reviewed and discussed in the following sections.

2.1 AISI SPECIFICATION

Realizing the need for special design specifications and in the absence of a factual background and research information, the AISI committee on Building Research and Technology (originally called the Committee on Building Codes) sponsored several research projects, starting in 1939, at several universities, including Cornell University and The University of Missouri-Rolla. As a result of these projects, the various editions of the American Iron and Steel Institute (AISI) Specification were published to promote the use and the development of thin-walled

cold-formed steel construction in the United States. In addition, AISI published the first Edition of the "Light Gage Steel Design Manual" in 1949. It was subsequently revised in 1956 and most recently in 1989.

The discussion in this section will be limited to the provisions of the AISI Specification related to the behaviour of compression flanges of cold-formed sections which are stiffened by straight edge stiffeners. According to the 1980 Edition of the AISI Specification, an element was deemed stiffened if it had an adequate stiffener on both of its edges. In order for a compression flange to be considered stiffened, the edge stiffener, that was bent at right angles to the stiffened element, had to satisfy a minimum overall width requirement of d_{min} (in.), where,

$$d_{\min} = 2.8t\left[\left(\frac{b_f}{t}\right)^2 - \frac{27600}{F_y}\right]^{\frac{1}{6}} \qquad (2.1)$$

where,

t = thickness of section (in.);

b_f = flat width of the flanges of section (in.); and

F_y = yield strength of the steel sheet used to form a section (ksi).

This requirement was considered sufficient to ensure yielding at the edges of the stiffened compression flanges.

Desmond (1978) carried out an extensive experimental investigation to determine the behaviour of cold-formed sections with stiffened and partially stiffened compression flanges. As shown in Figure 2.1, Desmond's experimental investigation involved cold-formed sections whose web was stiffened to prevent local

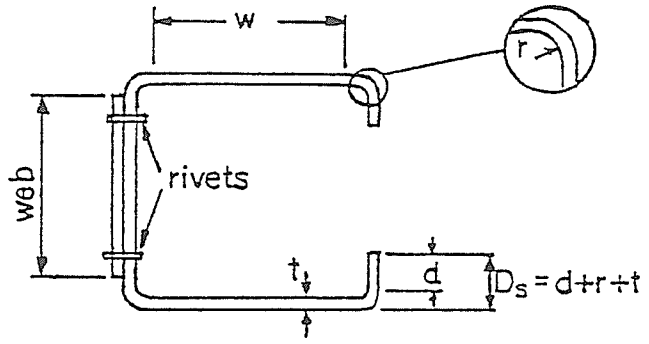

(a) Lipped channel

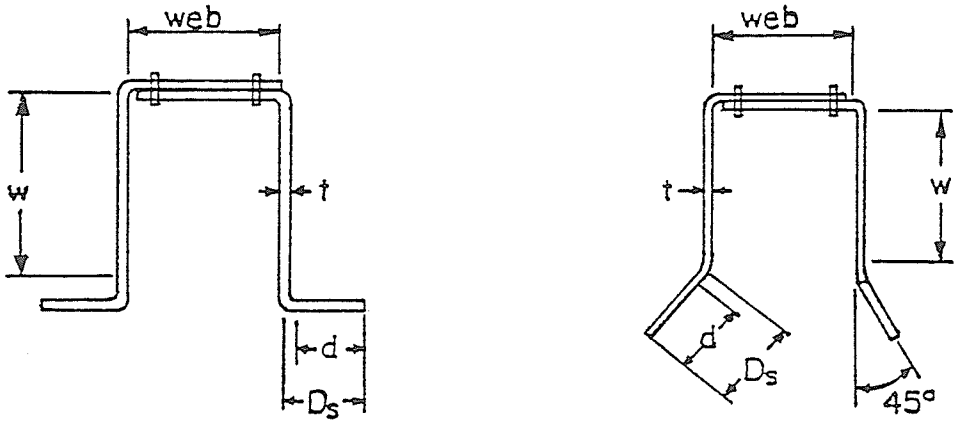

(b) Hat shaped sections

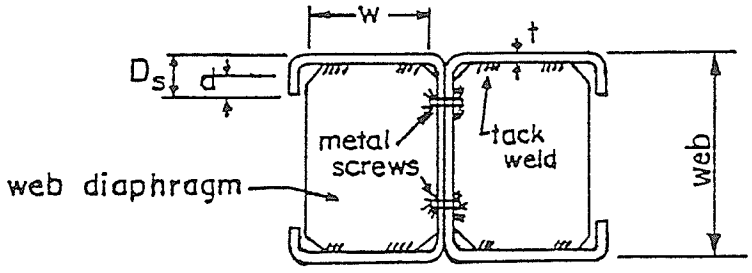

(c) Edge stiffened beam

Figure 2.1 Specimens Used in Desmond's Experimental Investigation

buckling. The local buckling interaction between web and flange elements was therefore excluded. The design guidelines for cold-formed sections in the 1986 and 1989 Edition of the AISI Specification were based on Desmond's work.

Cohen (1986) extended Desmond's work (1978) by studying the local buckling behaviour of cold-formed members subject to bending and compression. Cohen's results were used to support and clarify the AISI Specification (1986) criteria. Also, for locally unstable beam webs, effective width equations were developed from calibrations to the experimental data. The results of this investigation were proposed for the 1989 Edition of the AISI Specification.

The effect of residual stresses, produced in the forming process on the behaviour of cold-formed columns was investigated by Weng (1990). His results showed that the higher the level of residual stresses and geometric imperfections, the worse the agreement between experimental results and the AISI (1986) predictions.

The current design philosophy is to treat compression flanges as stiffened or partially stiffened elements and to compute the ultimate strength using the effective width approach. Basically, there is one effective width equation for all types of element and the post-buckling capacity of these elements depends on the plate buckling coefficient, k, which can be obtained from expressions provided by the code. In the following discussion relevant to the design specifications, the equation numbers shown are those used in the design specifications.

According to the effective width approach, the non-uniform stress after local buckling, is approximated by a uniform stress equal to the maximum stress with a part of the area being ineffective. The distribution and size of the effective area depend on the distribution and magnitude of the stress.

In the AISI Specification (1989), the effective width (b) of an uniformly compressed stiffened element is given as follows:

$$b = w \quad when \quad \lambda \leq 0.673 \qquad \textbf{(Eq. B2.1-1)}$$

$$b = \rho w \quad when \quad \lambda > 0.673 \qquad \textbf{(Eq. B2.1-2)}$$

where,

w = flat width as shown in Figure 2.2 (in.);

ρ = parameter determined as follows:

$$\rho = (1 - 0.22/\lambda)/\lambda \qquad \textbf{(Eq. B2.1-3)}$$

where,

λ = a slenderness factor determined as follows:

$$\lambda = \frac{1.052}{\sqrt{k}}\left(\frac{w}{t}\right)\sqrt{\frac{f}{E}} \qquad \textbf{(Eq. B2.1-4)}$$

where,

E = modulus of elasticity (ksi);

f = the critical stress of members (ksi); and

k = buckling coefficient defined as follows:

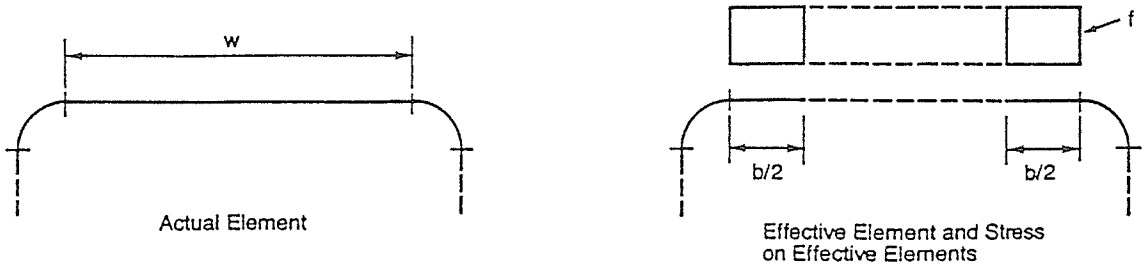

Figure 2.2 Stiffened Elements

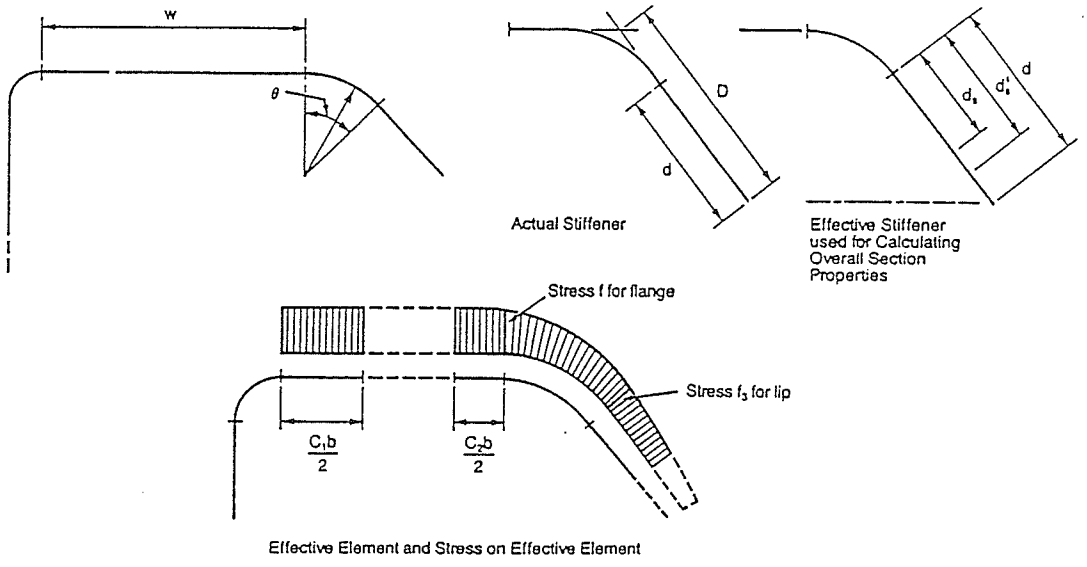

Figure 2.3 Elements with Edge Stiffener

$$k = [4.82 - 5(D/w)](I_s/I_a)^n + 0.43 \leq 5.25 - 5(D/w) \qquad \text{(Eq. B4.2-9)}$$

$$for \qquad 0.8 \geq D/w > 0.25$$

$$k = 3.57(I_s/I_a)^n + 0.43 \leq 4.0 \qquad \text{(Eq. B4.2-10)}$$

$$for \qquad D/w \leq 0.25$$

where,

I_a = the adequate moment of inertia of the stiffener which depends on the flat width-to-thickness ratio (w/t) of the flange (ksi) and is obtained as follows:

Case I: w/t $\leq$ S

$$I_a = o \quad (no\ edge\ stiffener\ needed) \qquad \text{(Eq. B4.2-2)}$$

Case II: S/3 < w/t < S

$$I_a / t^4 = 399[((w/t)/S) - 0.33]^3 \qquad \text{(Eq. B4.2-6)}$$

Case III: w/t > S

$$I_a / t^4 = [115(w/t)/S] + 5 \qquad \text{(Eq. B4.2-13)}$$

where,

S = $1.28\ (E / f)^{1/2}$;

n = 1/2 for Case II and 1/3 for Case III;

I_s = the moment of inertia of the edge stiffener about its own centroidal axis parallel to the flange (ksi) is defined as,

$$I_s = (d^3 t \sin^2\theta)/12 \qquad \text{(Eq. B4-2)}$$

where,

d = the flat width of the stiffener as shown in Figure 2.3 (in.).

Due to the non-uniform stress distribution in the flange and the edge stiffener, the effective widths of the flange and the edge stiffener are located as shown in Figure 2.3. The variables used in this figure are:

$$C_2 = \frac{I_s}{I_a} \leq 1 \qquad \text{(Eq. B4.2-7)}$$

$$C_1 = 2 - C_2 \qquad \text{(Eq. B4.2-8)}$$

$$d_s = d_s' \qquad \textit{for Case I} \qquad \text{(Eq. B4.2-4)}$$

$$d_s = d_s'(I_s/I_a) \leq d_s' \qquad \textit{for Case II , III} \qquad \text{(Eq. B4.2-12)}$$

where,

d_s' = the effective width of the edge stiffener (in.); and

d_s = a reduced effective width used for computing the overall effective section properties (in.).

For elements under a stress gradient, such as a web or any other adequately stiffened element, the k value is obtained as follows:

$$k = 4 + 2(1 - \psi)^3 + 2(1 - \psi) \qquad \text{(Eq. B2.3-4)}$$

where,

ψ = f_2 / f_1;

f_1, f_2 = stresses shown in Figure 2.4 calculated on the basis of effective section (ksi).

The effective widths, b_1, and b_2 (in.), as shown in Figure 2.4, are determined from the following formulas:

$$b_1 = b_e/(3 - \psi) \qquad \text{(Eq. B2.3-1)}$$

$$b_2 = b_e/2 \qquad For \quad \psi \leq -0.236 \qquad \text{(Eq. B2.3-2)}$$

where,

b_e = effective width , b (in.), determined with f_1 substituted for f and with k determined from Eq. B2.3-4.

$b_1 + b_2$ shall not exceed the compression portion of the web calculated on the basis of effective section

$$b_2 = b_e - b_1 \qquad For \quad \psi > -0.236 \qquad \text{(Eq. B2.3-3)}$$

The effective width, b , of unstiffened compression elements with uniform compression is determined from Eqs. B2.1-1 to B2.1-4 with the exception that k shall be taken as 0.43 and w as defined in Figure 2.5.

The effective width, b, of unstiffened compression elements and edge stiffeners with stress gradient is determined using the same equations but with $f = f_3$, as defined in Figure 2.3, and $k = 0.43$.

There is no provision pertaining to a partially stiffened flange with a stress gradient since the Specification (AISI, 1989) assumes Z-sections are not subject to twisting when subjected to bending about the strong axis. Thus, it is assumed that the stress in the flanges is uniform. However, if the principal axes are used as reference, the flanges and the edge stiffeners have a stress gradient.

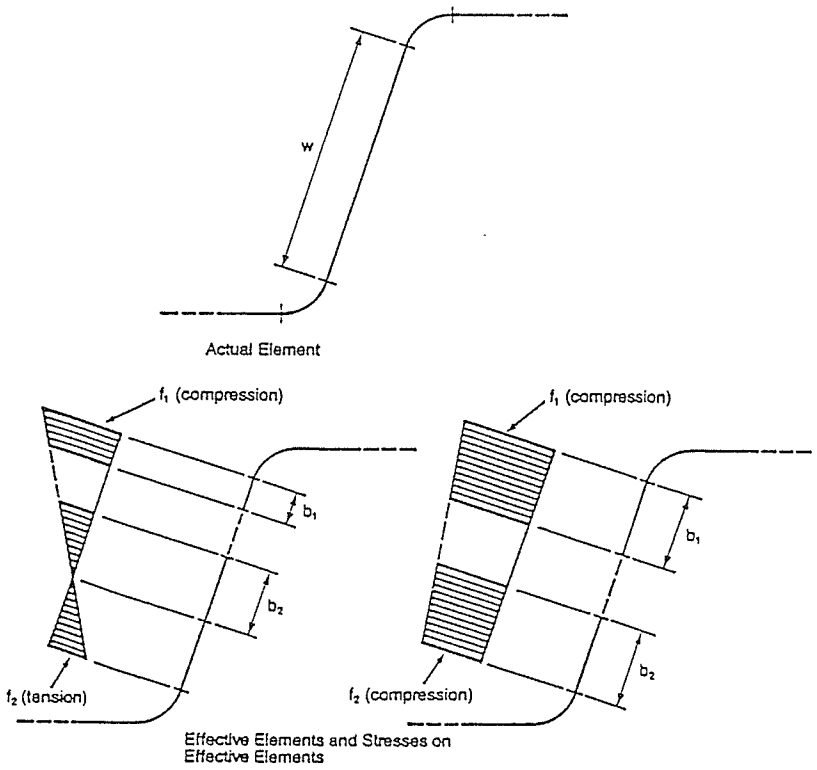

Figure 2.4 Stiffened Elements with Stress Gradient and Webs

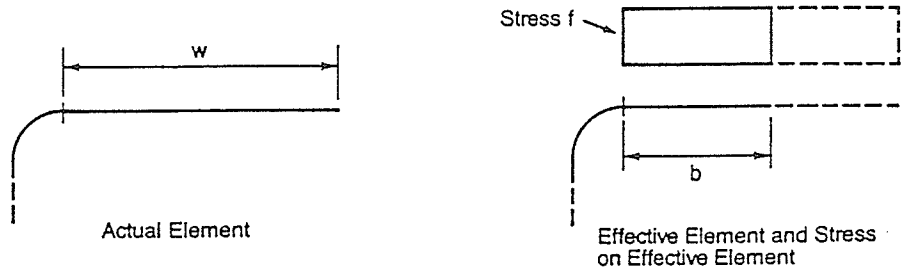

Figure 2.5 Unstiffened Elements with Uniform Compression

In the AISI Specification (1989), the maximum ratio of overall width of edge stiffener to flat width of the flange, D/b_f, and the maximum ratio of the flat width of the flange to the thickness of the section, d/t, are limited to 0.8 and 14, respectively. It is not clear in the Specification how the radius at the corners affects the behaviour of the section. Cohen and Pekoz (1986) have shown that the predicted values for the ultimate strength using the AISI Specification (1989) are unconservative if the maximum ratio, D/b_f, is greater than 1.0 or if the inside radius-to-thickness ratio, r_i/t, is greater than 1.5.

A summary of the AISI (1989) provisions governing the design of flexural members, compression members, and beam-columns is given below:

Flexural Members (Strength for bending only)

In flexural members, the applied moment must not exceed the allowable M_a calculated as follows:

$$M_a = M_n / \Omega_f \qquad \textbf{(Eq. C3.1-1)}$$

where,

M_n = smaller of the moment strength calculated according to yielding and lateral buckling given below, or the moment strength of unstiffened flanges section that was caused by the local buckling of unstiffened flange elements (kips-in.);

Ω_f = factor of safety for bending.

The effective yield moment based on section strength, M_n, is determined as follows:

$$M_n = S_e F_y \qquad \text{(Eq. C3.1.1-1)}$$

where,

S_e = elastic section modulus of the effective section based on the extreme compression fibre ($in.^3$).

For the laterally unbraced segments of singly-, doubly-, and point-symmetric sections subject to lateral buckling, M_n, is determined as follows:

$$M_n = S_c \frac{M_c}{S_f} \qquad \text{(Eq. C3.1.2-1)}$$

where,

S_f = elastic section modulus of the full unreduced section for the extreme compression fibre ($in.^3$);

S_c = elastic section modulus of the effective section calculated at a stress M_c/S_f in the extreme compression fibre ($in.^3$);

M_c = critical moment (kips-in.).

For Z-sections bent about the centroidal axis perpendicular to the web (x-axis) the critical moment, M_c, is determined as follows:

$$For \quad M_e \geq 2.78\,M_y \qquad M_c = M_y \qquad \text{(Eq. C3.1.2-12)}$$

$$For \quad 2.78\,M_y > M_e > 0.56\,M_y \qquad M_c = \frac{10}{9} M_y \left(1 - \frac{10 M_y}{36 M_e}\right) \qquad \text{(Eq. C3.1.2-13)}$$

$$For \quad M_e \le 0.56 M_y \qquad M_c = M_e \qquad \text{(Eq. C3.1.2-14)}$$

where,

M_y = moment causing initial yield at the extreme compression fibre of the full section (kips-in.),

$$M_y = S_f F_y \qquad \text{(Eq. C3.1.2-4)}$$

M_e = elastic critical moment (kips-in.),

$$M_e = \frac{\pi^2 E C_b d I_{yc}}{2 L^2} \qquad \text{(Eq. C3.1.2-16)}$$

where,

L = unbraced length of the member (in.);

I_{yc} = moment of inertia of the compression portion of a section about the gravity axis of the entire section parallel to the web, using the full unreduced section ($in.^4$).

d = total depth of the member (in.);

C_b = coefficient = 1.0.

Concentrically Loaded Compression Members

The axial load must not exceed P_a (kips) calculated as follows:

$$P_a = P_n / \Omega_c \qquad \text{(Eq. C4-1)}$$

where,

$$P_n = A_e F_n \qquad \text{(Eq. C4-2)}$$

A_e = effective area at the stress F_n ($in.^2$);

F_n (ksi) is determined as follows:

$$For \quad F_e > F_y/2 \qquad F_n = F_y(1 - F_y/4F_e) \qquad \text{(Eq. C4-3)}$$

$$For \quad F_e \leq F_y/2 \qquad F_n = F_e \qquad \text{(Eq. C4-4)}$$

F_e = the least of the elastic flexural, torsional and torsional-flexural buckling stress (ksi);

Ω_c = factor of safety for axial compression.

For Z-shapes, P_n should not be less than:

$$P_n = \frac{A\,\pi^2 E}{25.7\,(w/t)^2} \qquad \text{(Eq. C4-5)}$$

where,

A = area of the full cross section (in.^{2});

w = flat width of the unstiffened element (in.).

The AISI Specification (1989) is not clear as to how the critical stress, F_e, should be computed for Z-sections. This Specification governs sections not subject to torsional or torsional flexural buckling, sections which are doubly- or singly-symmetric sections subject to torsional or torsional-flexural buckling and non-symmetric sections. Z-Sections are point symmetric and they are subject to either lateral buckling or torsional buckling. Thus, F_e is the least of the following buckling stresses:

$$\sigma_{ex} = \frac{\pi^2 E}{(K_x L_x / r_x)^2} \qquad \text{(Eq. C3.1.2-7)}$$

$$\sigma_{ey} = \frac{\pi^2 E}{(K_y L_y / r_y)^2} \qquad \text{(Eq. C3.1.2-8)}$$

$$\sigma_t = \frac{1}{A r_o^2}\left[GJ + \frac{\pi^2 E C_w}{(K_t L_t)^2}\right] \qquad \text{(Eq. C3.1.2-9)}$$

where,

σ_{ex} = critical elastic lateral buckling stress with respect to the principal x-axis of the sections (ksi);

σ_{ey} = critical elastic lateral buckling stress with respect to the principal y-axis of the sections (ksi);

σ_t = critical elastic torsional buckling stress (ksi);

r_o = polar radius of gyration of the cross section about the shear centre (in.),

$$r_o = \sqrt{r_x^2 + r_y^2 + x_o^2} \qquad \text{(Eq. C3.1.2-10)}$$

r_x, r_y = radius of gyration of the cross section about the centroidal principal axes (in.);

G = shear modulus (ksi);

K_x, K_y, K_t = effective length factors for bending about the x- and y-axes, and for twisting;

L_x, L_y, L_t = unbraced length of member for bending about the x- and y-axes, and for twisting (in.);

x_o = distance from the shear centre to the centroid along the principal x-axis, taken as negative (in.);

J = St. Venant torsion constant of the cross section (in.^{4});

C_w = torsional warping constant of the cross section (in.^{6}).

Combined Axial Load and Bending

The axial force and bending moments must satisfy the following equations:

$$\frac{P}{P_a} + \frac{C_{mx} M_x}{M_{ax} \alpha_x} \leq 1.0 \qquad \text{(Eq. C5-1)}$$

$$\frac{P}{P_{ao}} + \frac{M_x}{M_{ax}} \leq 1.0 \qquad \text{(Eq. C5-2)}$$

where,

P = applied axial load (kips);

M_x = applied moments with respect to the centroidal axes of the effective section determined for the axial load alone (kips-in.);

P_a = allowable axial load determined from Eq. C4-1 (kips);

P_{ao} = allowable axial load determined from Eq. C4-1, with $F_n = F_y$ (kips);

M_{ax} = allowable moments about the centroidal axes determined from Eq. C3.1-1 (kips-in.),

$$\alpha_x = 1 - (\Omega_c P / P_{cr}) \qquad \text{(Eq. C5-4)}$$

$$P_{cr} = \frac{\pi^2 E I_b}{(K_b L_b)^2} \qquad \text{(Eq. C5-5)}$$

where,

P_{cr} = Euler buckling load with respect to the plane of bending (kips);

I_b = moment of inertia of the full cross section about the axis of bending (in.^{4});

L_b = actual unbraced length in the plane of bending (in.);

K_b = effective length factor in the plane of bending;

C_{mx} = coefficient = 1.0.

2.2 CSA STANDARD

In Canada, the Standard for the design of cold-formed steel members is the responsibility of Committee S136 of the Canadian Standard Association (CSA). The most recent edition of the Standard was published in 1989 and is designated CSA-S136-M89 (1989).

The 1984 Edition of the CSA Standard (1984) stated that, in order for a compression element to be treated as a stiffened element, it had to be stiffened along each longitudinal edge by the web, or edge, or other stiffeners, which had to provide sufficient rigidity for the compression element to reach yield. The edge stiffeners had to provide the following minimum moment of inertia:

$$I_{min} = (2B - 13)t^4 \geq 9t^4 \qquad (2.2)$$

where,

I_{min} = minimum allowable moment of inertia of stiffeners (of any shape) with respect to its own centroidal axis and parallel to the stiffened element (mm^4);

B = b/t, flat width-to-thickness ratio of the stiffened element;

b = flat width of the stiffened element (mm);

t = base steel nominal thickness (mm).

For edge stiffener bent at right angles to the stiffened element, the minimum overall width of the edge stiffener, d_{min} (mm), was given as:

$$d_{min} = t(24B - 156)^{\frac{1}{3}} \geq 4.8t \qquad (2.3)$$

These requirements were sufficient to ensure yielding at the edges of the flanges being stiffened.

In the 1989 Edition of the Standard (CSA, 1989), the minimum moment of inertia and the minimum overall width of edge stiffeners were eliminated and an unified approach (Pekoz, 1986) was adopted. According to this approach elements were classified as stiffened or partially stiffened. A series of empirical equations similar to those in the AISI Specification (1989), were adopted for computing the buckling coefficient of fully and partially stiffened compression flanges.

In the following sections the CSA Standard (1989) requirements for the effective width design of elements, the strength of members in bending, compression, and combined axial load and bending, are discussed.

According to the effective design width of elements in compression, when W (w/t) exceeds W_{lim}, the flat width, w, shall be replaced by an effective width. The effective width is determined as follows:

Case I: When $W \leq W_{lim}$,

$$B = W$$

Case II: When $W > W_{lim}$,

$$B = 0.95\sqrt{kE/f}\left[1 - \frac{0.208}{W}\sqrt{kE/f}\right]$$

where,

$$W_{lim} = 0.644\sqrt{kE/f}$$

k = buckling coefficient defined in Table 2.1; the variables used in Table 2.1 are as follows:

d, w, d_i = calculated stress in compression element.

$$I_r = I_s / I_a$$

I_s = moment of inertia of fully effective cross sectional area of stiffener about its own centroidal axis parallel to the element to be stiffened (mm^4),

$$I_s = t\,d^3 \sin^2\theta / 12$$

I_a = required moment of inertia for an adequate stiffener that allows the adjacent compressive element to behave as a fully stiffened element (mm^4). It is obtained as follows:

Case I: When $W < W_{lim1}$,

$$I_a = 0 \quad (\textit{no edge stiffener needed})$$

Case II: When $W_{lim1} < W < W_{lim2}$,

$$I_a = 399\,t^4\,(W/W_{lim2} - 0.33)^3$$

Table 2.1 Buckling Coefficient for Elements in Compression Under Uniform Stress with a Simple Edge Stiffener (as shown in Figure 2.6)

		$d_i/w \leq 0.25$	$0.25 < d_i/w \leq 0.8$
Case II	$I_r \geq 1$	$k = 4$	$k = 5.25 - 5(d_i/w)$
	$I_r < 1$	$k = 3.57(I_r)^{1/2} + 0.43$	$k = [4.82 - 5(d_i/w)](I_r)^{1/2} + 0.43$
Case III	$I_r \geq 1$	$k = 4$	$k = 5.25 - 5(d_i/w)$
	$I_r < 1$	$k = 3.57(I_r)^{1/3} + 0.43$	$k = [4.82 - 5(d_i/w)](I_r)^{1/3} + 0.43$

Note: *In Table 1, $d/t \leq 14$*

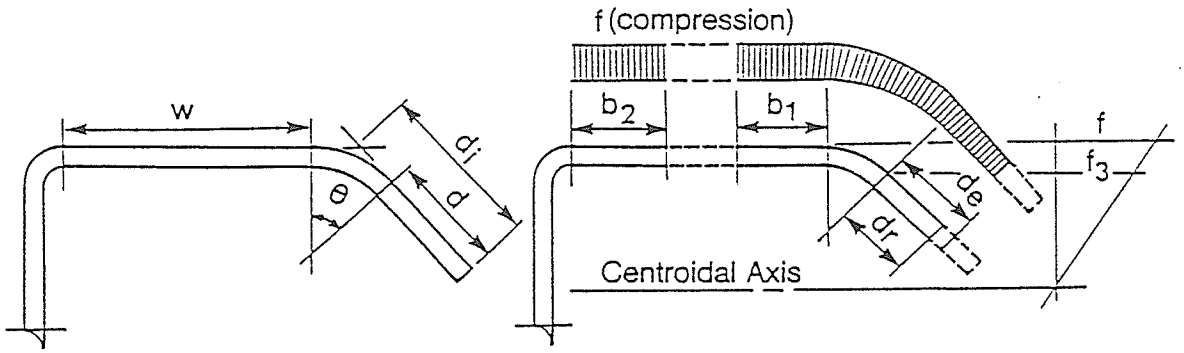

Figure 2.6 Example of Edge-Stiffened Flange Element Subjected to Uniform Compressive Stress

Case III: When $W > W_{lim2}$,

$$I_a = t^4\left[115\left(W/W_{lim2}\right) + 5\right]$$

where for Cases I, II, and III,

$$W_{lim1} = 0.644\sqrt{kE/f} \qquad with \quad k = 0.43$$

$$W_{lim2} = 0.644\sqrt{kE/f} \qquad with \quad k = 4$$

Due to the non-uniform stress distribution in the flange and the edge stiffener, the effective widths of the flange and the edge stiffener are located as shown in Figure 2.7. The variables used in this figure are:

$$b_1 = I_r Bt/2 \le Bt/2$$

$$b_2 = Bt - b_1$$

$$d_r = d_e \qquad for\ Case\ I$$

$$d_r = d_e I_r \le d_e \qquad for\ Case\ II,\ III$$

where,

b_1, b_2 = effective widths illustrated in Figure 2.7 (mm);

d_e = effective width of stiffener illustrated in Figure 2.7 determined with $W = d/t$ and $f = f_3$ (mm);

d_r = reduced effective width of stiffener illustrated in Figure 2.7 to be used in calculating overall effective properties (mm).

For elements under a stress gradient, such as a web or any other adequately stiffened element, the k value is obtained as follows:

$$k = 4 + 2(1 + q)^3 + 2(1 + q) \qquad when \quad 0 \leq q \leq 1$$

$$k = 6(1 + q)^2 \qquad when \quad 1 < q \leq 3$$

where,

$q = f_2 / f_2$;

f_1, f_2 = calculated stresses shown in Figure 2.7 (MPa).

The effective widths, b_1, and b_2, as shown in Figure 2.7, are determined from the following formulas;

$$b_1 = Bt/(3 + q)$$

$$b_2 = Bt/(1 + q) - b_1$$

where,

b_1, b_2 = effective widths illustrated in Figure 2.7 (mm);

B = b/t, calculated with $f = f_1$.

The effective width, b = Bt, of unstiffened compression elements with uniform compression is determined with k = 0.43 and W = w/t, as shown in Figure 2.8, whereas the effective width, d = Bt, of unstiffened compression elements and edge stiffeners gradient is determined with k = 0.43, $f = f_3$, and W = d/t, as shown in Figure 2.6.

A summary of the CSA Standard (1989) governing the design of flexural members, compression members, and beam-columns is given below:

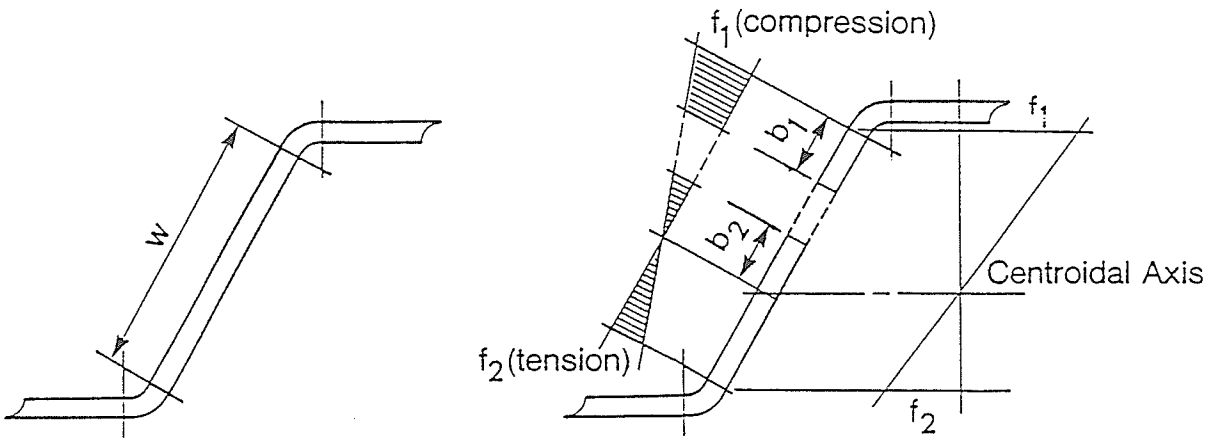

Figure 2.7 Example of Stiffened Web Element Subjected to Stress Gradient (Compression and Tension)

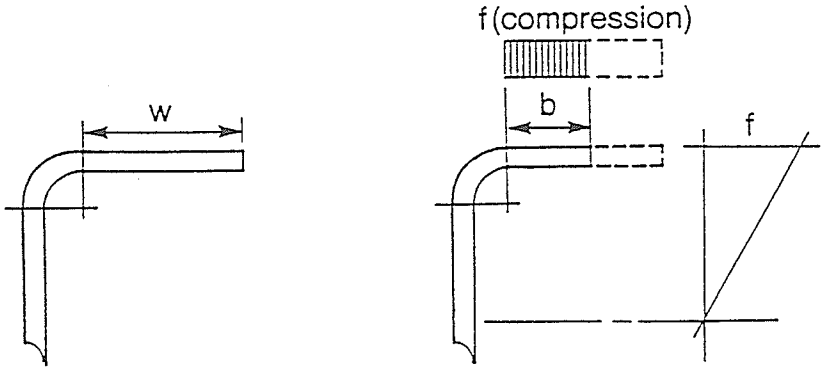

Figure 2.8 Example of Unstiffened Flange Element Subjected to Uniform Compression Stress

Members in Bending (Strength for bending only)

The moment resistance of member in bending is determined as follows:

$$M_r = S_c F_c$$

$$M_r = S_{tn} F_u$$

$$M_r = S_t F_y$$

where,

F_c = compressive limit stress calculated in accordance with either the yielding or the lateral buckling criteria (MPa);

S_c = compressive section modulus based on the moment of inertia of the effective cross sectional area divided by the distance from the centroidal axis to the extreme compressive fibre (mm^3);

S_t = tensile section modulus based on the moment of inertia of the effective gross cross sectional area divided by the distance from the centroidal axis to the extreme tensile fibre (mm^3);

S_{tn} = tensile section modulus based on the moment of inertia of the effective net cross sectional area divided by the distance from the centroidal axis to the extreme tensile fibre (mm^3).

Laterally Supported Members

F_c is calculated based on initiation of yielding (MPa);

$F_c = F_y$

Laterally Unsupported Members

For Z-shaped members, F_c is calculated as follows:

$$(a) \quad when \quad F_b > F'/2 \qquad F_c = F' - \frac{(F')^2}{4F_b} = \leq F_y$$

$$(b) \quad when \quad F_b \leq F'/2 \qquad F_c = F_b$$

where F_b (MPa) is calculated as follows:

$$F_b = \frac{0.833}{2S_{xc}} C_b r_o A \sqrt{F_{ey} F_t}$$

$$F_{ex} = \frac{\pi^2 E}{(K_x L_x / r_x)^2}$$

$$F_{ey} = \frac{\pi^2 E}{(K_y L_y / r_y)^2}$$

$$F_t = \frac{1}{A r_o^2} \left[GJ + \frac{\pi^2 E C_w}{(K_t L_t)^2} \right]$$

$$F' = 1.11 F_y$$

where,

F_{ex} = critical elastic lateral buckling stress with respect to the principal x-axis of the sections (ksi);

F_{ey} = critical elastic lateral buckling stress with respect to the principal y-axis of the section (ksi);

F_t = critical elastic torsional buckling stress (ksi);

S_{xc} = compressive section modulus of the fully effective cross sectional area about the centroidal x-axis perpendicular to the web, I_x divided by the distance from the centroidal axis to the extreme compressive fibre (mm^3).

For Z-shaped members with unstiffened flanges and $F_c < F_y$, the moment resistance is limited to:

$$M_r = \frac{k \pi^2 E S_{cf}}{12 (1 - \mu^2) W^2}$$

where,

k = 0.43;

S_{cf} = compressive section modulus based on the moment of inertia of the fully effective cross sectional area divided by the distance from the centroidal axis to the extreme compressive fibre (mm^3).

Members in Compression (Concentrically Loaded)

The compressive resistance, C_r (kN), is determined by:

$$C_r = A_e F_a$$

where, the compressive limit stress, F_a (MPa), is determined as follows:

$$(a) \quad when \ F_p > F_y/2 \qquad F_a = F_y - \frac{(F_y)^2}{4 F_p}$$

$$(b) \quad when \ F_p \leq F_y/2 \qquad F_a = F_p$$

where,

A_e = effective cross sectional area at the stress F_a (mm^2);

F_p = critical elastic buckling stress, being the least of the stresses for Euler-flexural, torsional, or torsional-flexural elastic buckling, multiplied by the coefficient 0.833 (MPa).

For any sections that can be shown to be not critical in torsional buckling or not subject to torsional-flexural buckling, F_p is given by:

$$F_p = 0.833 F_e$$

$$F_e = \pi^2 E / (KL/r)^2$$

where,

KL/r = the greater of the effective slenderness ratios about the principal axes;

K = effective length factor;

r = radius of gyration of the fully effective cross sectional area (mm).

For Z-shapes, C_r is not less than:

$$C_r = \frac{k \pi^2 E A}{12 (1 - \mu^2) W^2}$$

where,

k = 0.43.

For point-symmetric open sections, such as Z-sections that may be subject to torsional buckling and that are not braced against twisting, F_p equal to the lesser of $0.833F_e$ or $0.833F_t$.

Combined Axial Load and Bending

When subject to both axial compression and bending, members must be proportioned to meet the following requirements:

$$(a) \qquad \frac{C_f}{C_r} + \frac{M_{fx}}{M_{rx}} \leq 1.0$$

where,

C_f = axial compressive load in the member due to factored loads (kN);

C_r = $A_e F_y$ (kN);

A_e = effective cross sectional area at the stress F_y (kN);

M_{rx} = moment resistance with C_b = 1 (kN-m);

M_{fx} = maximum moments due to axial compression load (kN-m).

$$(b) \qquad \frac{C_f}{C_r} + \frac{\omega_x M_{fx}}{M_{rx}\alpha_x} \leq 1.0$$

where,

ω_x = coefficient = 1.0;

α_x = amplification factor, equal to [1 - C_f/C_e];

C_e = AF_e (kN).

CHAPTER 3

THEORETICAL MODELS

Differential equations for the lateral-torsional buckling of beams were originally developed by Goodier (1941). These equations were extended to cover lateral-torsional buckling of undistorted sections by Vlasov (1961) and further to include continuous elastic supports by Timoshenko and Gere (1961). Haussler (1964) used the equations to develop an iterative procedure for determining the elastic critical stress of thin-walled steel beams. In his theoretical model, Haussler assumed that the elastic critical stress was equal to the critical stress of an equivalent compression component. This equivalent compression component consisted of the compressive flange, the edge stiffener, and one-sixth of the overall width of the web element. Wikstrom (1971) developed a simplified method for the design of panel-braced thin-walled steel beams by analyzing the beams as though the compression side of the member was supported by an elastic foundation. He assumed that the elastic foundation was provided by the panel, the adjacent flange, and part of the web. The theory of elastically stabilized beams (Haussler, 1964) was extended by Pekoz (1983) to cover cold-formed steel channel and Z-section used as roof members braced by sheathing attached along the tension flange. Lars (1986) using a similar model showed a satisfactory agreement with experimental results involving Z and C profiles under both gravity and uplift loads. Marsh (1985), and Lau and Hancock (1987) solved the simultaneous differential equations presented by

Timoshenko and Gere (1961) and proposed a number of analytical procedures. The procedures developed by Lau and Hancock (1987) were used to obtain the distortional buckling stress on the flange-edge component of thin-walled channel section columns, shown in Figure 3.1. Their model is based on the principle of a column on an elastic foundation, where the column consists of an edge stiffened flange and the elastic foundation is provided by the web.

In the present study, the model suggested by Lau and Hancock (1987) was modified and used for the analysis of the column Z-sections. The model developed by Pekoz (1983) and Lars (1986) was modified and used in the analysis of the beam Z-sections. Therefore, the flange-edge stiffener component of Z-section columns and the equivalent column of Z-section beams investigated in this research project, are assumed to fail by distortional buckling. In the following sections, the assumptions made in the development of the theoretical models are discussed. The governing differential equations are presented, along with the general closed form solutions, and followed by the specific simplified expressions for computing the strength of typical column, beam, and beam-column sections.

3.1 ASSUMPTIONS

The assumptions regarding the behaviour of the cold-formed steel Z-section with straight edge stiffeners, shown in Figures 3.2 and 3.3, for column and beam, respectively, are as follows:

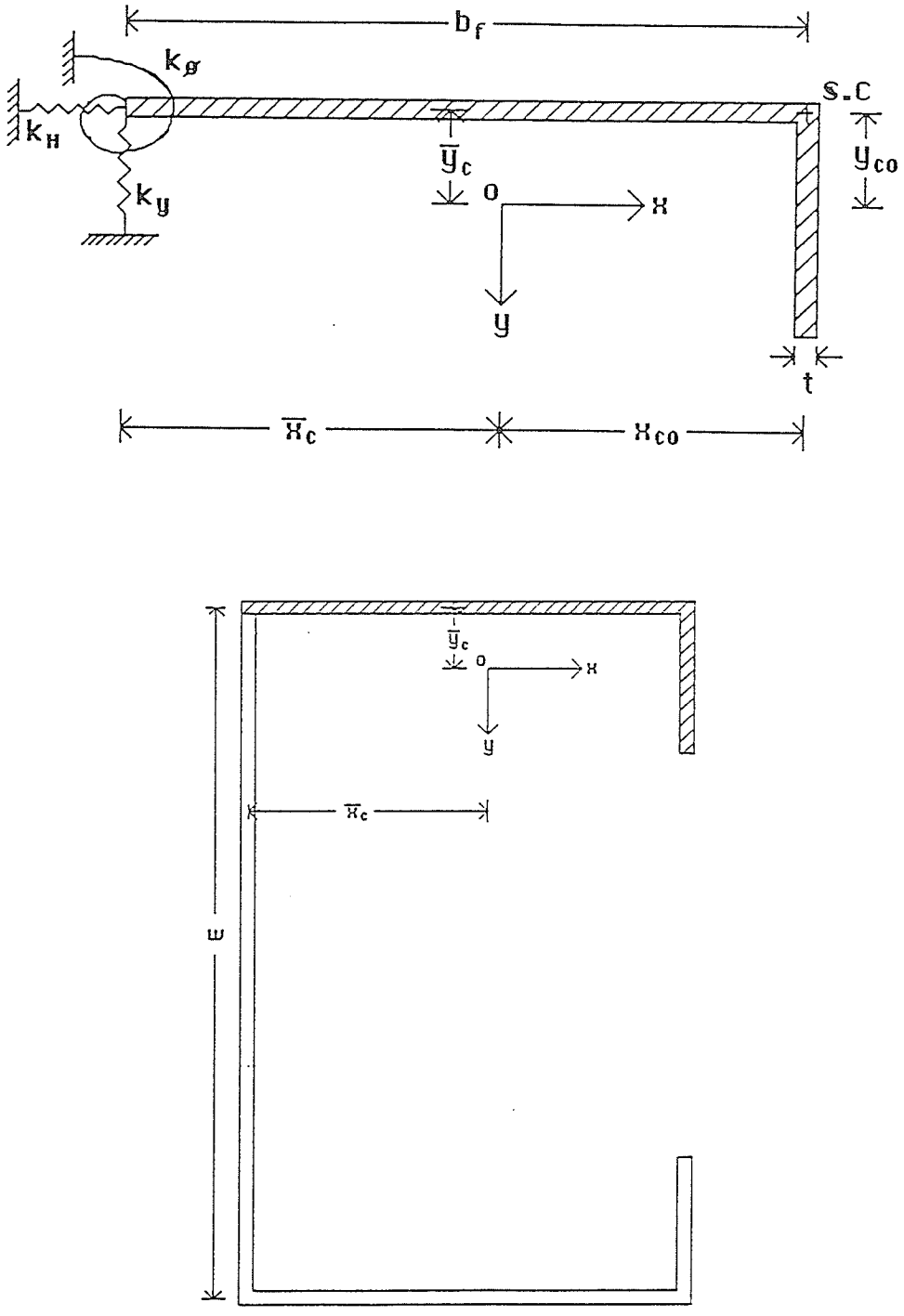

Figure 3.1 Flange-Edge Stiffener Component on a Continuous Elastic Foundation

1) For columns, the elastic critical stress of the whole section is equal to the distortional buckling stress of an undistorted flange-edge stiffener component. This component consists of the edge stiffener and the flange element, as shown in Figure 3.2. The web of sections is assumed to be partially destabilized by the uniform longitudinal compressive stress. The web can provide only vertical support to the flange-edge stiffener component.
2) For beams, the elastic critical stress is equal to the distortional buckling stress of an undistorted equivalent column. This column consists of the edge stiffener, top flange, and one-sixth of the overall width of the web, as shown in Figure 3.3. The web of sections is assumed to be partially destabilized by the linear longitudinal stress gradient. The continuous foundation was assumed to be located at the web-flange junction on the tension side of the beam. It was also assumed that once the web becomes locally unstable, it was no longer able to contribute to the bending capacity of the member. Five-sixths of the overall width of the web were therefore assumed to be ineffective in this theoretical model.
3) The lateral restraint in the transverse plane to the web is assumed to be small and ignored in the analysis.
4) The corners at the flange-edge stiffener junction and the flange-web junction are assumed to be curved, as this is the case in cold-formed sections, and they are included in the evaluation of the cross sectional properties.

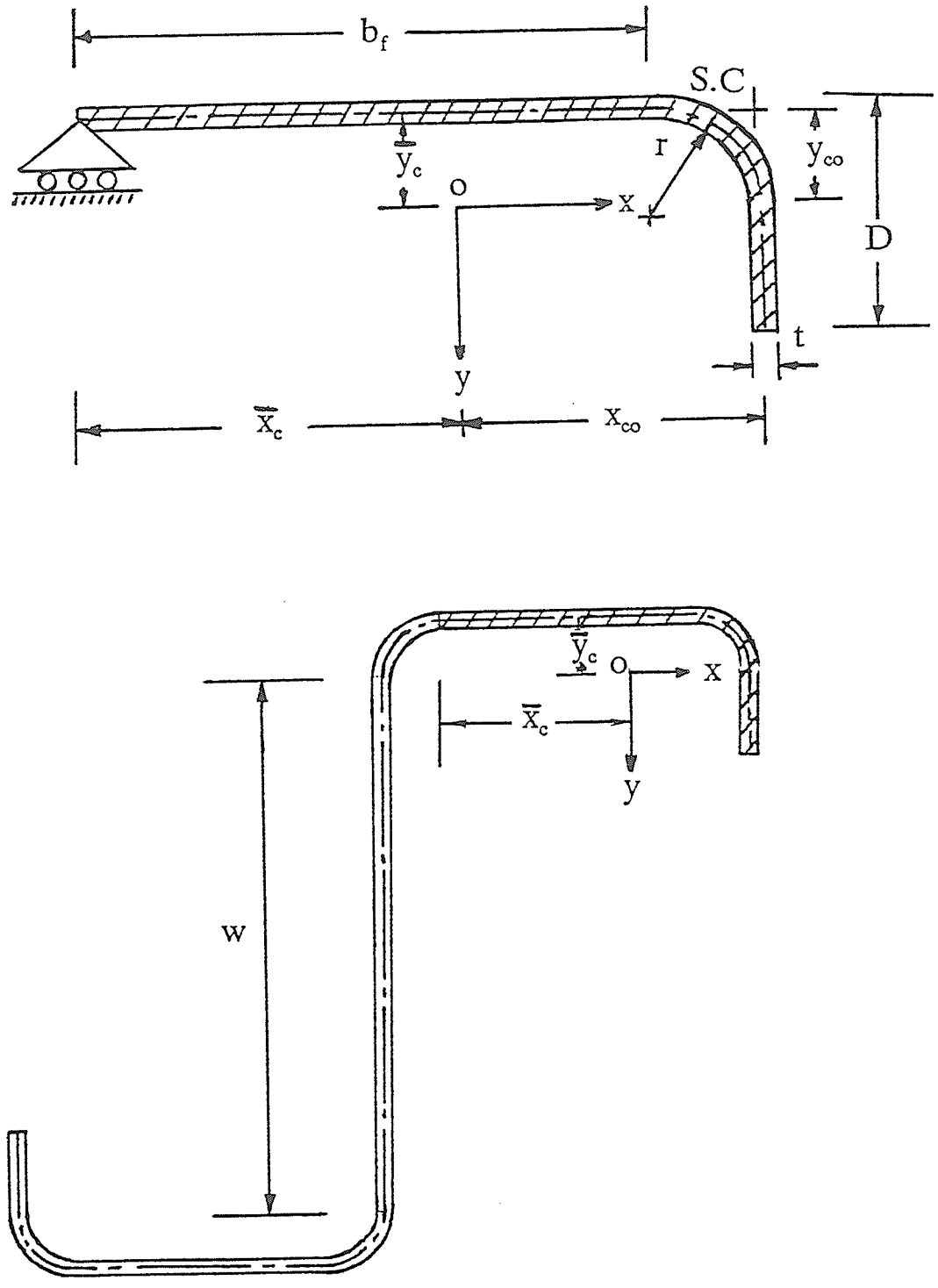

Figure 3.2 Theoretical Model of a Flange-Edge Stiffener Component for Cold-Formed Steel Z-Section Column

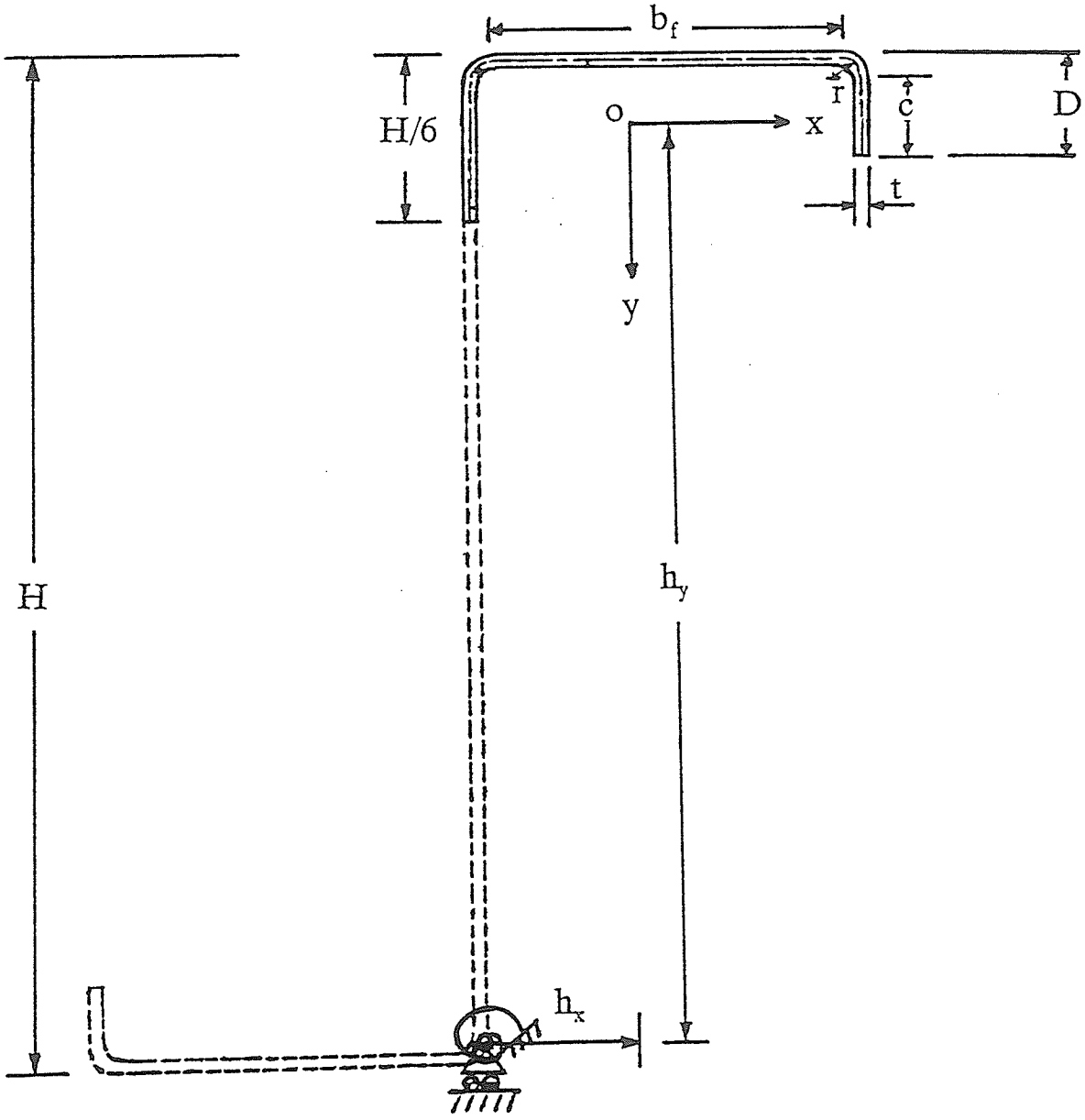

Figure 3.3 Theoretical Model of an Equivalent Column for Cold-Formed Steel Z-Section Beam

5) The inelastic distortional buckling stress is taken into account using CRC (Canadian Research Council) curve (Jhonston, 1976).

3.2 THE GOVERNING DIFFERENTIAL EQUATIONS

By considering equilibrium of forces in the plane of the cross section and the equilibrium of moments about the shear centre, the resulting three simultaneous differential equations were obtained as follows:

$$EI_{cy}\frac{d^4u}{dz^4} + EI_{cxy}\frac{d^4v}{dz^4} + P\left(\frac{d^2u}{dz^4} - (y_{co} - e_y)\frac{d^2\phi}{dz^2}\right) + k_x\left[u - (y_{co} - h_y)\,\phi\right] = 0 \tag{3.1}$$

$$EI_{cx}\frac{d^4v}{dz^4} + EI_{cxy}\frac{d^4u}{dz^4} + P\left(\frac{d^2v}{dz^4} - (x_{co} - e_x)\frac{d^2\phi}{dz^2}\right) + k_y\left[v - (x_{co} - h_x)\,\phi\right] = 0 \tag{3.2}$$

$$EC_w\frac{d^4\phi}{dz^4} - \left[GJ_c - P\left(e_y\beta_1 + e_x\beta_2 + \frac{I_{co}}{A}\right)\right]\frac{d^2\phi}{dz^2} - P\left((x_{co} - e_x)\frac{d^2v}{dz^2} - (y_{co} - e_y)\frac{d^2u}{dz^2}\right)$$

$$+ k_x\left[u + (y_{co} - h_y)\,\phi\right](y_{co} - h_y) - k_y\left[v - (x_{co} - h_x)\,\phi\right](x_{co} - h_x) + k_\phi\,\phi = 0 \tag{3.3}$$

where,

$$\beta_1 = \frac{1}{I_{cx}}\left(\int_A y^3dA + \int_A x^2y dA\right) - 2y_{co} \tag{3.4}$$

$$\beta_2 = \frac{1}{I_{cy}}\left(\int_A x^3dA + \int_A x y^2 dA\right) - 2x_{co} \tag{3.5}$$

$$I_{co} = I_{cx} + I_{cy} + A_d\left(x_{co}^2 + y_{co}^2\right) \tag{3.6}$$

where,

A_d = cross sectional area of the flange-edge stiffener component or the equivalent column (in.^{2});

E = elastic modulus of the cold-formed steel (ksi);

G = elastic shear modulus of the cold-formed steel (ksi);

P = applied compressive force on the flange-edge stiffener (kips);

J_c = St. Venant torsional constant of the flange-edge stiffener or the equivalent column ($in.^4$);

C_w = warping constant of the flange-edge stiffener or the equivalent column ($in.^4$);

I_{cx}, I_{cy} = second moments of area of the flange-edge stiffener or the equivalent column with respect to the geometric x- and y-axes ($in.^4$);

I_{cxy} = product second moment of area of the flange-edge stiffener or the equivalent column with respect to the geometric x- and y-axes ($in.^4$);

I_o = polar second moment of area of the flange-edge stiffener or the equivalent column with respect to the shear centre ($in.^4$);

x, y = x- and y-coordinates of the flange-edge stiffener or the equivalent column (in.);

x_{co}, y_{co} = x- and y-coordinates of the shear centre (in.);

h_x, h_y = x- and y-coordinates of the supported edge (in.);

e_x, e_y = x- and y-coordinates of the eccentric load on the equivalent column with respect to the centroid (in.);

k_x, k_y, k_ϕ = stiffnesses of lateral and rotational restraints (kips/in., kips-in./rads);

u, v, z, ϕ = deflections in the x-, y- and z-coordinates of the shear centre axis and angle of rotation of section with respect to this axis (in.).

In Equations 3.1 and 3.2, the first two terms present the bending of the section with respect to the geometric x- and y-axes, the third term presents the intensities of lateral forces acting on the slightly rotated cross section caused by the applied compressive force P, and the last term indicates the intensities of lateral reaction forces acting along the elastic supports. In Equation 3.3, the first three terms are derived from non-uniform torsion of a thin-walled open cross section, whereas the last three terms are the torque caused by the two lateral reactions and the torsional restraint at the elastic supports, respectively.

3.3 THE GENERAL THEORETICAL EXPRESSIONS

The general closed form solutions were obtained from solving the simultaneous differential equations (Equations 3.1 to 3.6) by applying the assumptions discussed in Section 3.1. Thus, the general theoretical expressions involving the distortional buckling stress can be expressed as follows:

$$\sigma_{cr} = \sigma_{dcr} \qquad if \quad \sigma_{dcr} \leq \frac{F_y}{2} \tag{3.7}$$

and,

$$\sigma_{cr} = F_y \left(1 - \frac{F_y}{4\sigma_{dcr}}\right) \qquad if \quad \sigma_{dcr} > \frac{F_y}{2} \tag{3.8}$$

where,

$$\sigma_{dcr} = \frac{P}{A_d} \tag{3.9}$$

and,

$$P = \Lambda - \sqrt{\Lambda^2 - \Omega} \tag{3.10}$$

$$\Lambda = -\alpha_B / 2\alpha_A \tag{3.11}$$

$$\Omega = \alpha_C / \alpha_A \tag{3.12}$$

where,

$$\alpha_A = \frac{\gamma_y^2 - \gamma_h^2 + 2\gamma_x\gamma_h - \xi}{\eta E} \tag{3.13}$$

$$\alpha_B = \varphi_1 - 2\varphi_2\gamma_y + I_{cy}\left(\gamma_h^2 - 2\gamma_x\gamma_h + \xi\right) + \frac{GJ_c + \frac{k_\phi}{\eta}}{\eta E} \tag{3.14}$$

$$\alpha_C = E\varphi_2^2\eta - I_{cy}\left(E\varphi_1\eta + GJ_c + \frac{k_\phi}{\eta}\right) \tag{3.15}$$

$$\gamma_x = x_{co} + e_x \tag{3.16}$$

$$\gamma_y = y_{co} + e_y \tag{3.17}$$

$$\gamma_h = x_{co} + \overline{x_c} \tag{3.18}$$

$$\gamma_o = y_{co} + \overline{y_c} \tag{3.19}$$

$$\varphi_1 = C_w + I_{cx}\gamma_h^2 \tag{3.20}$$

$$\varphi_2 = I_{cxy}\gamma_h \tag{3.21}$$

$$\varphi_3 = \varphi_1 + \gamma_o\left(I_{cy}\gamma_o - 2\varphi_2\right) \tag{3.22}$$

$$\xi = \frac{I_{co}}{A_d} - e_y\beta_1 - e_x\beta_2 \tag{3.23}$$

$$\eta = \sqrt{\frac{k_\phi}{E\varphi_3}} \tag{3.24}$$

$$k_\phi = \frac{Et^3}{4w} \tag{3.25}$$

where,

F_y = yield strength of the cold-formed steel (ksi);

σ_{dcr} = elastic distortional buckling stress of the flange-edge stiffener (ksi);

σ_{cr} = inelastic distortional buckling stress of the flange-edge stiffener (ksi);

x_c, y_c = x- and y-coordinates of the flange-edge stiffener or the equivalent column with respect to the centroid (in.);

t = thickness of the cold-formed section (in.);

w = flat width of the web element (in.);

k_ϕ = stiffness of the rotational restraint (kips-in./rads).

The rotational stiffness of the restraint is due to the bending resistance of the web only. It can be obtained from the load-deflection relationship of a cantilever consisting of a unit width of the section fixed on one flange and loaded along the other flange, as shown in Figure 3.4. The test result of a single specimen loaded in this fashion is shown in this figure. The shape of the line in Figure 3.4 then represents a measure of the stiffness rotational restraint.

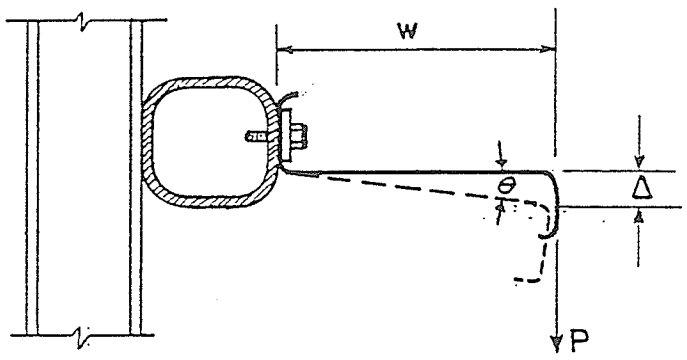

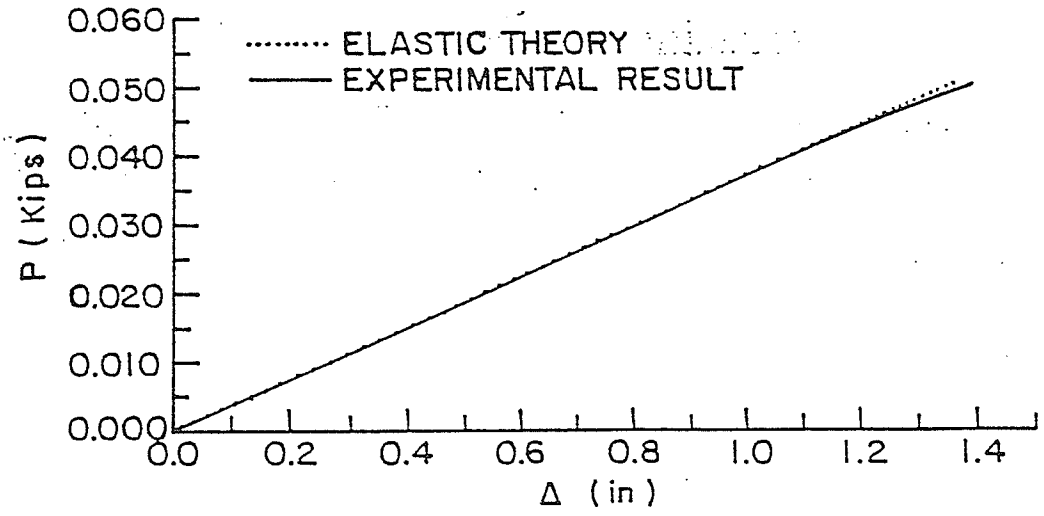

Figure 3.4 Set-Up to Determine Load-Deflection Relationship for Obtaining Rotational Restraint

3.4 THE SIMPLIFIED THEORETICAL EXPRESSIONS

The primary objective in developing the theoretical models was to provide simplified design procedures for cold-formed sections subjected to distortional buckling. Two theoretical models were developed: one for members subjected to direct compression, and the second for members subjected to bending. By combining these two models in the form of an interaction equation, a simplified expression for beam-columns was also obtained. Each of these theoretical models is discussed separately in the following sections.

3.4.1 Column Model

The strength of a Z-section under direct compression is computed in accordance with its failure behaviour. First type of failure, distortional buckling of the flange-edge stiffener component takes place first followed by buckling of the web, as shown in Figure 3.5(a). The maximum capacity of the section is the product of the distortional buckling stress of the flange-edge stiffener and the gross cross sectional area of the section. Second type of failure, local buckling of the web takes place first followed by distortional buckling of the flange-edge stiffener component, as shown in Figure 3.5(b). The post-buckling strength of the web may be taken into consideration by using the distortional buckling stress of the flange-edge stiffener as the critical stress of the section. In this study, in order to develop a simplified expression it was assumed that the locally unstable web element causes instability of the flange-edge stiffener. The post-buckling strength of the web was not

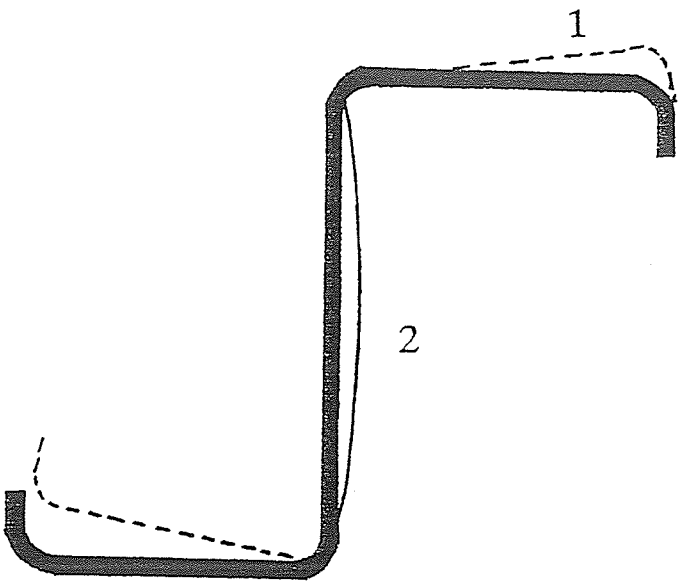

(a) Distortional Buckling of the Flange Precedes Local Buckling of the Web

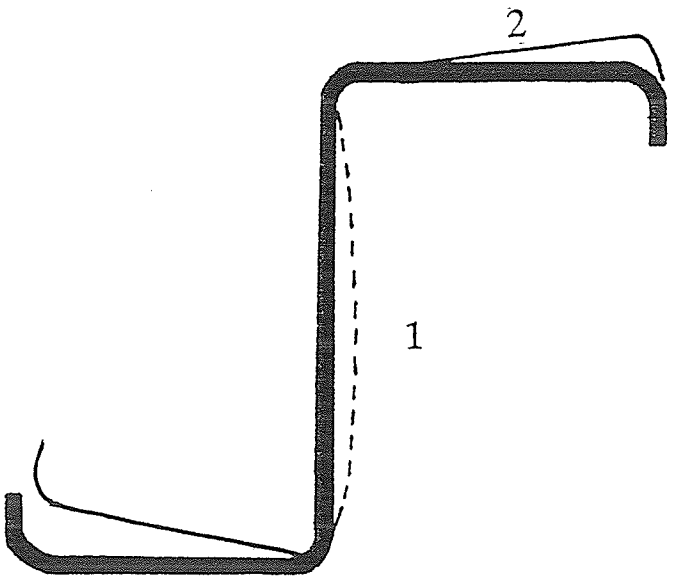

(b) Local Buckling of the Web Precedes Distortional Buckling of the Flange

Figure 3.5 Distortional Buckling Behaviour of Cold-Formed Z-Section

developed. By ignoring this post-buckling strength, a conservative estimate of the load-carrying capacity of the section is then computed as follows: i.e.,

$$P_{cr} = \sigma_{cr} A \tag{3.26}$$

where,

P_{cr} = load-carrying capacity of Z-section column (kips);

A = gross cross sectional area of the Z-section (in.^{2}).

σ_{cr} = inelastic distortional buckling stress of the flange-edge stiffener using the CRC curve (Jhonston, 1976), Equations 3.7 and 3.8 (ksi);

The distortional buckling stress of the flange-edge stiffener component was computed as follows:

$$\sigma_{dcr} = E(\tau - \sqrt{\tau^2 - 4.2\psi}) \,/\, 5NA_d \tag{3.27}$$

$$\tau = I_{cx} x_{co} + 2\overline{y}_c I_{cxy} + 0.9\frac{J_c N}{V} + \frac{I_{cy} V}{x_{co}} \tag{3.28}$$

$$\psi = V\left(I_{cx} I_{cy} - I_{cxy}^2\right) + \frac{I_{cy} J_c N}{x_{co}} \tag{3.29}$$

$$N = V\left(\frac{I_{cx} w}{t^3}\right)^{0.5} \tag{3.30}$$

$$V = \overline{x}_c^2 + \frac{I_{cx} + I_{cy}}{A_d} \tag{3.31}$$

where,

σ_{dcr} = elastic critical stress in the compressive flange at the extreme fibre which is caused by the distortional buckling stress of the flange-edge stiffener (ksi);

x_{co} = x-coordinate of the shear centre of the flange-edge stiffener (in.);

= $0.5\ b_f$ for flanges without edge stiffeners,

= $b_f + r$ for flanges with edge stiffeners bent at right angle,

= $b_f + r \tan(\theta/2)$ for flanges with sloping edge stiffeners.

b_f = flat width of the flanges (in.);

r = centerline bend radius of the flange-edge stiffener junction (in.);

θ = angle between flange and edge stiffener element (degrees);

A_d = gross cross sectional area of the flange-edge stiffener (in.^{2});

$\overline{x_c}$, $\overline{y_c}$ = as shown in Figure 3.2 (in.);

I_{cx}, I_{cy} = moments of inertia of the flange-edge stiffener with respect to the geometric x- and y-axes, respectively (in.^{4});

I_{cxy} = product moment of inertia of the flange-edge stiffener with respect to the geometric x- and y-centroidal axes, respectively (in.^{4});

J_c = St. Venant torsional constant of the flange-edge stiffener (in.^{4}).

In evaluating the load-carrying capacity of Z-sections, failure by lateral buckling about the weak principal axis or failure by torsional buckling, must be checked. Thus, σ_{dcr} in Equations 3.7 and 3.8 is either the critical stress

corresponding to member instability (lateral or torsional buckling) or the distortional buckling stress (Equation 3.27), whichever is smaller.

3.4.2 Beam Model

The bending capacity of the beam was limited by the distortional buckling capacity with no post-buckling strength taken into account; i.e,

$$M_{cr} = S_x \sigma_{cr} \tag{3.32}$$

where,

M_{cr} = bending capacity of Z-section beams (kips-in.);

S_x = elastic section modulus of the gross cross sectional area with respect to the geometric x-axis (in.^{3});

σ_{cr} = critical stress of the compressive fibre flange which is caused by the distortional buckling stress of the equivalent column and is taken the inelastic stress using the CRC curve (Jhonston, 1976), Equations 3.7 and 3.8 (ksi).

The distortional buckling stress of the equivalent column was taken as the critical stress at its geometric centroid. The critical stress, at the outer compressive fibre of the beam, was then computed as the product of this distortional buckling stress and the distance from the neutral axis of the beam to its outer compressive fibre, divided by the distance from the neutral axis to the centroid of the equivalent column. The simplified expressions, therefore, lead to the following:

$$\sigma_{dcr} = \frac{\sigma_c d_c}{d} \tag{3.33}$$

where,

σ_{dcr} = elastic critical stress at the outer compressive fibre of the section (ksi);

d_c = distance from the neutral axis of the section to its extreme compressive fibre (in.);

d = distance from the neutral axis of the section to the centroid of the equivalent column (in.).

and,

σ_c = elastic distortional buckling stress of the equivalent column defined as:

$$\sigma_c = \frac{E}{2A_c}\left[(\alpha_1+\alpha_2) - \sqrt{(\alpha_1+\alpha_2)^2 - 4\alpha_3}\ \right] \tag{3.34}$$

where,

$$\alpha_1 = \frac{\eta}{\chi_1}\left(\chi_2 + \frac{GJ_c}{E\eta}\right) + \frac{k_\phi}{\chi_1 E\eta} \tag{3.35}$$

$$\alpha_2 = \eta\left(I_{cy} - \frac{2y_{co}\chi_3}{\chi_1} + \frac{I_{cy}y_{co}^2}{\chi_1}\right) \tag{3.36}$$

$$\alpha_3 = \eta\left(\alpha_1 I_{cy} - \frac{\eta\chi_3^2}{\chi_1}\right) \tag{3.37}$$

$$\chi_1 = h_x^2 + \frac{I_{cx}+I_{cy}}{A_c} \tag{3.38}$$

$$\chi_2 = C_w + I_{cx}(x_{co}-h_x)^2 \tag{3.39}$$

$$\chi_3 = I_{cxy}(x_{co}-h_x) \tag{3.40}$$

$$\chi_4 = \chi_2 + (y_{co}-h_y)\left(I_{cy}(y_{co}-h_y)-2\chi_3\right) \tag{3.41}$$

$$\lambda = \pi\left(\frac{E\chi_4}{k_\phi}\right)^{\frac{1}{4}} \tag{3.42}$$

$$k_\phi = \frac{Et^3}{4w} \tag{3.43}$$

$$\eta = \left(\frac{\pi}{\lambda}\right)^2 \tag{3.44}$$

where,

A_c = gross cross sectional area of the equivalent column (in.^{2});

I_{cx}, I_{cy} = moments of inertia of the component with respect to the geometric x- and y-axes (in.^{4}), respectively;

I_{cxy} = product moment of inertia of the component with respect to the geometric x- and y-centroidal axes (in.^{4});

J_c = St. Venant torsional constant of the equivalent column (in.^{4});

C_w = torsional warping constant of the equivalent column (in.^{6});

x_{co}, y_{co} = x- and y-coordinates of the shear centre of the equivalent column (in.), respectively;

h_x, h_y = as shown in Figure 3.3;

3.4.3 Beam-Column Model

To obtain the load-carrying capacity of Z-section beam-columns, the simplified expressions developed for columns and beams were used in a strength interaction equation as follows:

$$\frac{P/A}{P_{cr}/A} + \frac{M_x/S_x}{M_{cr}/S_x} \leq 1.0 \tag{3.45}$$

or,

$$\frac{P}{P_{cr}} + \frac{M_x}{M_{cr}} \leq 1.0 \tag{3.46}$$

where,

P = applied axial load (kips);

P_{cr} = distortional compressive load in the absence of any bending computed according to Equation 3.26 (kips);

M_x = applied moment with respect to the geometric x-axis (kips-in.);

M_{cr} = critical moment with respect to the geometric x-axis, in the absence of any axial loads, computed according to Equation 3.32 (kips-in.).

In the experimental study, the bending moment was created by the eccentric application of the axial load. This load was applied along the web at a distance e_y from the centroid of the section. Thus,

$$M_x = Pe_y \tag{3.47}$$

where,

e_y = distance of the eccentrically loading location with respect to the centroid (in.).

Substituting Equation 3.47 into Equation 3.46 and rearranging the terms by considering the load level at which a structure becomes unstable, the eccentric load (P) of the beam-columns can be obtained as follow:

$$P = \frac{P_{cr}}{1 + \frac{e_y P_{cr}}{M_{cr}}} \tag{3.48}$$

An alternative interaction equation would be to use a quadratic function, instead of the linear function represented by Equation 3.45. The strength interaction equation would then be expressed as:

$$\left(\frac{P/A}{P_{cr}/A}\right)^2 + \left(\frac{M_x/S_x}{M_{cr}/S_x}\right)^2 \leq 1.0 \tag{3.49}$$

or,

$$\left(\frac{P}{P_{cr}}\right)^2 + \left(\frac{M_x}{M_{cr}}\right)^2 \leq 1.0 \tag{3.50}$$

Substituting Equation 3.47 into Equation 3.50 and rearranging the terms by considering the load level at which a structure becomes unstable, the eccentric load of the beam-columns (P) can be computed as follow:

$$P = \frac{P_{cr}}{\sqrt{1 + \left(\frac{e_y P_{cr}}{M_{cr}}\right)^2}} \tag{3.51}$$

As in the case of columns and beams, the load-carrying capacity of beam-columns obtained from Equations 3.48 and 3.49, does not take into account the post-buckling capacity of the sections.

CHAPTER 4

FINITE ELEMENT ANALYSIS

The ANSYS finite element analysis program developed by Swanson Analysis system, Inc., (1979) is based on classical engineering concepts. Through proven numerical techniques, these concepts can be formulated into matrix equations that are suitable for analysis using the conventional finite element method.

The system to be analyzed is presented by a mathematical model consisting of discrete regions (elements) connected at a finite number of points (nodes). The primary unknowns in an analysis are the degrees of freedom for each node in the finite element model. Degrees of freedom may include displacements, rotations, and are defined by the elements attached to the node. Corresponding to the degrees of freedom, a stiffness matrix is generated, as appropriate, for each element in the model. The element matrices are then assembled to form a set of simultaneous equations that can be processed in the solution phase.

The program's solution phase uses the frontal method to solve this set of equations. The frontal solution procedure simultaneously assembles and solves an overall stiffness matrix from the individual element matrices. This procedure progressively moves through the model, element by element, introducing the equations corresponding to the particular element degrees of freedom. At the same time, degrees of freedom are solved and deleted (using Gaussian elimination) from the matrix as soon as possible. The degree of freedom set present in the assembled

matrix is known as the wavefront, which expands and contracts as degrees of freedom are introduced to and deleted from the matrix.

The ANSYS finite element analysis program is based on a governing equation constructed by using an appropriate mathematical relation of stiffness matrix. The following sections discuss the applicability of the ANSYS finite element analysis program to the case of cold-formed steel Z-section members. The general corresponding finite element formulations are also presented in the discussion. The primary objective of using the finite element analysis in this study was to determine how the ANSYS finite element analysis program would predict the failure mode and the buckling capacity of various Z-sections tested.

4.1 QUADRILATERAL SHELL ELEMENT

The analysis is based on the four-node quadrilateral shell finite element depicted in Figure 4.1. The element has six degrees of freedom at each node: translations in the nodal x, y, and z directions and rotations about the nodal x, y, and z axes. The nodal displacements are shown in Figure 4.1 as u, v, and w. This element has both bending and membrane capabilities. Therefore, there are stiffness matrices for membrane action and bending in the analysis. For the membrane analysis, 2 x 2 integration points are used and shape functions are expressed as:

$$u = \frac{1}{4}\left[u_I(1-s)(1-t) + u_J(1+s)(1-t) + u_K(1+s)(1+t) + u_L(1-s)(1+t)\right] \tag{4.1}$$

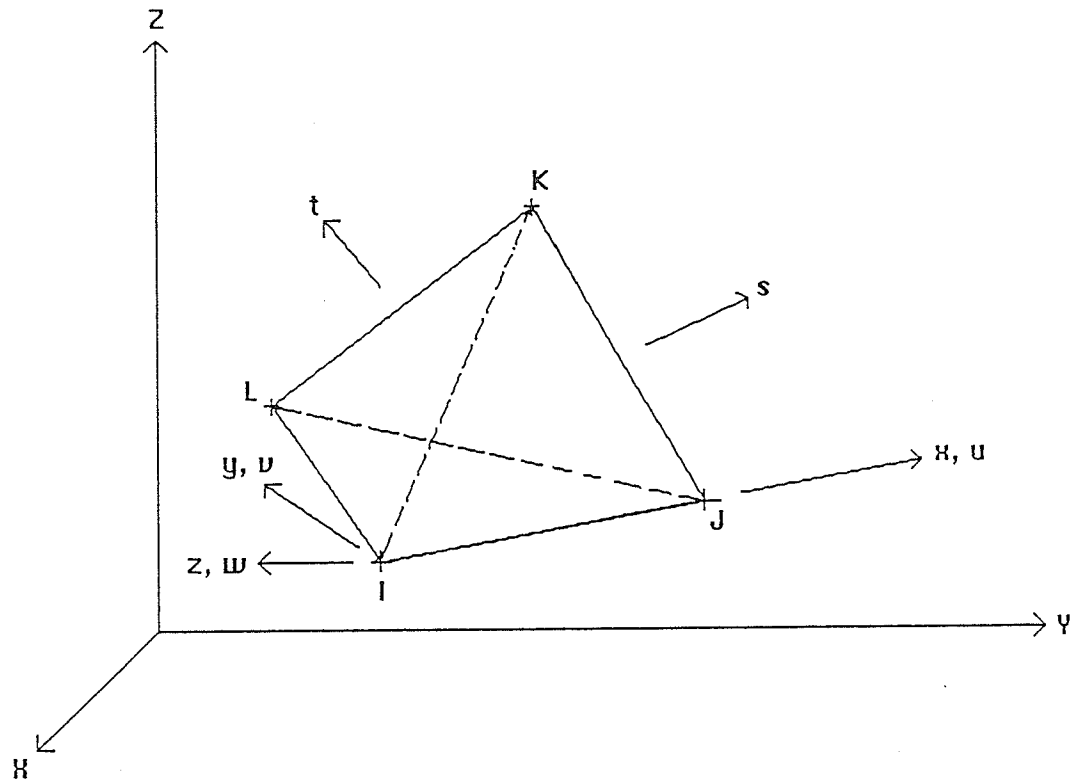

Figure 4.1 Relative Four-Node Quadrilateral Shell Element

where,

U_I, U_J, U_K, and U_L = u-displacement (in x-direction) of nodes I, J, K, and L;

s, t = element coordinates.

For the bending analysis, four triangles are used for shape functions. These triangles are overlaid as shown in Figure 4.1 Nodes I, J, and K are connected to from a triangle. The remaining triangles connect nodes I, J, L, nodes K, L, I, and nodes K, L, J. Three integration points are used for each triangle.

The four-node quadrilateral shell finite element of an orthotropic material the stress is related to the strains by:

$$(\sigma) = [D](\epsilon) \tag{4.2}$$

where,

(σ) = stress vector;

[D] = elasticity matrix;

(ϵ) = strain vector.

In evaluating the nodal and centroidal stresses, the element integration point stress equation is expressed as:

$$(\sigma) = [D][B](u) \tag{4.3}$$

where,

[B] = the strain-displacement matrix, which is based on the element shape functions, must be evaluated at each integration point;

(u) = nodal displacements vector.

The stresses are calculated using interpolation of the integration point stresses in the element natural coordinate system. Triangles type of geometries with three integration points are used to determine the stresses where the assumed stress variation is expressed as:

$$\sigma_i = a + bs + ct \tag{4.4}$$

where,

σ_i = assumed stress variation;

a, b, c = coefficients.

In the current configuration of the quadrilateral element, a least squares fitting procedure for the bending stresses was applied by using data from all three integration points of each of the four triangles.

4.2 NONLINEAR BUCKLING ANALYSIS

The analysis type is important for determining the stability of any load-carrying structure. Stability analysis is used to determine either the load level at which a structure becomes unstable or a structure is stable at a particular load level. Two types of stability analyses are available in the ANSYS finite element analysis program: linear (eigenvalue) buckling and nonlinear buckling. The nonlinear buckling is the one that was used in the study of the behaviour and capacity of Z-section members.

To determine buckling loads more accurately, nonlinear buckling analysis should be used. Nonlinear buckling analysis is essentially an application of large deflection which will be described in the following section of "Nonlinearities". This nonlinear buckling analysis also includes a snap-through analysis where the structure reaches a second stable state after buckling if the load continues to increase.

4.3 NONLINEARITIES

Nonlinearlities cause the response of a structure or component to vary disproportionately with the applied forces. Realistically, all structures are nonlinear in nature, but not always to a degree that the nonlinearities have a significant effect on an analysis. However, if the analyst determines that nonlinearities affect the behaviour of a structure to the extent that they cannot be ignored, a nonlinear analysis is required.

The ANSYS finite element analysis program carries out nonlinear buckling analyses by performing a series of successive linear approximations. Each linear approximation requires one pass, or iteration, through the equation solver. In a nonlinear buckling analysis, the structure's stiffness matrix and/or load vector varies with the applied load and is therefore unknown. To solve the problem, the ANSYS finite element analysis program uses an incremental procedure based on the Newton-Raphson method, in which a series of linear iterations converges to the actual nonlinear solution.

The number of iterations in the solution process can be specified by either the user or default. Because the number of iterations needed to approach convergence is usually not known, a convergence checking feature is available in the program. Convergence checking compares the results of each iteration with the previous iteration. If the change from one iteration to the next is judged to be insignificant, the ANSYS finite element analysis program considers the solution to be converged and stops the iterative process.

In this nonlinear buckling analysis, two types of nonlinearities are used. These nonlinearities are classified into two categories: material and geometric which are discussed in the following sections.

4.3.1 Material Nonlinearities

A material nonlinearity exist when stress is not proportional to strain. The ANSYS finite element analysis program can simulate both nonlinear stress/strain relationships (plasticity and nonlinear elasticity). This is accomplished by using the Newton-Raphson method, in which the stiffness matrix is updated each iteration to form the tangent stiffness matrix.

The Newton-Raphson equation is as follows:

$$[K_T](\Delta u) = (F) - (F^{el}) \tag{4.5}$$

where,

$[K_T]$ = the tangent stiffness matrix;

(Δu) = the nodal displacement increment vector;

(F) = the forcing function;

(F^{el}) = the elastic load vector.

To fully account for plastic material behaviour in an analysis, three important concepts have been considered: the yield criterion, the flow rule, and the hardening law. The yield criterion describes the three-dimensional stress state by computing a single-valued equivalent stress, which is compared against the uniaxial yield strength to determine when the material will yield. The flow rule predicts the direction in which yielding will occur. The hardening law, which is applicable to materials that strain-harden, describes how the yield surface expands or changes as yielding progresses.

The ANSYS finite element analysis program uses the von Mises yield criterion to predict when yielding will begin. For equivalent stress this criterion is as follows:

$$\sigma_{eq} = \sqrt{\frac{1}{2}\left[(\sigma_1 - \sigma_2)^2 + (\sigma_2 - \sigma_3)^2 + (\sigma_3 - \sigma_1)^2\right]} \qquad (4.6)$$

where,

σ_1, σ_2, and σ_3 = the principal stresses which are calculated from the stress components by the cubic equation.

Yielding begins when $\sigma_{eq} = F_y$, the uniaxial yield strength.

The flow rule used in the ANSYS finite element analysis program is associated with the von Mises yield criterion so that the increment in plastic strain

is normal to the yield surface. This associated flow rule is based on the Prandtl-Reuss flow equation:

$$(d\epsilon^{pl}) = \lambda\left(\frac{\partial Q}{\partial \sigma}\right) \tag{4.7}$$

where,

λ = the multiplier determining the amount of plastic strain;

Q = a function of stress (termed the plastic potential) determining the direction of plastic strain.

The flow rule is associative (that is, Q is the yield function) for all yield criteria in the ANSYS finite element analysis program.

Hardening laws determine how a material's yield surface is changed once the material has been loaded into its plastic range. In strain hardening materials, subsequent reloading will cause the material to yield again only if the load exceeds the previous stress level. Two kinds of hardening laws are presented in the ANSYS finite element analysis program: isotropic hardening and kinematic hardening. Isotropic hardening describes a yield surface which expands the same in all directions, and implies that an increase in tensile yield stress results in an equal increase in compressive yield stress. Kinematic hardening, which is more realistic, predicts an increase in tensile yield stress, and produces a corresponding decrease in compressive yield strength. Therefore, a material that was initially isotropic will become anisotropic after yielding. This is known as the Bauschinger effect.

A particular combination of yield criterion, flow rule, and hardening law describe a unique material behaviour. To use the ANSYS finite element program

for the analysis of cold-formed steel members, the Classical Bilinear Kinematic Hardening procedure was used. Classical Bilinear Kinematic Hardening describes general metallic materials that are considered to be bilinear, having one elastic and one plastic slope. This option is applicable to most common, initially isotropic, engineering meterials. The von Mises yield criterion was also used, as well as the Prandtl-Reuss flow equations. Kinematic hardening accounts for the Bauschinger effect. In the present study, this kinematic hardening (Plastic material behaviour) was applied to the cold-formed steel Z-sections through the explicit use of established nonlinear stress/strain relationships. Two stress/strain relationships were used, one for the corner portions and the other for the flat portions of members. These stress/strain relationships, shown as curves A and B of Figure 4.2, provide the yield strength of the material at the corners and the flat portions of members, 75 and 50 ksi, respectively.

4.3.2 Geometric Nonlinearities

Geometric nonlinearities occur when the displacements of a structure significantly change its stiffness. The ANSYS finite element analysis program can account for these types of geometric nonlinear effects using large deflection and stress stiffening concepts.

Large deflection presents a change in stiffness resulting from a change in element spatial orientation as the structure deflects. In general, the ANSYS finite element analysis program solves large deflection problems by updating the element

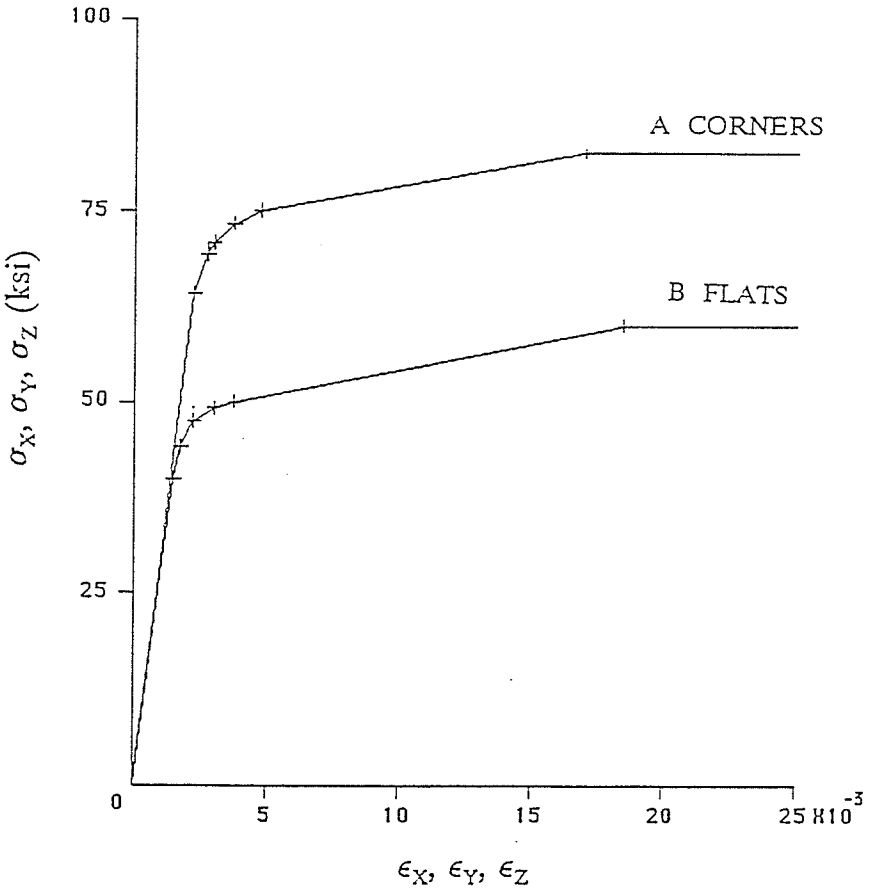

Figure 4.2 The Explicit Stress/Strain Relationships Used in the ANSYS Program

orientations as the structure deflects. Since the stiffness is affected by the displacements, an iterative solution is required to solve for changes in stiffness at each iteration. The ANSYS finite element analysis program uses an incremental Newton-Raphson procedure based on an updated tangent stiffness matrix:

$$[K]_{i-1}(\Delta u)_i = (F) - (F^{el})_{i-1} \tag{4.8}$$

where,

$[K]_{i-1}$ = the stiffness matrix based on deformed geometry from the (i-1) iteration;

$(\Delta u)_i$ = the incremental displacement vector,

$(u)_i = (u)_{i-1} + (\Delta u)_i$;

$(u)_i$ = the displacement vector at the current iteration;

(F) = the applied force vector;

$(F^{el})_{i-1}$ = the elastic force vector based on displacement for iteration (i-1).

With each iteration, Δu becomes smaller and smaller as the successive iterations converge to the solution. The ANSYS finite element analysis program's optional convergence checking feature can be used to stop the iterative process when Δu becomes smaller than the user-specified or the default criterion.

Stress stiffening, also known as geometric stiffening, accounts for an increase or decrease in structural stiffness based on the stress state. This analysis option is also applied to the case of cold-formed steel members since this type of structures is weak in bending resistance.

The ANSYS finite element analysis program uses the stress state of a structure to calculate a stiffness matrix, [S], which is added to the normal stiffness matrix, [K], to solve for the new displacements. Accordingly, the governing equation for a static analysis using stress stiffening is:

$$[\,[K] + [S]\,](u) = (F) \tag{4.9}$$

where,

[[K]+[S]] = the tangent stiffness matrix based on deformed geometry.

In summary, the governing equation for a nonlinear buckling analysis of cold-formed steel Z-section in the present study is:

$$\left[\,[K_T] + [S_T]\,\right]_{i-1} (\Delta u)_i = (F) - \left(F^{el}\right)_{i-1} \tag{4.10}$$

where,

$[\,[K_T]+[S_T]\,]_{i-1}$ = the tangent stiffness matrix based on deformed geometry from the (i-1) iterations.

4.4 MODELLING OF SECTIONS

The analysis of three cold-formed Z-sections was carried out using an educational version of the ANSYS program operated by using the VAX/VMS system computer station at the Interactive Graphic Computer Facility of The University of Manitoba. Three types of section were analyzed: a column, a beam, and a beam-column section. The residual stresses of the sections were not taken into consideration in the analysis of these sections. To prevent local distortion at point

of concentrated nodal loads at the end supports of these sections, the thickness of the elements at each end, was increased from 0.059 to 0.59 inches. Also, to prevent a rigid body rotation of the sections about their longitudinal axes, a roller support was used at each flange-web junction of the end supports, as shown in Figure 4.3. The loading factor obtained from the ANSYS analysis was used to compute the failure load of these sections. The modelling of the sections and their results are discussed in the following sections.

4.4.1 Column Section

An 18 inch specimen with 0.25 inch flat width of edge stiffeners, 1.5 inch flat width of flanges, and 4.0 inch flat width of web element, was chosen for the analysis. To simulate the pin-ended condition, where shortening of the member is permitted only in the longitudinal direction, a roller at one end and a simple support at the other end, located at the centroid of the cross section, were assumed. A unit axial load was applied on the roller end support at the centroid of the cross section. The finite element mesh of the section, for an input data batch file, is shown in Figure 7.3. The modelling of the same section produced by the ANSYS program prior to the analysis is shown in Figure 4.4.

The deformed configuration of the section produced by the ANSYS program is shown in Figure 4.5. The failure mode of the cross section was by distortional buckling of the flange-edge stiffener component, as shown in Figure 4.6. The predicted load of this section was 14.3 kips, compared to the experimental value of

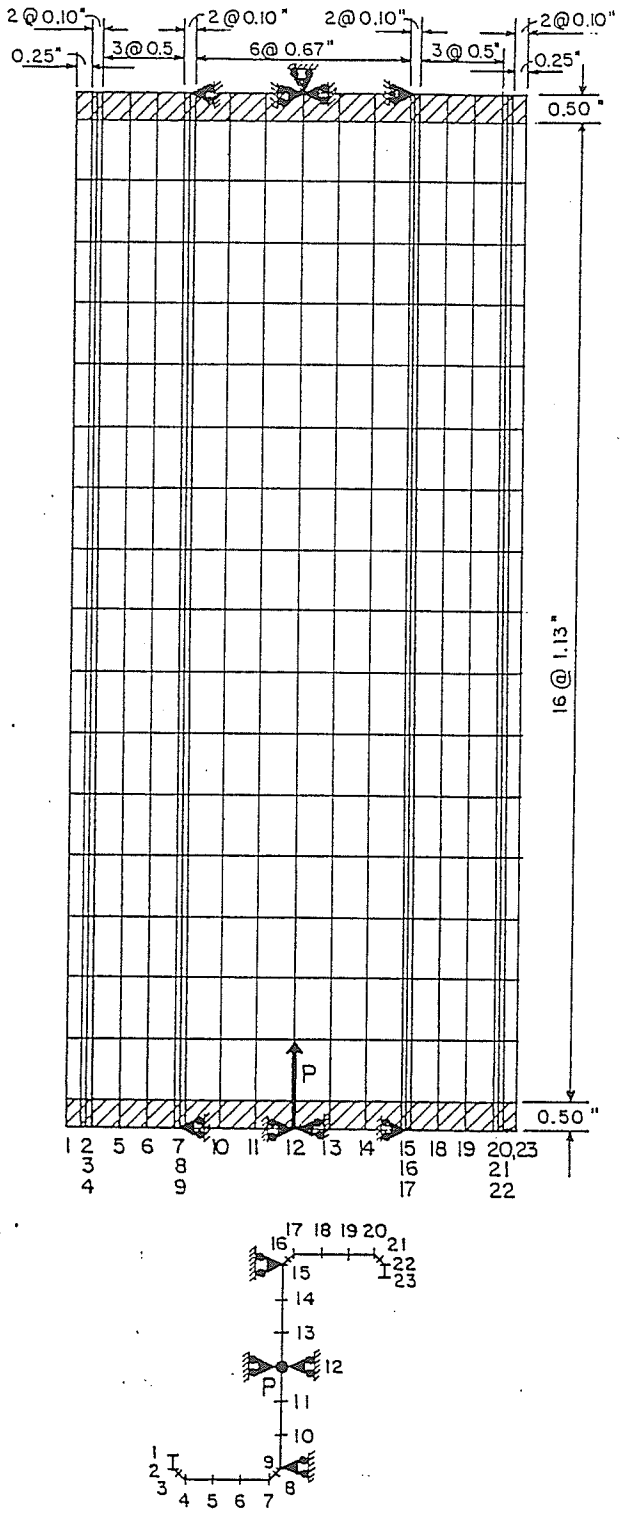

Figure 4.3 The Finite Element Mesh of Column Section

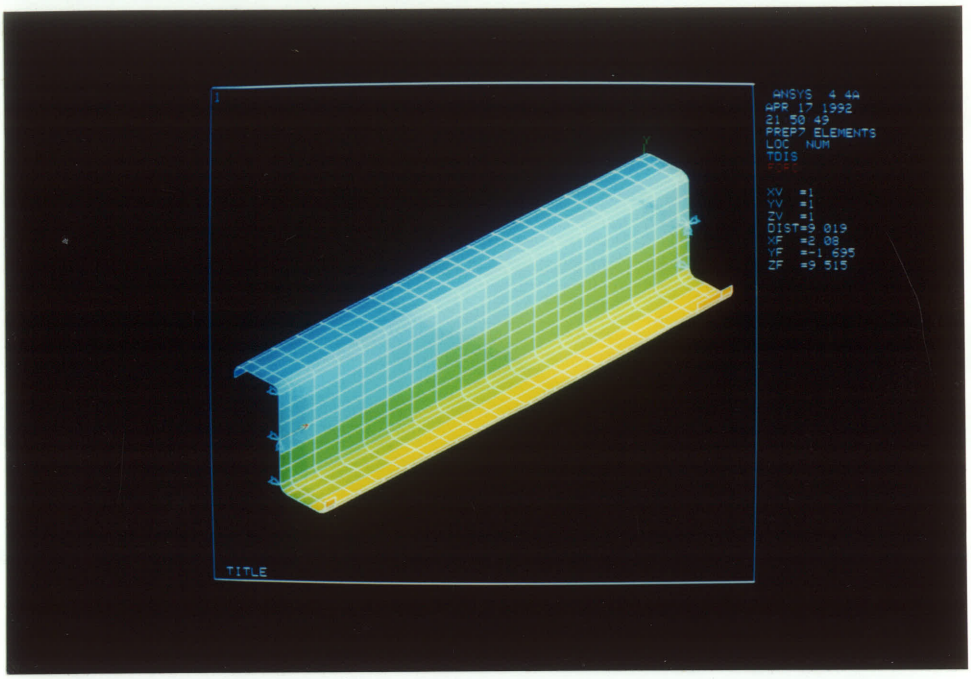

Figure 4.4 ANSYS Modelling of the Column

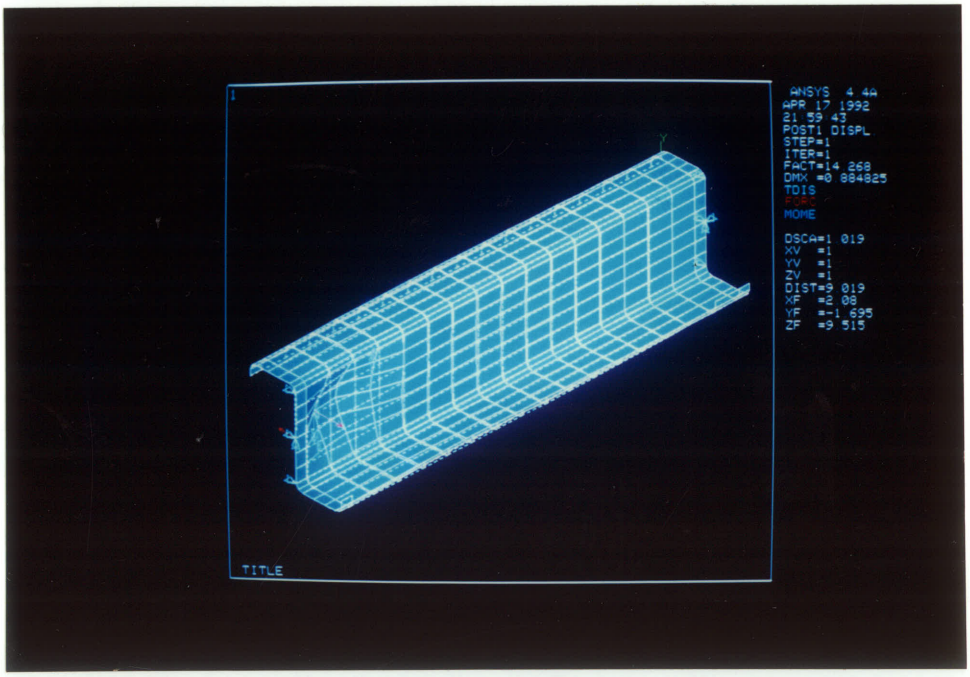

Figure 4.5 The Deformed Configuration of the Column

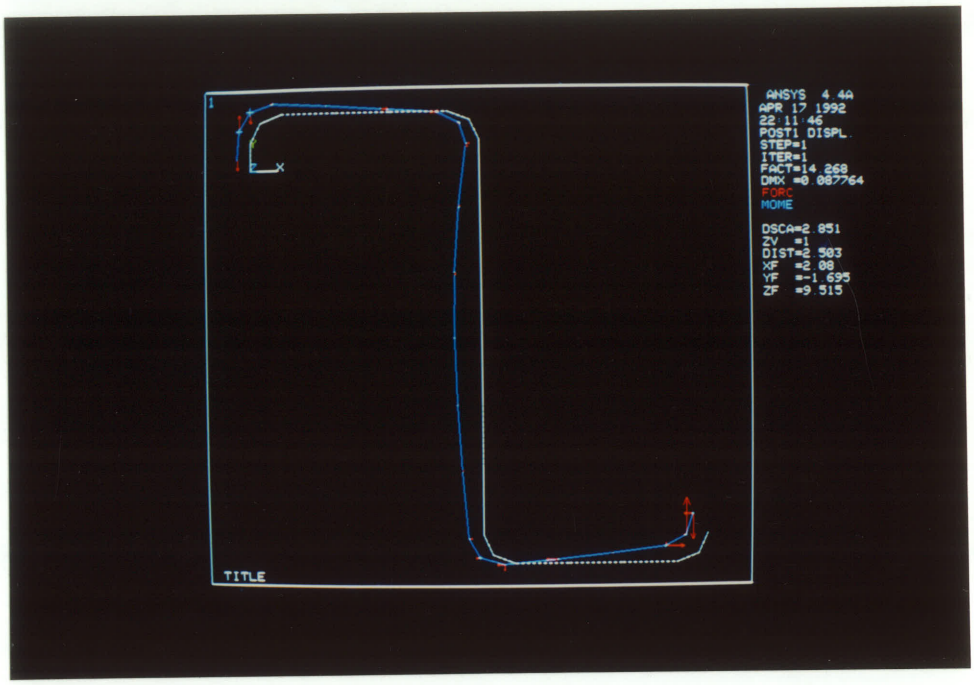

Figure 4.6 The Failure Mode of the Cross Sectional Column

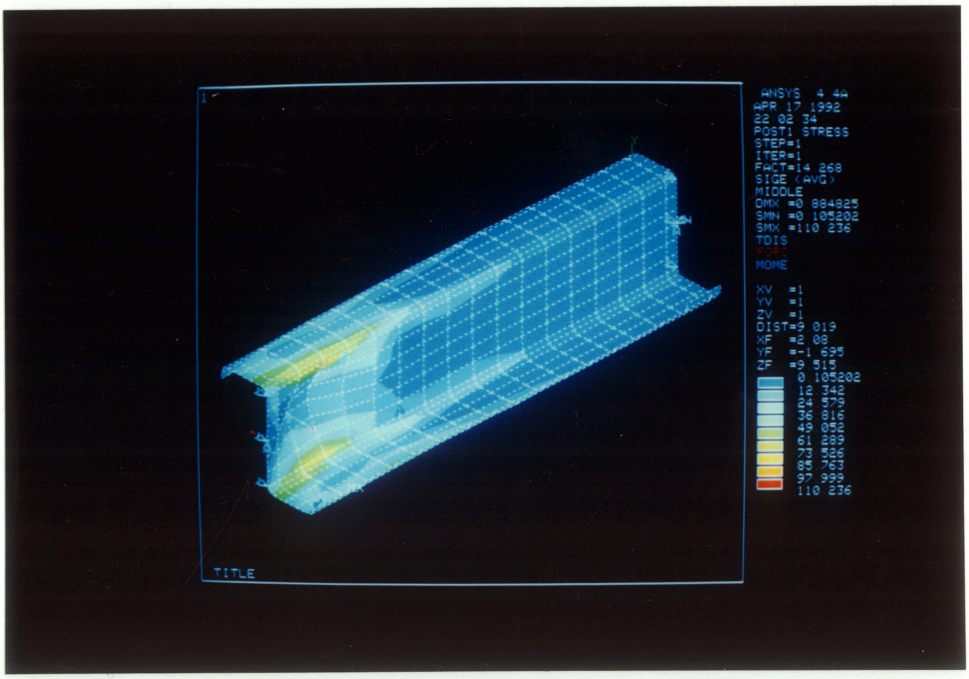

Figure 4.7 The Stress Distribution of the Column

17.5 kips. The difference in the results could be attributed to the fact that the ANSYS analysis does not take into account the post-buckling strength of the section.

The stress distribution in this member is shown in Figure 4.7. The level of the distributed stresses is presented by the tone of colours. The darker the colours, the higher the stress level. As shown in this figure, the highest stress level appears to be at the corners or the junctions of the section which is in good agreement with the basic elastic theory described by Winter (1959).

4.4.2 Beam Section

A 54 inch specimen with 0.75 inch flat width of edge stiffeners, 2.7 inch flat width of flanges and 7.7 inch flat width of web element, was chosen for this analysis. To simulate the pin-ended condition used in the actual test set-up of the experimental investigation, a simple support at the centroid of the cross section was assumed to act at one end and a roller support was assumed to act at the other end. These supports were used to allow for shortening of the member in the longitudinal direction. Also, to simulate the lateral supports used in the test set-up to brace the Z-section against twisting, three roller supports were applied on the plane of the web, at midspan and at a distance of 14.25 inches from each end of the member, as shown in Figure 4.8. The loads were applied at the third points, located 14.25 inches from each end of the member. The finite element mesh of section, for an input data batch file, is shown in Figure 4.8, while the modelling of section produced by the ANSYS program prior to the analysis is shown in Figure 4.9. The deformed

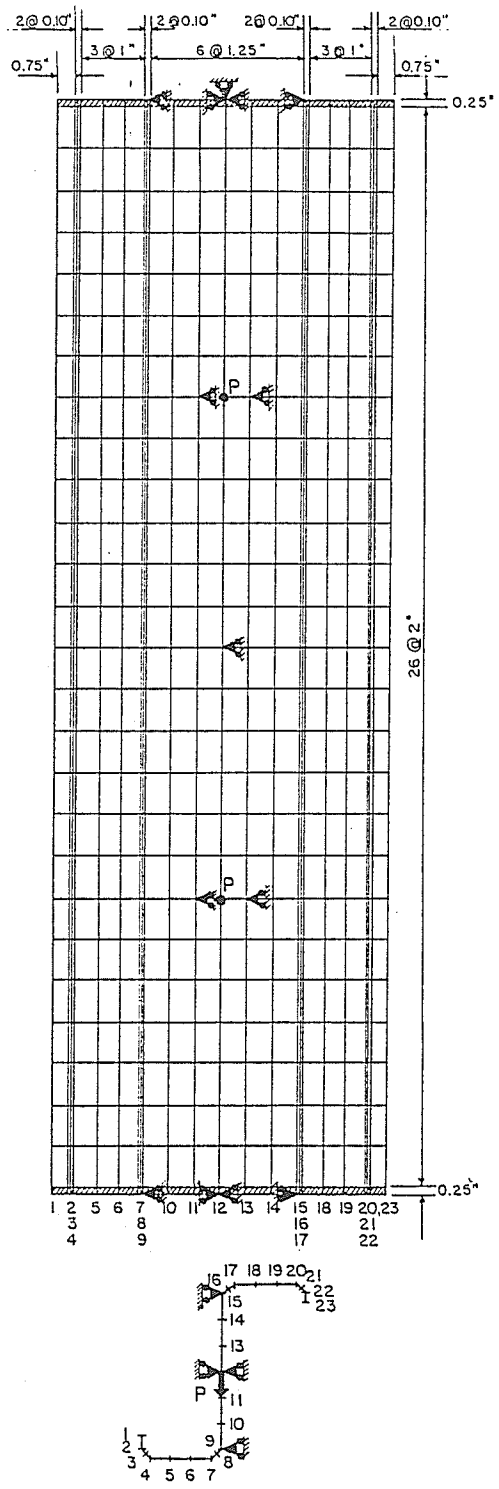

Figure 4.8 The Finite Element Mesh of Beam Section

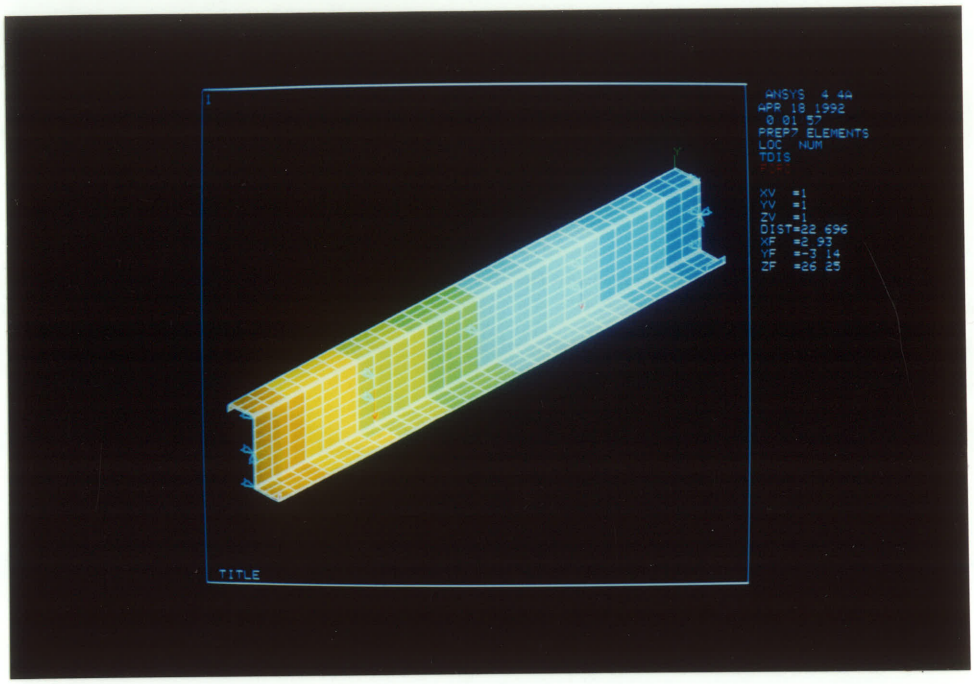

Figure 4.9 ANSYS Modelling of the Beam

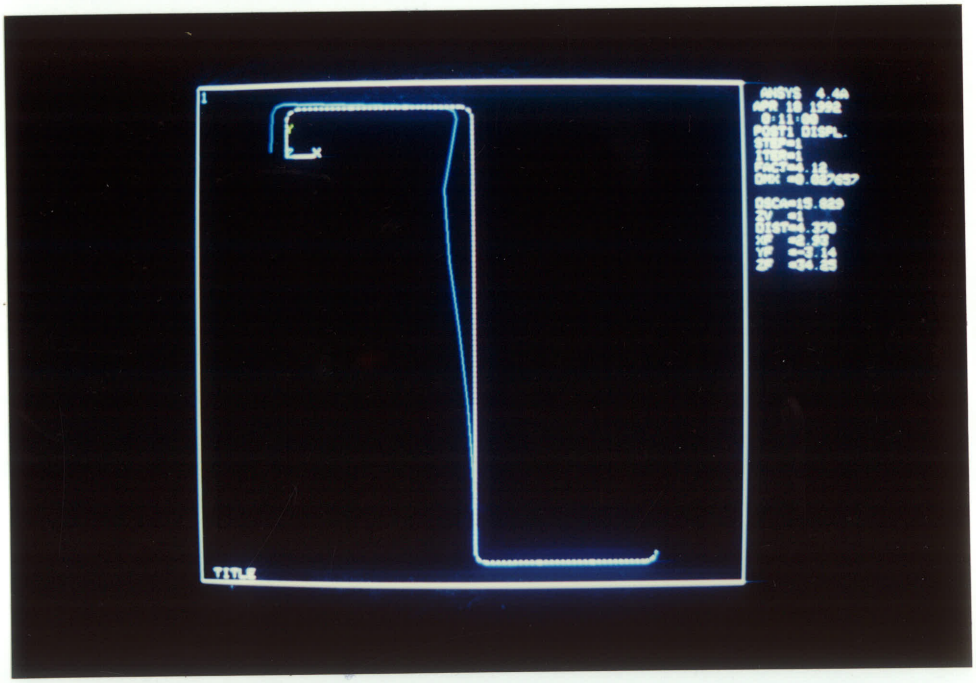

Figure 4.10 The Failure Mode of the Cross Sectional Beam

cross sectional configuration of the member, shown in Figure 4.10, indicates that distortional buckling of the flange-edge stiffener component took place. The computed bending capacity of the member was 58.7 kips-in., compared to 58.8 kips-in. measured during testing. The ANSYS result in remarkably close to the experimental result.

4.4.3 Beam-Column Section

A 24 inch specimen was used in this case. This section had 0.75 inch flat width of edge stiffeners, 2.7 inch flat width of flanges and 7.7 inch flat width of web element. To simulate the pin-ended condition, where shortening of the member is permitted only in the longitudinal direction, a roller at one end and a simple support at the other end, located at the centroid of the cross section were used, as shown in Figure 4.11. Also shown in this figure, A unit axial load was applied on the roller end support, at one of the web-flange junctions, while the modelling of section produced by the ANSYS program is shown in Figure 4.12. The deformed configuration of the cross section, shown in Figure 4.13, indicates that in the beam-column section, as in the case of the column and the beam members, distortional buckling of the flange-edge stiffener component took place. The predicted capacity was 5.9 kips, compared to 9.2 kips measured during testing.

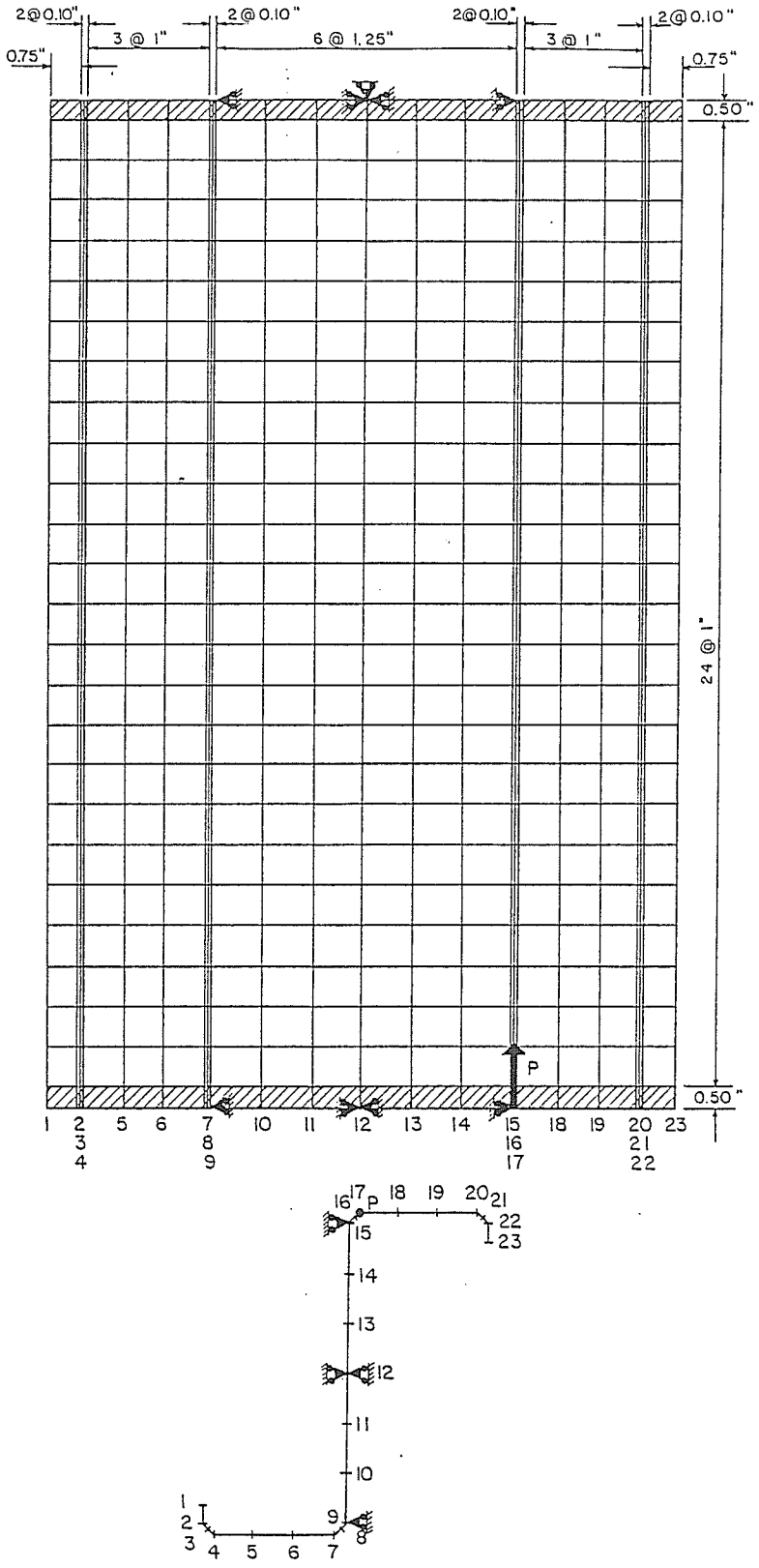

Figure 4.11 The Finite Element Mesh of Beam-Column Section

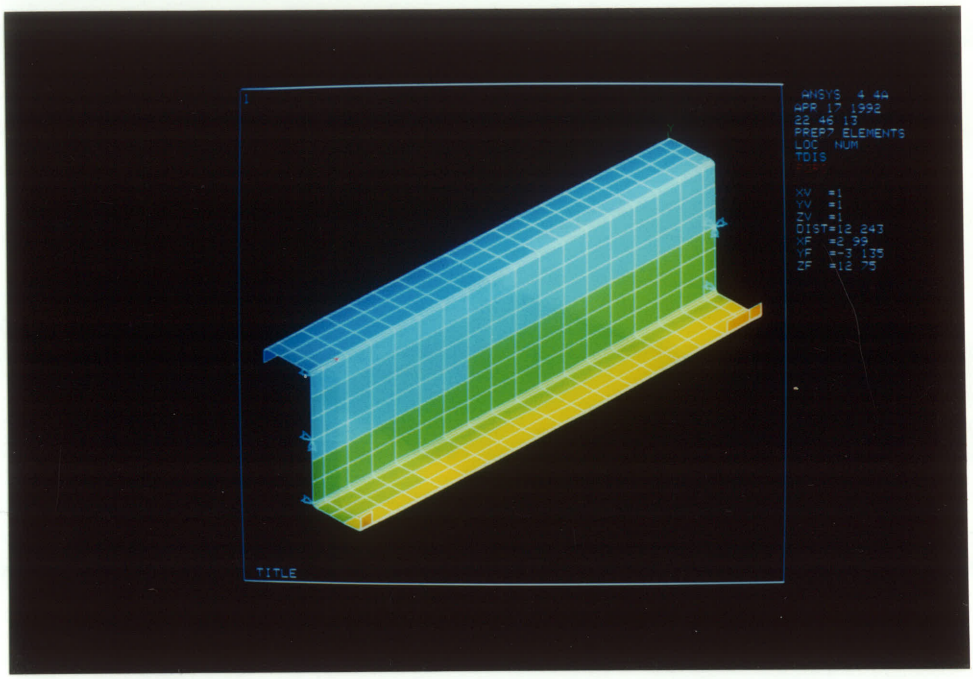

Figure 4.12 ANSYS Modelling of the Beam-Column

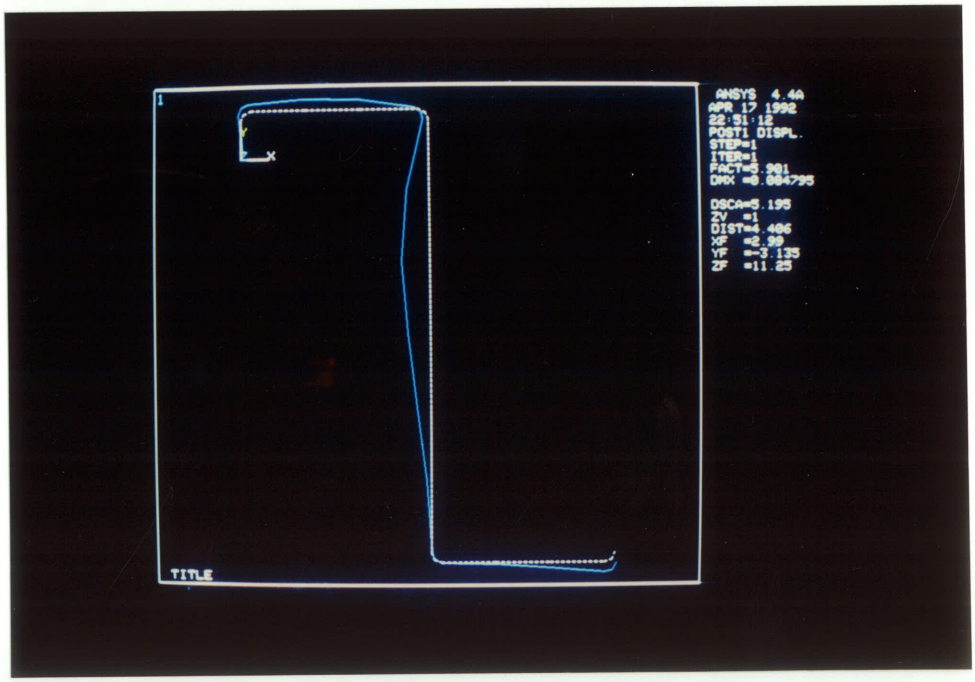

Figure 4.13 The Failure Mode of the Cross Sectional Beam-Column

CHAPTER 5

EXPERIMENTAL INVESTIGATION

An experimental investigation of the effect of partially stiffened flanges on the behaviour of cold-formed sections was carried out by Mulligan (1983). Using channel sections, Mulligan pointed out that the flange-edge stiffener component of the sections collapsed suddenly due to distortional buckling. In these cases, the sections showed little post-buckling strength.

Sudharmapal (1988) conducted on experimental investigation involving cold-formed Z-sections loaded in direct compression. An important parameter in the tests was the angle between the edge stiffener and the flange. The specimens were designed in such a way as to preclude web buckling prior to flange buckling. The experimental results were in good agreement with the results predicted by the AISI Specification (1986).

Purnadi (1990) extended Sudharmapal's work and investigated cold-formed Z-section steel members subjected to combined axial load and bending. Purnadi's research showed that the edge stiffener angle had a direct influence on the behaviour of the Z-sections. The experimental results showed that for Z-sections whose web was not subject to local buckling, edge stiffener angles greater than 30 degrees ensured adequate stiffening against distortional buckling.

The distortional buckling of cold-formed steel Z-section columns was also studied by Rosner et al (1989) who carried out an experimental investigation on Z-

sections with edge stiffeners transverse to the flanges. That investigation was extended by Martens et al (1989) to cover sloping edge stiffeners and angled edge stiffeners. Le et al (1990) extended Rosner's work to cover sections susceptible to local buckling of the web element.

An extensive review of the literature has shown that there is limited experimental information on the distortional buckling behaviour of cold-formed steel Z-sections. The behaviour of such sections with the web-flange buckling interaction has not been adequately addressed in the design specifications (AISI, 1989 and CSA, 1989). The need to study this interaction, a behavioral phenomenon which is missing in the design specifications, is significant. The present experimental investigation thus is designed to study the distortional buckling of cold-formed steel Z-sections susceptible to local buckling of the web element.

5.1 TEST SPECIMENS

The test specimens were made from a cold-formed steel sheet with a nominal thickness of 0.059 inches. The specimens were manufactured in a commercial fabrication shop by shearing the flat sheet to the correct width and length and then forming it to the desired Z-section configuration, using a press-break. The dimensions of specimens were specified within the tolerance of 1%. The imperial unit was used throughout the experimental program.

A typical Z-section specimen is shown in Figure 5.1. A three-part specimen designation system was used. For example, specimen 1.5-1.0-1 has a nominal flat

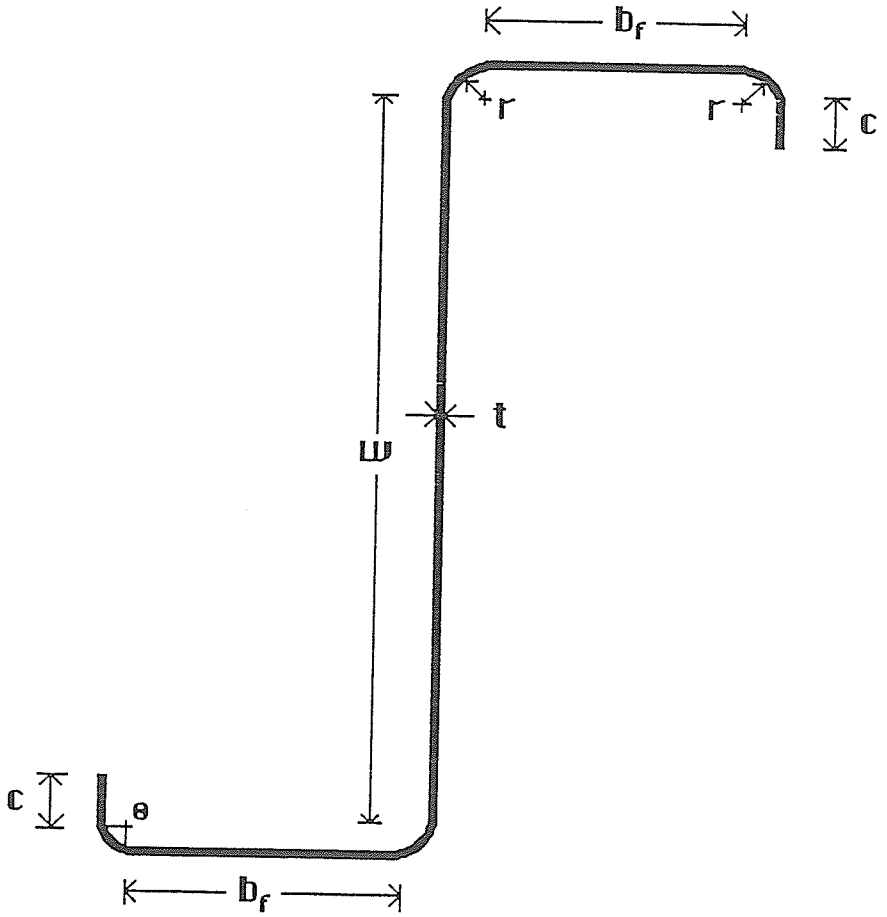

t = thickness
w = flat width of web
b_f = flat width of flange
c = flat width of edge stiffener
r = centerline radius (flange-web or flange-edge stiffener junctions)
θ = angle (flange-edge stiffener junction)

Figure 5.1 Typical Cross Section

width of flange, b_f, of 1.5 inches, and a nominal flat width of edge stiffener, c, of 1.0 inch. The last term, 1, identifies the specimen within its category.

A complete list of the parameters used, along with the number of specimens tested in each category, is given in Table 5.1. In the table, column (8) shows a group of specimens with unstiffened flanges. In these specimens there was no curved portion of edge stiffeners. Column (9) shows a group of specimens where the edge stiffeners had only a curved portion and no flat width. The sections tested are typical of those used in practice, except that the dimensions of the edge stiffeners were purposely varied to determine the effect of distortional buckling on the behaviour of the section.

Of the 123 specimens, 85 were tested as columns under concentric loading, 20 were tested as beams under pure bending, and 18 were tested as beam-columns under eccentric axial loading. The column specimens were grouped into three categories with lengths, of 18, 24, and 48 inches. For the 18 inch specimens, the total number of specimens considered was: (3 different flanges) x (5 different edge stiffeners) x (3 specimens) = 45 specimens. For the 24 and 48 inch specimens, the total number of specimens was: (1 flange) x (10 different edge stiffeners) x (2 specimens) = 20 specimens. The beam specimens were 54 inches long and the total number was: (1 different flange) x (10 different edge stiffeners) x (2 specimens) = 20 specimens. The beam-column specimens had lengths of 24 and 48 inches. For each length, the total number of specimens was: (1 different flange) x (9 different edge stiffeners) x (1 specimen) = 9 specimens.

TABLE 5.1 List of Test Variables and Number Specimens Tested
(Numbers in Brackets Indicate Numbers of Specimens Tested)

Specimen Type	L	θ	r	t	w	b_f	c (in.)									
	(in.)	(°)	(in.)	(in.)	(in.)	(in.)	-	0.00	0.15	0.25	0.50	0.75	1.00	1.25	1.50	2.00
(1)	(2)	(3)	(4)	(5)	(6)	(7)	(8)	(9)	(10)	(11)	(12)	(13)	(14)	(15)	(16)	(17)
Columns	18	90	0.28	0.059	4.0	1.50	[3]	-	-	[3]	[3]	[3]	[3]	-	-	-
	18	90	0.28	0.059	4.0	2.00	[3]	-	-	[3]	[3]	[3]	[3]	-	-	-
	18	90	0.28	0.059	4.0	2.50	[3]	-	-	[3]	[3]	[3]	[3]	-	-	-
	24	90	0.12	0.059	7.7	2.70	[2]	[2]	[2]	[2]	[2]	[2]	[2]	[2]	[2]	[2]
	48	90	0.12	0.059	7.7	2.70	[2]	[2]	[2]	[2]	[2]	[2]	[2]	[2]	[2]	[2]
Beams	54	90	0.12	0.059	7.7	2.70	[2]	[2]	[2]	[2]	[2]	[2]	[2]	[2]	[2]	[2]
Beam-Columns	24	90	0.12	0.059	7.7	2.70	[1]	[1]	[1]	[1]	[1]	[1]	[1]	[1]	[1]	-
	48	90	0.12	0.059	7.7	2.70	[1]	[1]	[1]	[1]	[1]	[1]	[1]	[1]	[1]	-

The specimen lengths were chosen to permit various interactive modes of failure. The short specimens were chosen so that yielding would be reached before lateral buckling, thus allowing local or distortional buckling after yielding had commenced. The longer specimens were designed so that local and distortional buckling of the cross section and its interaction with the overall buckling of the members could be studied.

5.1.1 Dimensions and Properties of Specimens

To measure the actual dimensions of the specimens and to determine their properties, a technique was used which utilized spray paint impressions taken from the ends of each specimen. Each specimen was placed upright on a white sheet of paper and paint was sprayed around the specimen on the paper so that an outline of the cross sectional shape was left on the paper. Figure 5.2 shows a typical outline. Measurements were performed using a vernier calliper to an accuracy of 0.0004 inch. The lengths of the specimens were measured using a tape measure to an accuracy of 0.004 inch. The paint was removed from the ends of each specimen before determining the plate thickness at two locations from each element component. To account for any distortion of the edge caused by the shearing process of the steel sheet before forming, the thickness of the section was measured at approximately 1.0 inch away from the edge and at several locations around the cross section.

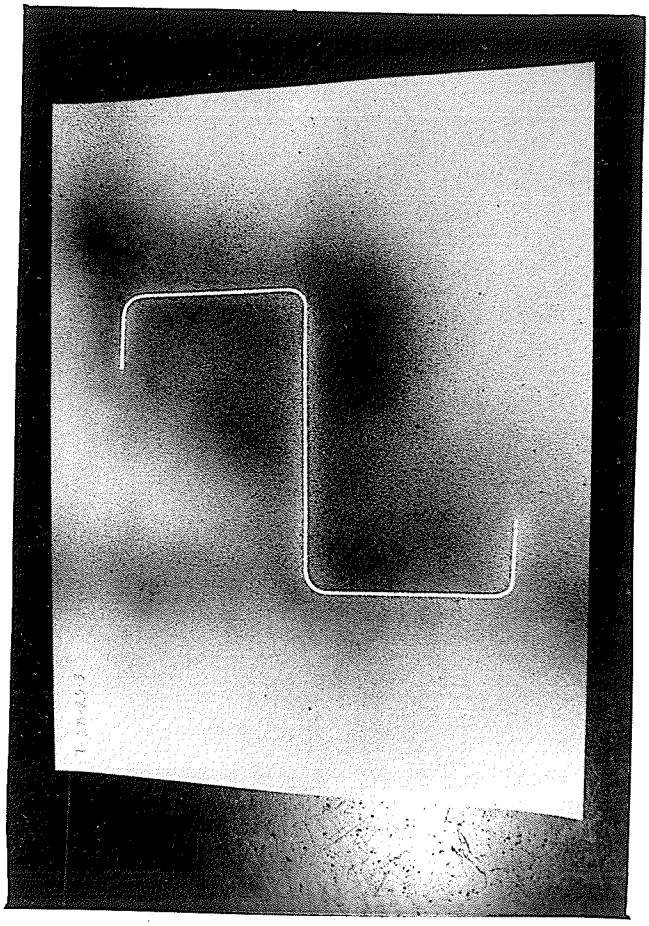

Figure 5.2 Typical Spray Paint Outline
(Not to Scale)

The average values of the cross sectional dimensions taken from both ends of each specimen were determined and the cross sectional properties were calculated. The average cross sectional dimensions, and the corresponding computed cross sectional properties such as area, moments of inertia, and torsional and warping constants, are presented in Tables B.1 to B.8, and Tables B.9 to B.16 in Appendix B.

5.1.2 Material Properties

To determine the material properties of the specimens, a series of tension tests were performed. Test coupons were cut from flat sheets as well as from randomly selected specimens which showed the smallest amount of damage due to testing. The tension tests were conducted in accordance with ASTM E 8M-85, Standard Methods of Tension Testing of Metallic Materials (1985).

Figure 5.3 shows the locations from which test coupons were obtained. A typical X-Y plot of tensile load versus elongation for a virgin coupon is given in Figure 5.4. Typical load-elongation plots for coupons cut from the flange and from the curved part of a section are given in Figures 5.5 and 5.6, respectively. The static yield strength was obtained using the 0.2% offset method. Table 5.2 lists the mechanical properties of the tensile coupons. The results given in this table indicate that there were two sets of steel sheets used in the investigation. The first set was used to form the 18 inch long specimens, the second to form the 24, 48, and 54 inch long specimens. For the first set, the average yield strength was 51.61 ksi (std dev

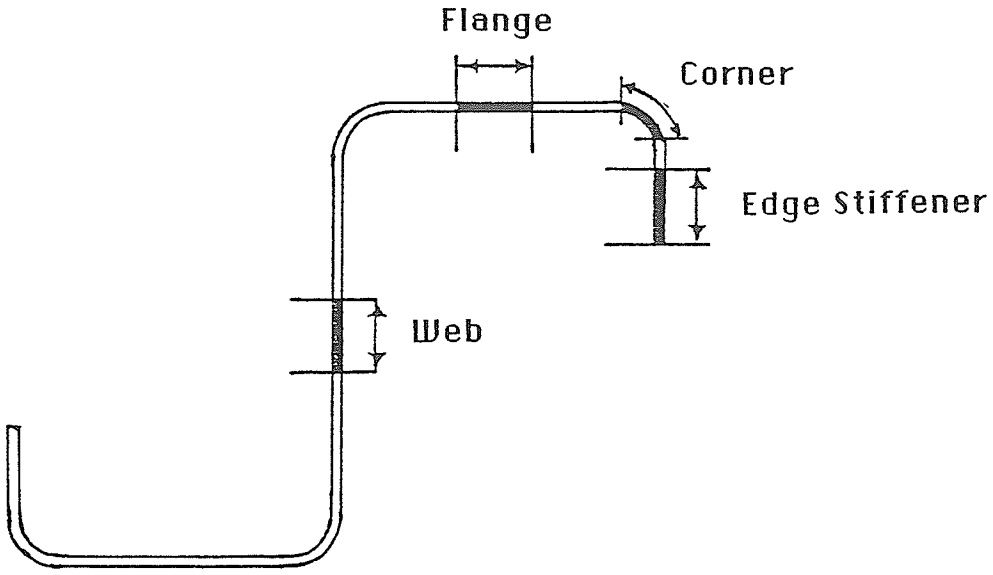

Figure 5.3 Locations of Tension Test Coupons

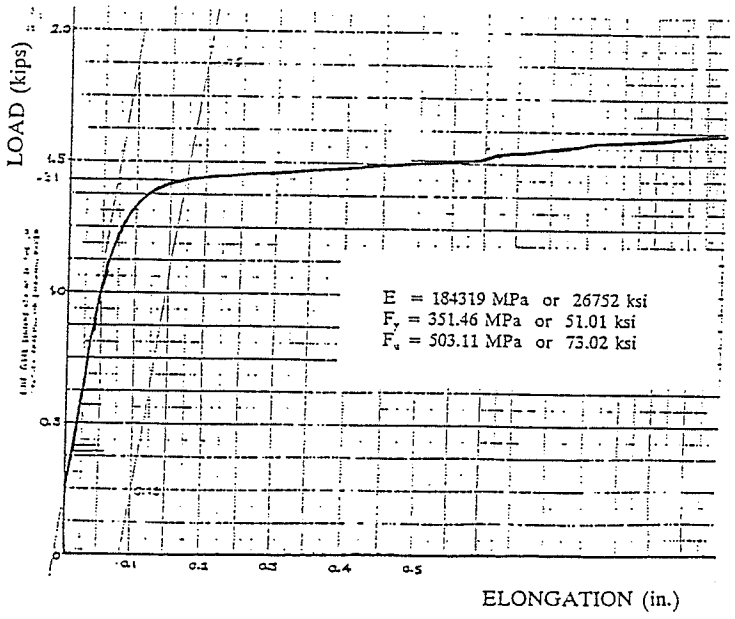

Figure 5.4 Typical X-Y Plot of Loads Versus Elongation for Tension Test Coupons Cut from Metal Sheets

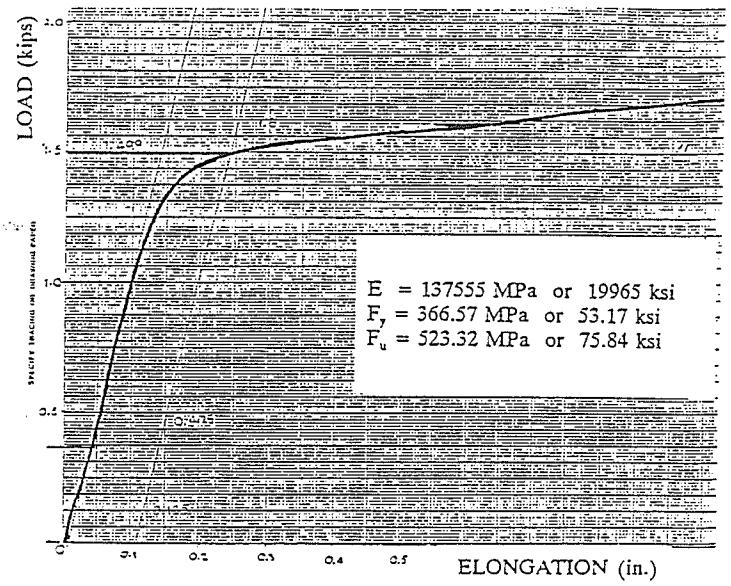

Figure 5.5 Typical X-Y Plot of Loads Versus Elongation for Tension Test Coupons Cut from Flange of a Section

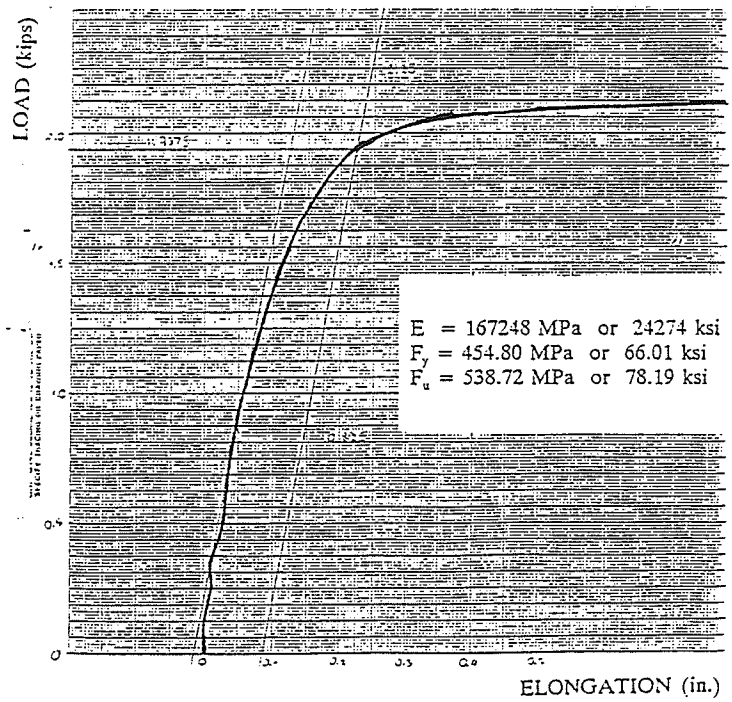

Figure 5.6 Typical X-Y Plot of Loads Versus Elongation for Tension Test Coupons Cut from Curved Part of a Section

TABLE 5.2 Mechanical Properties of Tensile Coupons

Coupon Locations (1)	Coupon Specimens (2)	18 in. Z-Sections			24, 48 and 54 in. Z-Sections		
		F_y (ksi) (3)	F_u (ksi) (4)	ϵ (%) (5)	F_y (ksi) (6)	F_u (ksi) (7)	ϵ (%) (8)
Virgin Sheet	1	51.01	73.02	28.40	47.95	71.07	29.28
	2	51.74	74.52	30.22	47.08	72.78	30.74
	3	52.53	74.96	22.55	47.71	72.08	29.88
	4	51.32	74.74	28.10	45.97	70.05	29.10
Flange	1	51.11	75.43	27.24	47.03	71.47	29.48
	2	52.27	75.56	27.56	47.56	70.66	30.74
	3	53.17	75.84	26.76	-	-	-
	4	50.54	75.31	27.22	-	-	-
Web	1	53.59	75.23	25.50	46.03	70.73	30.68
	2	52.82	74.77	27.24	47.64	71.55	28.22
Edge Stiffener	1	51.61	74.97	26.48	47.56	70.40	29.28
	2	51.77	69.99	22.70	46.34	67.36	28.56
Corner	1	65.86	75.58	21.24	75.21	86.84	27.06
	2	67.69	76.78	21.32	76.48	88.04	30.92
	3	66.01	78.19	21.02	73.33	88.42	25.70

= 0.66) for virgin sheet, 52.07 ksi (std dev = 1.05) for the flat portions of test specimens (i.e., flanges, web and edge stiffeners) and 66.73 ksi (std dev = 0.92) for the corner coupons. The average yield strength of corner coupons was 29% higher than that of the virgin sheet and 28% higher than that of the flat portion coupons, since the effect of cold-work at the corner coupons was greater than the one at the flat portion coupons. For the second set, the average yield strength was 47.18 ksi (std dev = 0.88) for the virgin sheet, coupons cut from flat portions, the average yield strength was 47.03 ksi (std dev = 0.69) and 75.01 ksi (std dev = 1.58) for the flat portions. The average yield strength of corner coupons was 59% higher than that of the virgin sheet and 59% higher than that of the flat portion coupons. In the present study, a yield strength of 52.07 ksi was used for the 18 inch specimens, and 47.03 ksi was used for the 24, 48, and 54 inch specimens

For both groups of specimens, there was less than a 0.01% difference between the average yield strength of flat coupons cut from the specimens and that of the flat coupons cut from the virgin sheet. However, there was approximately ± 5% difference between the average measured yield strength and the 50 ksi value specified by the supplier. Also, there was not statistically compared of the material properties between these two groups of specimens. The difference of average yield strength was too large to consider these two groups of specimens to be produced from the same steel material.

According to ASTM A607-90a Standard (1991) for Grade 50 Class 1 cold-rolled high strength low-alloy steel sheet, the minimum requirement for tensile

strength (F_u), yield strength (F_y), and percent elongation (ϵ) are 65 ksi, 50 ksi, and 20%, respectively. Material tests by the producer must comply with these values. However, the tests by the producer are limited to the end of the coil for coil products. Design considerations must recognize that variations in strength levels may occur throughout the untested portions of the coil, but, in general, yield levels will not be less than 90% of the minimum values specified. The absolute minimum requirements of tensile strength and yield strength in accordance with this Standard are therefore 58.5 and 45 ksi, respectively. Both sets of steel sheet were manufactured in accordance with ASTM A607-90a steel sheet. The results of the tensile coupons, shown in Table 5.2, are within the acceptable limits.

5.2 TEST EQUIPMENT

5.2.1 Test Equipment for Column and Beam-Column Tests

To avoid end effects such as fixing moments due to end conditions, the supports for the specimens had to be designed as "pin-ended" connections. To prevent tilting of the specimens during testing, the supports had to allow for rotation. This was achieved by the use of the hemispherical loading cylinder shown in Figure 5.7, and an end plate arrangement attached at the end of the specimen. This pin-ended condition permitted longitudinal movement while the ends of the specimen were free to rotate and twist with respect to any axis.

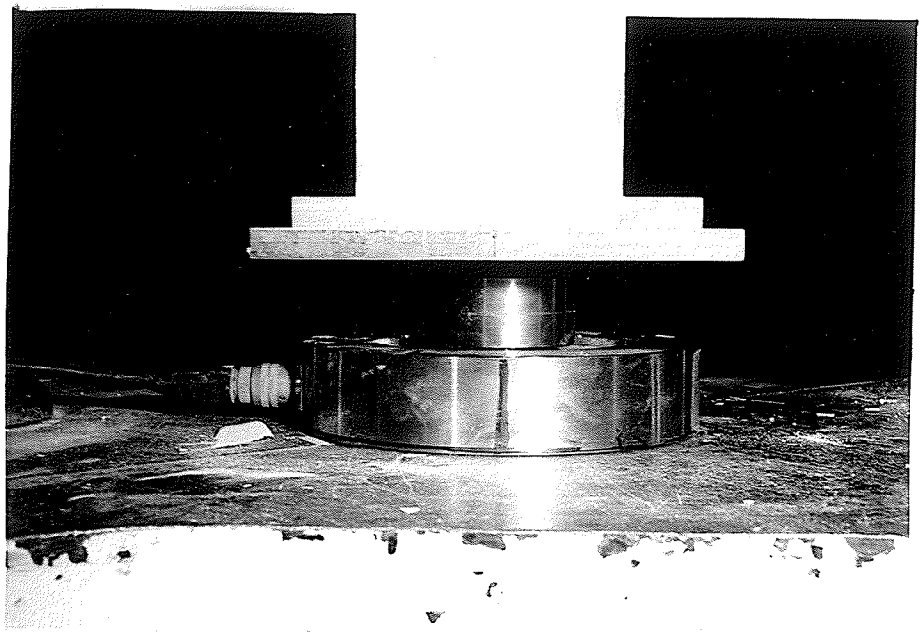

Figure 5.7 Loading Cylinder with an End Plate Arrangement Attached at an End of Specimen

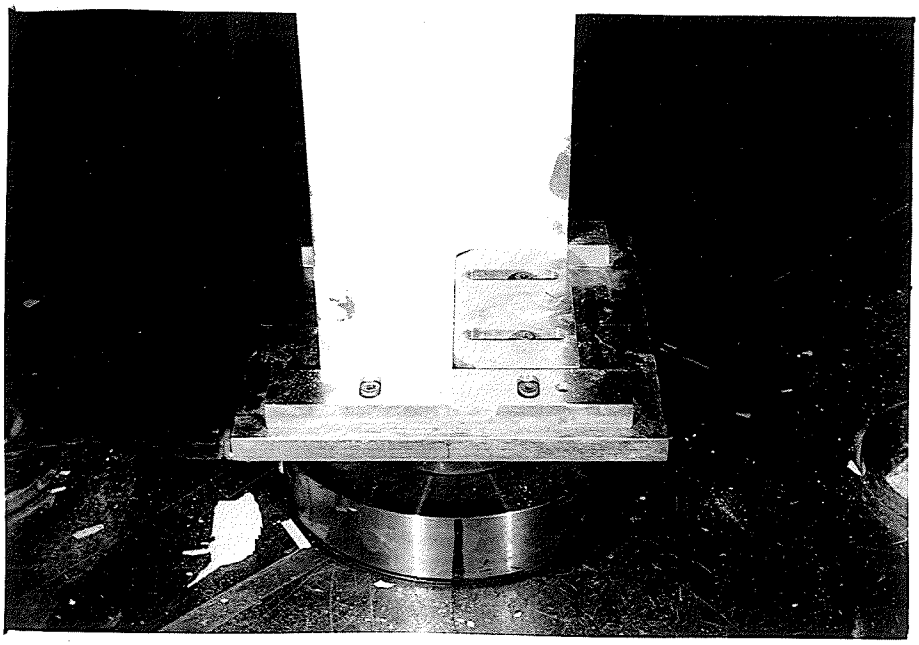

Figure 5.8 The End Plate with 18 inch Long Specimen in Place

The load was applied by a 60 kips capacity Riehle testing machine and measured by a 50 kips load cell. The applied load had to be distributed uniformly over the entire cross section of the specimen. This was achieved by placing a rigid steel plate at each end of the specimen. For the 18 inch specimens, the plates were high strength cold-formed steel with dimensions of 7.5 x 7.5 x 0.5 inches, as shown in Figure 5.8. For the 24 and 48 inch specimens, 15 x 15 x 0.75 inch, hot-rolled steel plates were used with dimensions of 15 x 15 x 0.75 inches, as shown in Figure 5.9.

To provide lateral support to the ends of the specimen and to prevent the specimen from slipping off the support plates after local buckling, 0.5 inch thick adjustable bars were bolted to the support plates, as shown in Figure 5.10. The adjustable bars were designed to accommodate any size of test section.

For the 18 inch specimens, a small circular "dent" was made on the reverse side of the end plates, in the exact geometric centre of sections. The centroid of the cross section was placed to coincide with the "dent" location. The hemispherical loading cylinders rested in the dent and was restrained from moving during testing. This arrangement ensured that the load was applied concentrically to each specimen.

A similar end plate arrangement was used for the 18 and 24 inch long specimens, as shown in Figure 5.11. However, to provide an easier and more accurate method of setting up the specimen, 1.0 inch high steel angle sections, were welded to the plates to form a groove. These angle sections were also used to prevent the specimen and the plates from slipping off the hemispherical loading cylinders during advanced stages of loading. Rubber spacers were placed around the

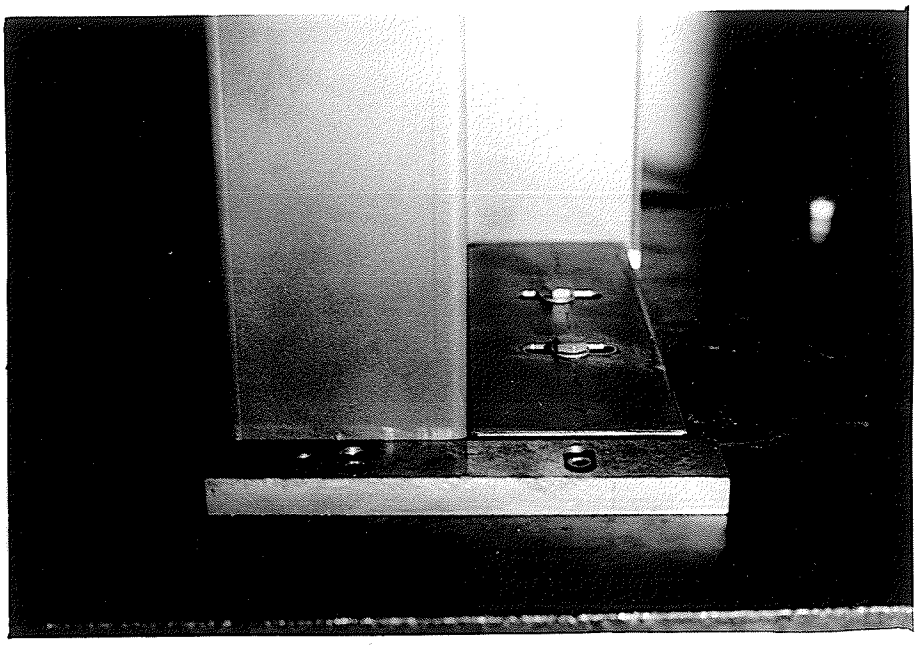

Figure 5.9 The End Plate with 24 inch Long Specimen in Place

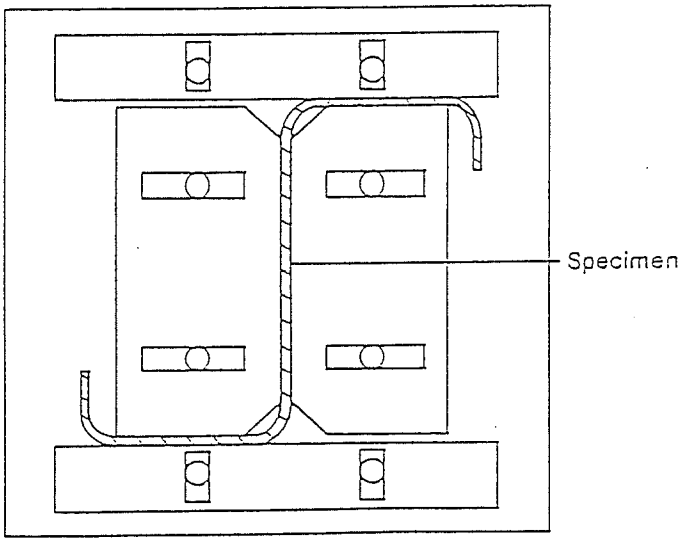

Figure 5.10 Plane View of Support Plate with Specimen in Place

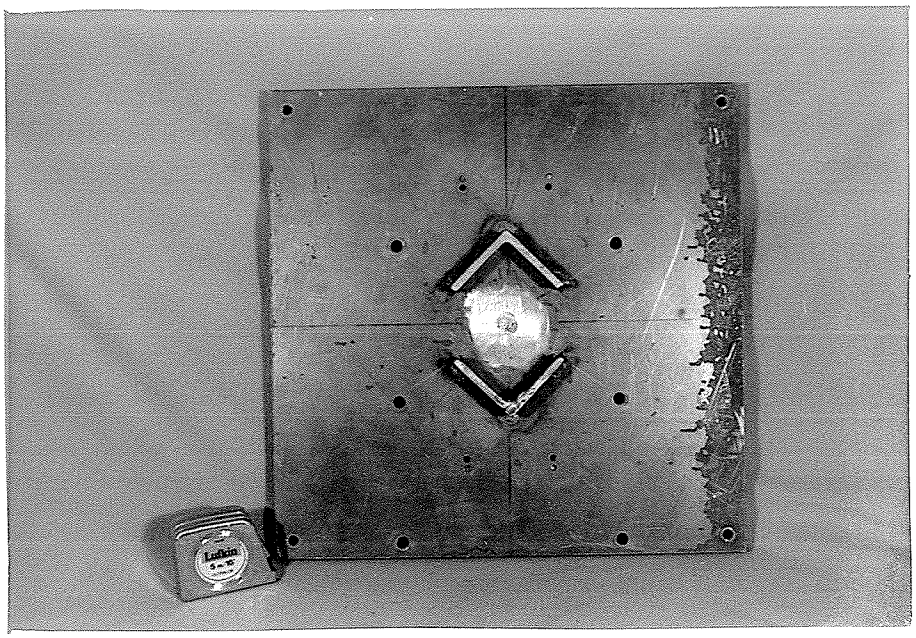

Figure 5.11 The Reverse Side of 15 x 15 x 0.75 inch Support Plate

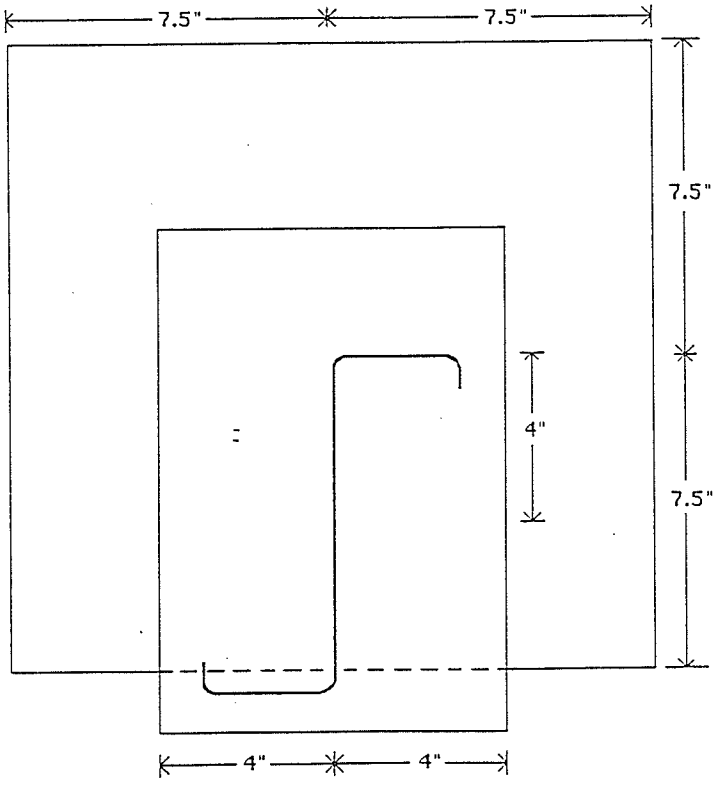

Figure 5.12 The 12 x 8 x 0.5 inch End Plate Used for Beam-Column Tests

inside of the grooves so that the hemispherical loading cylinder would fit into the groove with the smallest possible amount of resistance.

For the beam-column tests, specimens were welded to 12 x 8 x 0.5 inch hot-rolled steel end plates, as shown in Figure 5.12. The end plates were bolted to the support plates. The geometric centroid of the specimen on the end plates was 4.0 inches from the centre of the support plate. One of the flange-web junctions of each specimen was aligned with the geometric centroid of the support plate, as shown in Figure 5.12. This connection was designed to accommodate the large rotation which was expected during testing. After each test, the end plates were removed and cleaned by grinding prior to reuse. Typical set-up and a loading diagram with specimen in place are shown in Figures 5.13 and 5.14 for the column tests, whereas they are shown in Figures 5.15 and 5.16 for the beam-column tests.

5.2.2 Test Equipment for Beam Tests

The test set-up, shown in Figure 5.17, allowed the testing of each specimen as a simply supported beam under two concentric loads applied at the third points. A schematic diagram of the test equipment with the specimen in place is shown in Figure 5.18. The load was transferred to the third points via a hollow structural section spreader beam and applied through 1.2 inch diameter x 6.0 inch long rollers located as shown in Figure 5.19. The rollers were placed on steel box sections which were fastened to the webs of the specimen, thus ensuring loading through the webs. Since Z-section beam tend to bend and twist during loading, the specimens were

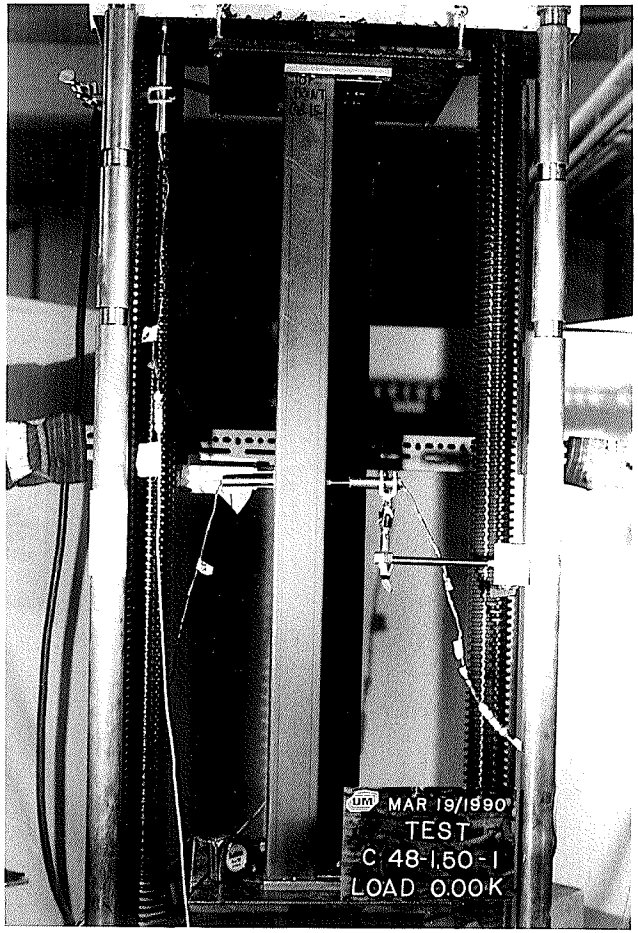

Figure 5.13 The Test Set-Up for a Typical Column Specimen

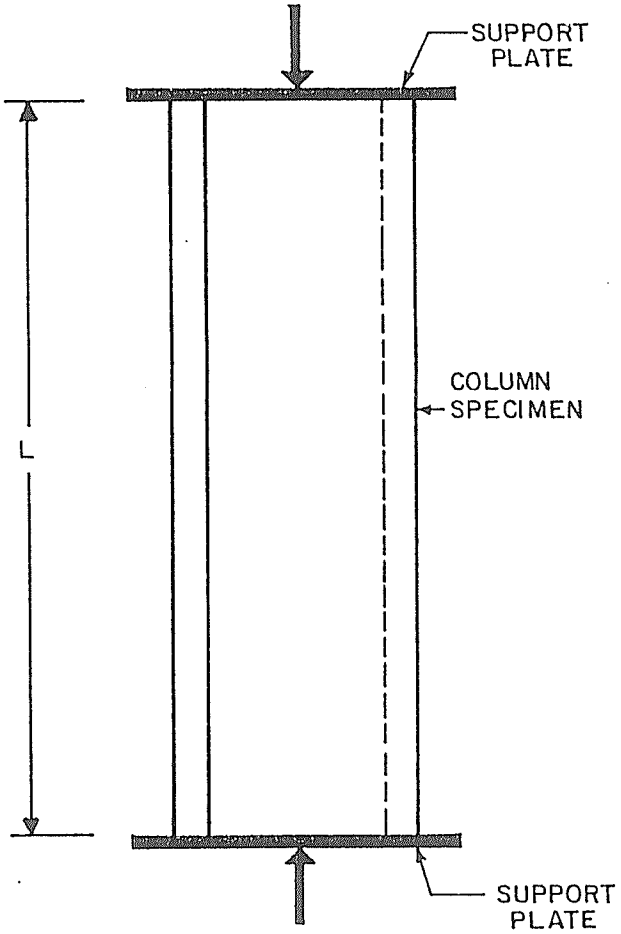

Figure 5.14 A Loading Diagram for the Column Tests

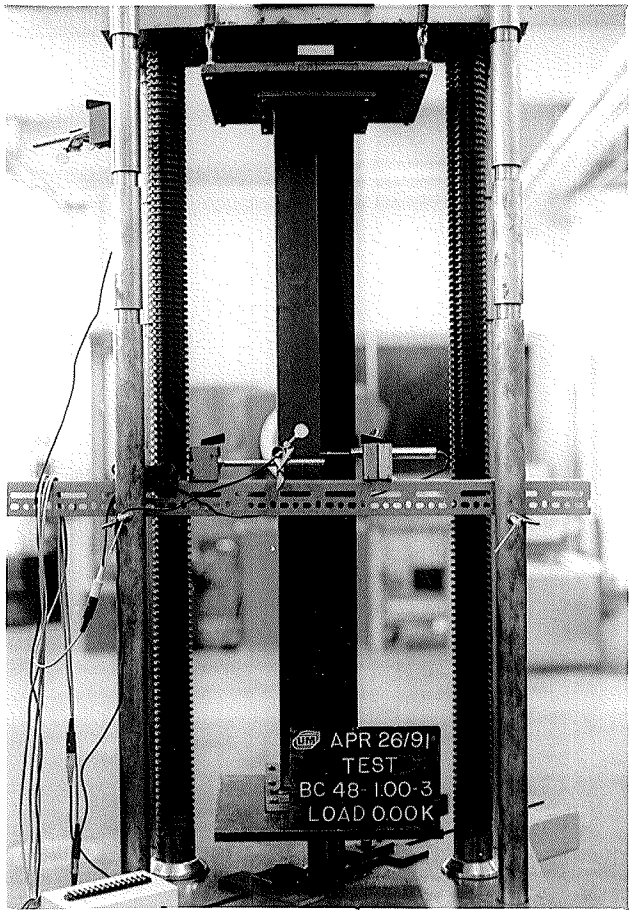

Figure 5.15 The Test Set-Up for a Typical Beam-Column Specimen

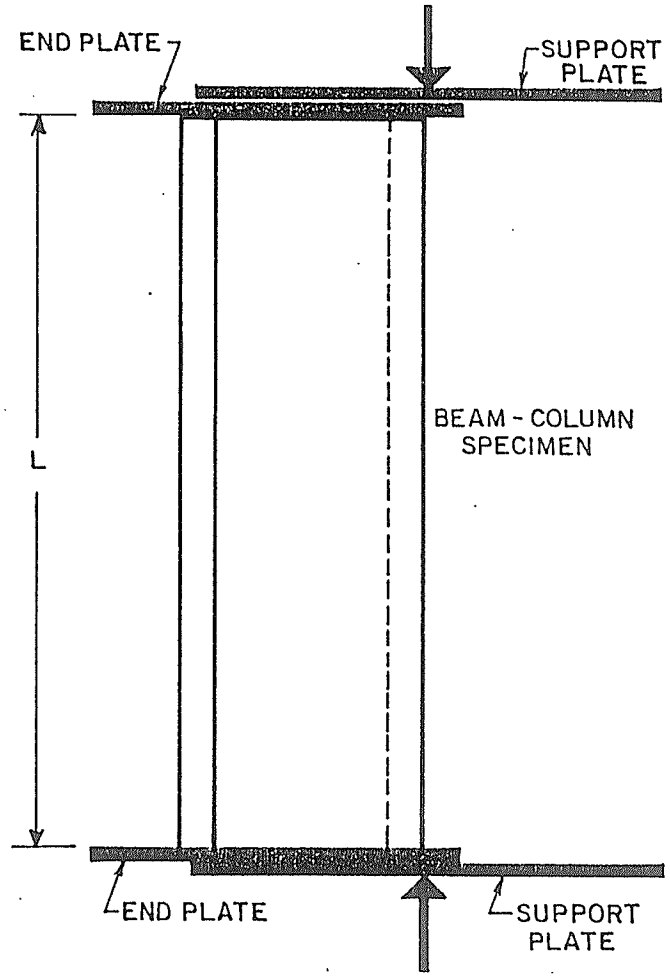

Figure 5.16 A Loading Diagram for the Beam-Column Tests

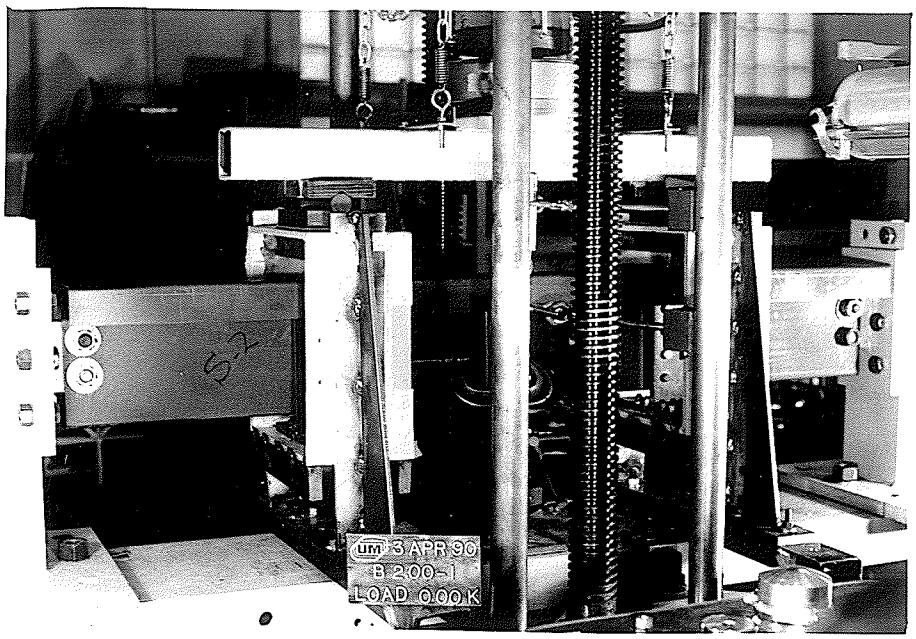

Figure 5.17 The Test Set-Up for a Typical Beam Specimen

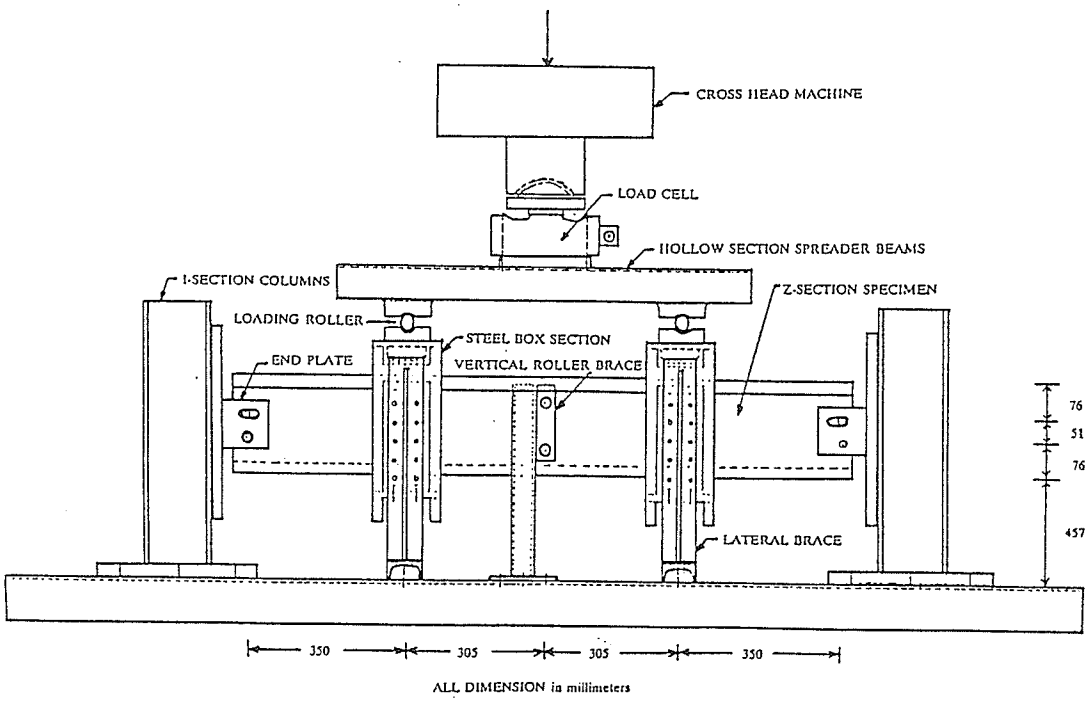

Figure 5.18 The Schematic Diagram of Test Set-Up for Beam Tests

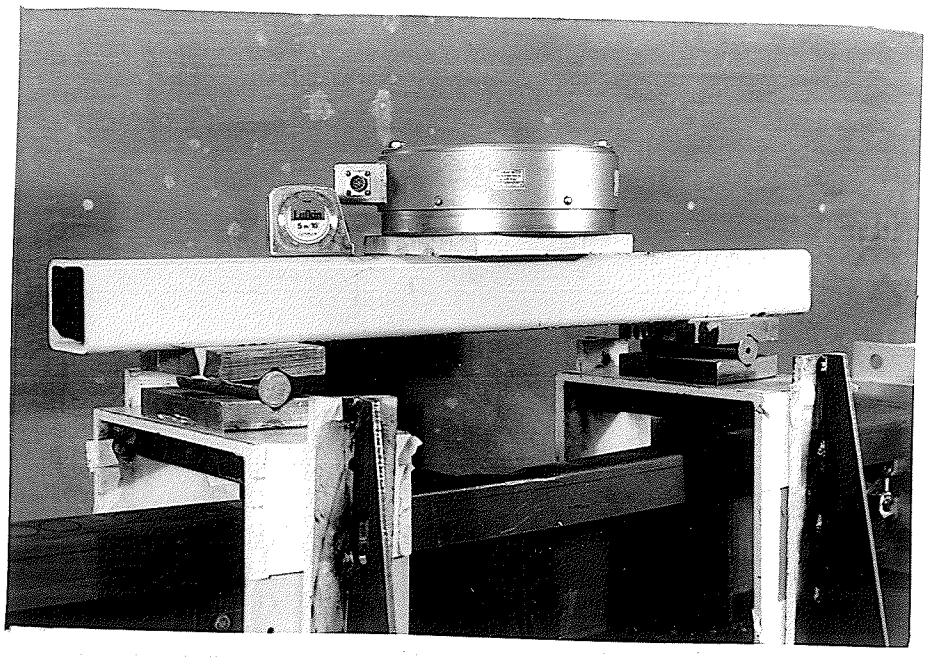

Figure 5.19 Hollow Section Spreader Beam and Two Sets of Rollers

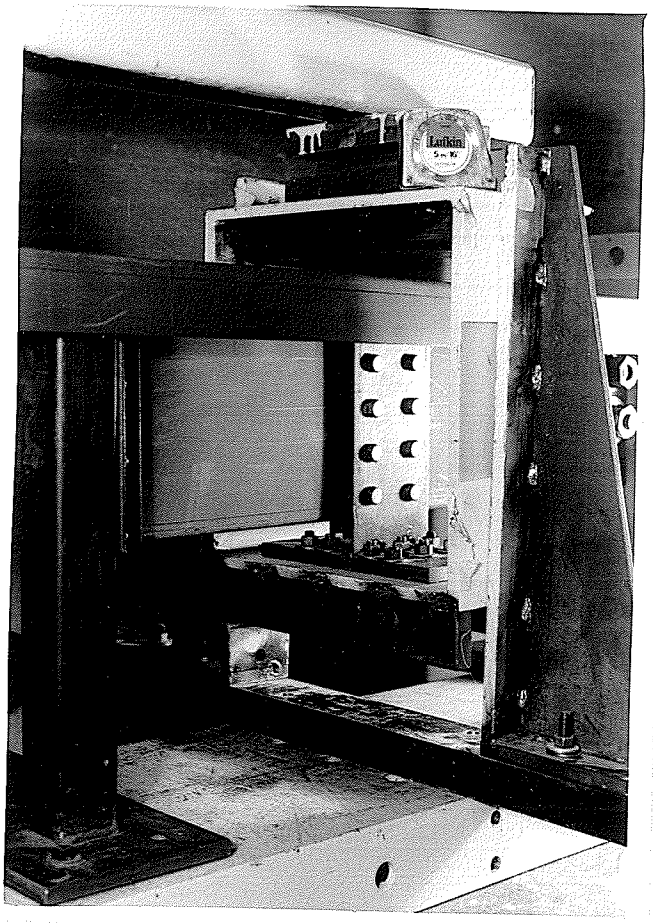

Figure 5.20 Steel Box Section

braced at midspan and at the loading locations. The lateral braces which consisted of 3.0 inch wide x 19.0 inch long steel bars, were used to brace the steel box sections, as shown in Figure 5.20. An additional brace consisting of a vertical roller was provided at the midspan, as shown in Figure 5.21. The specimen was loosely fastened at the ends to steel plates which were connected to hot-rolled steel I-section columns, as shown in Figure 5.22. Slotted holes were used to allow for rotation of the specimens in the plane of loading.

5.3 INSTRUMENTATION

The basic instrumentation for all specimens consisted of LVDTs (Linearly Variable Differential Transducers) and load cells connected to a data acquisition system. For the 18 inch column specimens, one LVDT measured the longitudinal axial deformation. For the 24 and 48 inch column and beam-column specimens, three LVDTs were used, one to measure deformation in the longitudinal direction, the other two, as shown in Figure 5.23, to monitor mid-height displacements perpendicular to the flanges at the flange-edge stiffener junction, and perpendicular to the web at a flange-web junction.

For the 54 inch beam specimens, four LVDTs were used, as shown in Figure 5.24. One measured the vertical deflection in the plane of the web at midspan, perpendicular to the bottom flange at a flange-web junction. The second measured the out-of-plane lateral displacement at midspan, perpendicular to the web at the top flange-web junction. The third measured the vertical displacement of the

Figure 5.21 The Additional Brace by Vertical Roller

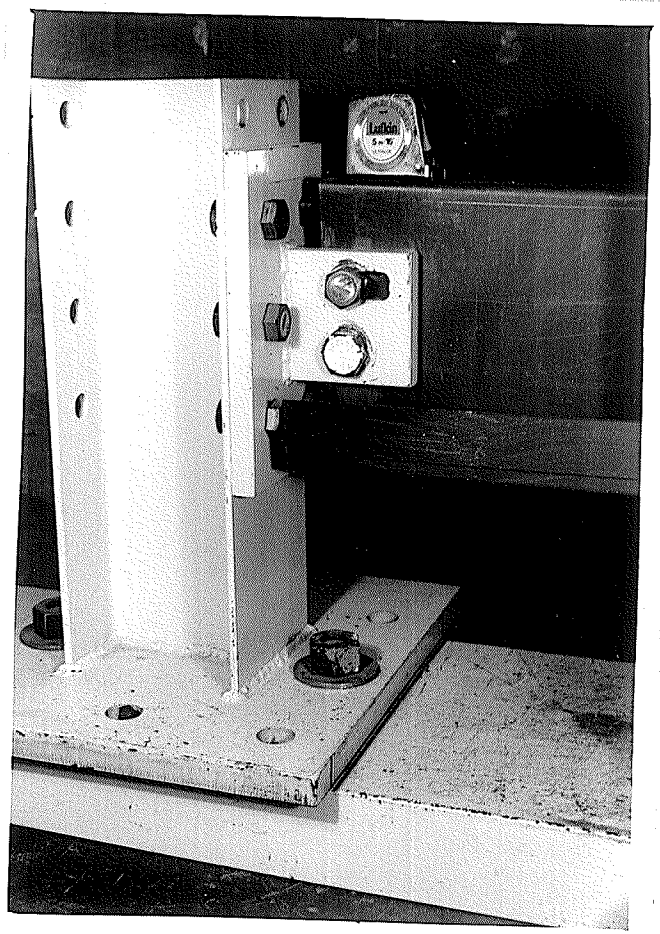

Figure 5.22 Hot-Rolled Steel I-Section Columns and the End Plate

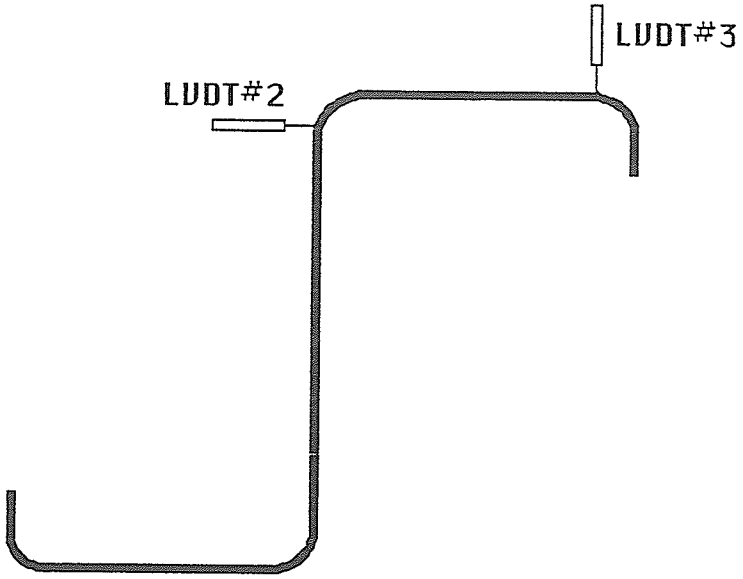

Figure 5.23 LVDTs Placed on the 24 and 48 inch Column Specimens

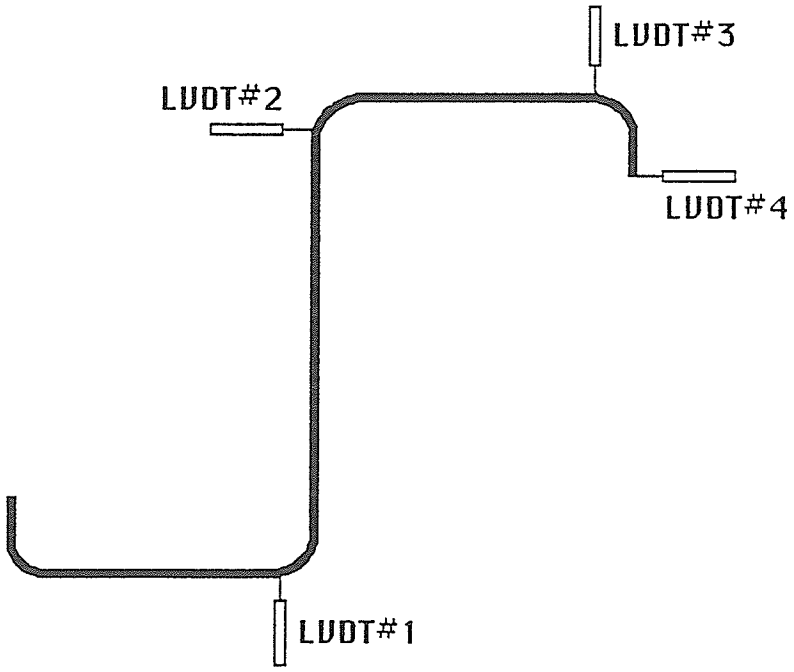

Figure 5.24 LVDTs Placed on Beam Specimen

flanges, perpendicular to the top flange at the flange-edge stiffener junction located at midspan. The fourth measured the midspan lateral displacement of the edge stiffener, perpendicular to the edge stiffener at its free edge. The load versus vertical displacement (LVDT #1) was monitored continuously using a Hewlett Packard 7044A X-Y recorder.

All data signals were fed into a TECMAR 12-Bit, 16 Channels Analog to Digital Convertor Board, installed in an IBM PC computer. Results were logged on to the hard disk for subsequent analysis.

5.4 TEST PROCEDURES

In the case of the 18 inch column tests, the support plates were first placed at each end of the specimen and the entire assembly was placed between the loading spheres which were fastened to the testing machine. In the case of the 24 and 48 inch column tests, the support plates were first attached to the loading spheres and then the specimens were placed between support plates. In both cases, once the specimen was placed between the support plates, a carpenter's level was used to adjust the specimen to a vertical position. A longitudinal centerline marked on both specimen and supports was used to adjust the specimen to a concentrically loaded position for testing.

For the beam tests, the procedure was described in section 5.2.2. The maximum load was converted to the bending capacity, for each specimen, by taking one half of the maximum load multiplied by the distance between the bolt line at

the end supports and the centerline of the fastener arrangement where the webs were connected to the box sections. The one half load was used in analysis. In practice, however, the load may not evenly distributed to each 1.2 inch diameter x 6.0 inch long rollers located, as shown in Figure 5.19, on the steel box sections.

In the case of the beam-column tests, the end plates were welded to the specimen. The entire assembly was placed between loading points, with an eccentricity of 4.0 inches. Once the specimen was set-up, it was adjusted to a vertical position which was confirmed using a carpenter's level.

For all tests, once a specimen was set-up, an approximately 0.3 kips load was applied to hold it in place and allow the positioning of the LVDTs. To ensure that the buckling behaviour of the specimen was observed, a rate of loading of 0.5 kips/min was used. A data acquisition system was used to record the load and the displacements at five-second intervals. During the tests, each specimen was observed closely for signs of local buckling or deformation. A 12-inch ruler was used to detect any local irregularities in the web, flanges and edge stiffeners by moving the longitudinal edge of the ruler parallel to the longitudinal surface of the specimen. After a specimen failed, the type of failure, location of failure, and ultimate load obtained from the testing machine were recorded. For both column and beam-column specimens, 60 minutes was needed to conduct the test with 30 minutes for loading. For beam specimens, 120 minutes was needed to conduct the test with 25 minutes for loading.

CHAPTER 6

EXPERIMENTAL AND ANALYTICAL RESULTS

In this chapter, experimental observations are discussed. Analytical results, using North American design specifications (AISI, 1989 and CSA, 1989), theoretical models, and ANSYS finite element analysis, are presented. The evaluation of the analytical results through the comparison between the experimental and analytical results is made.

6.1 EXPERIMENTAL RESULTS

It was observed that the failure modes of all specimens depended on the width of the edge stiffeners. The predominant mode of failure, for specimens without edge stiffeners or with narrow edge stiffeners, was distortional buckling of the flange-edge stiffener component followed by local buckling of the web. On the other hand, specimens with wider edge stiffeners, initially suffered localized buckling of the web followed by distortional buckling of the flange-edge stiffener component. In columns and beam-columns, the flange-edge stiffener tended to rotate with respect to the compression flange-web junction, as shown in Figure 6.1(a). For beam tests, the compression portion of the beam tended to rotate with respect to the tension flange, as shown in Figure 6.1(b).

A typical column specimen with edge stiffeners after failure is shown in Figure 6.2(a), while one without edge stiffeners is shown in Figure 6.2(b). Typical

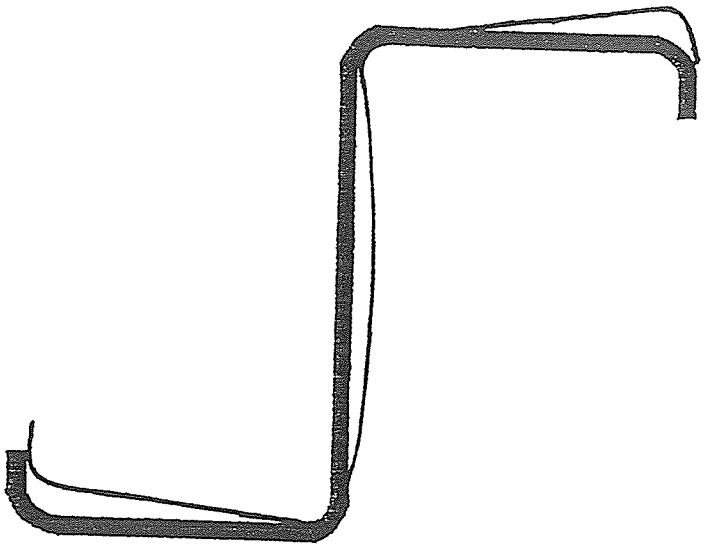

(a) Distortional Buckling of Column and Beam-Column Specimens

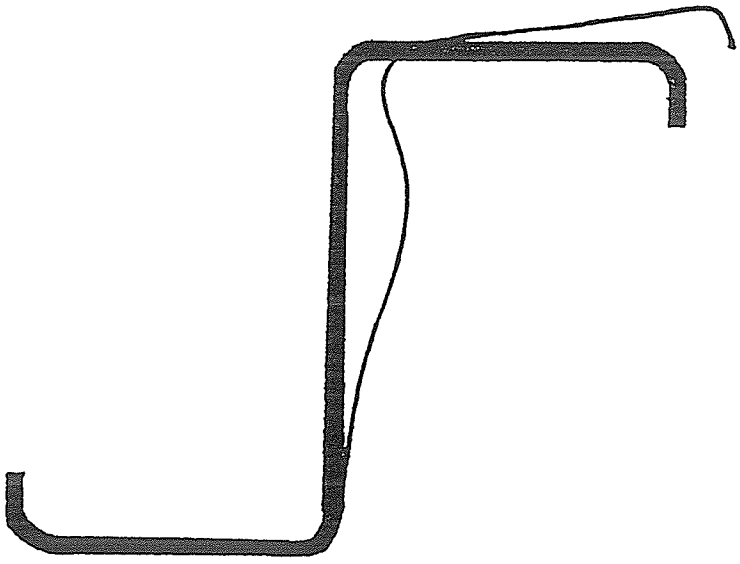

(b) Distortional Buckling of Beam Specimens

Figure 6.1 Schematic Diagrams of Distortional Buckling of Specimens

(a) Column Specimen with Edge Stiffeners

(b) Column Specimen without Edge Stiffeners

Figure 6.2 Typical Post-Test Z-Section Column Specimens with and without Edge Stiffeners

beam specimens with and without edge stiffeners after failure are shown in Figure 6.3, and typical beam-column specimens with and without edge stiffeners are shown in Figures 6.4(a) and 6.4(b).

A typical X-Y plot of the longitudinal axial load versus axial deformation is shown in Figure 6.5 for the column specimen without edge stiffeners. For the column specimens with edge stiffeners, typical X-Y plots are presented in Appendix C, Figures C.1 to C.5. A typical X-Y plot of load versus vertical deflection at midspan is shown in Figure C.6 for the beam specimen with edge stiffeners, whereas Figure C.7 shows a similar plot for the beam specimen without edge stiffeners. Also, typical X-Y plots for the beam-column specimens with and without edge stiffeners are shown in Figures C.8 and C.9, respectively.

The experimental results for all specimens are reported in Tables 6.1 to 6.8. Tables 6.1 to 6.3 present the results of the 18 inch column specimens with 1.5, 2.0, and 2.5 inch nominal flat widths of flanges, while Tables 6.4 and 6.5 list the results of the 24 and 48 inch column specimens, respectively. Table 6.6 provides the results of beam specimens, and Tables 6.7 and 6.8 give the results of the 24 and 48 inch beam-column specimens, respectively. In this table, the second and third columns present longitudinal axial deformation (δ) and experimental loads (P_{Test}) for the column and beam-column tests, and for the beam tests they present vertical deflection (δ) and experimental bending capacities (M_{Test}). In the same table the analytical results are also given.

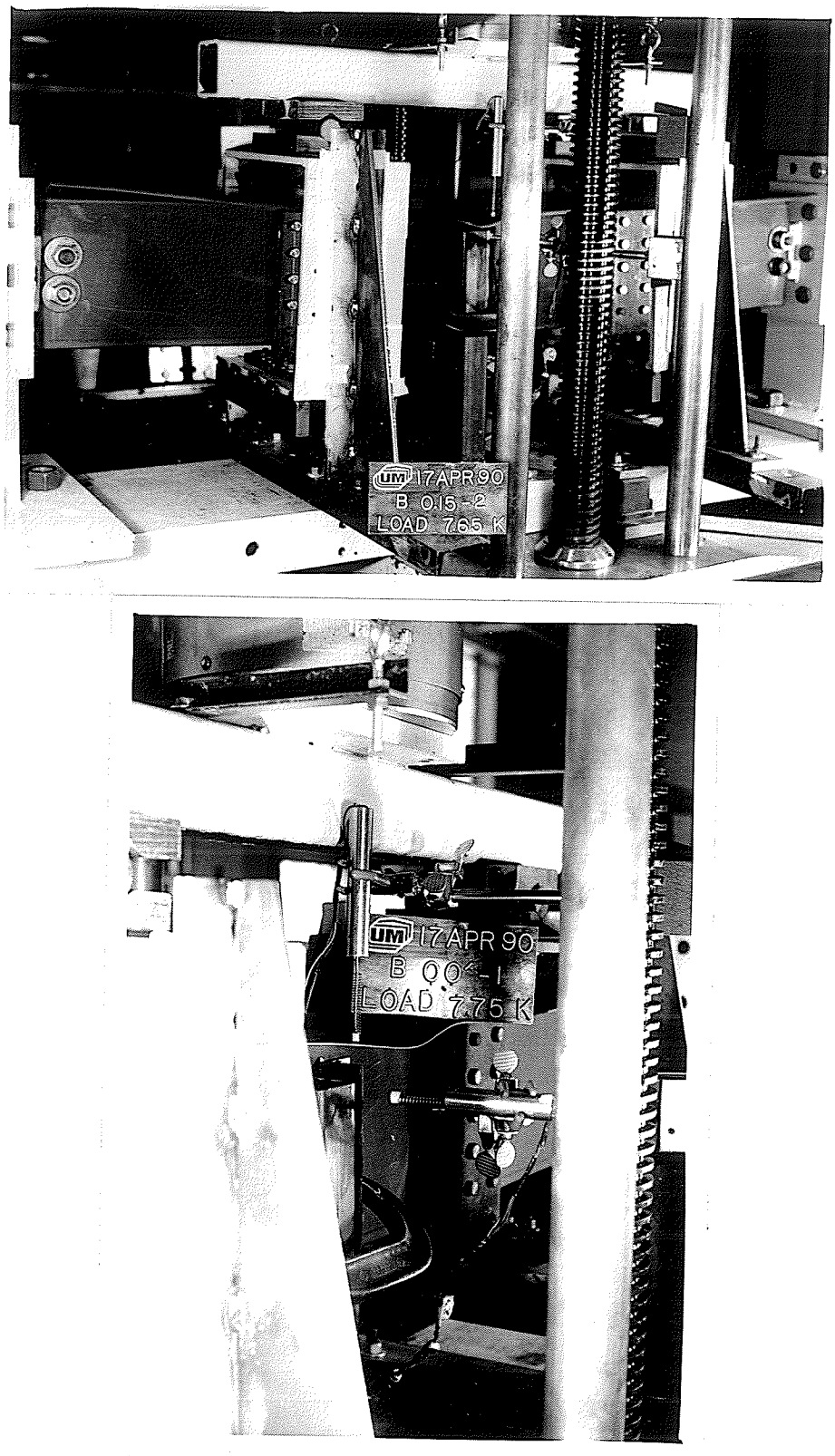

Figure 6.3 Typical Post-Test Z-Section Beam Specimens with and without Edge Stiffeners

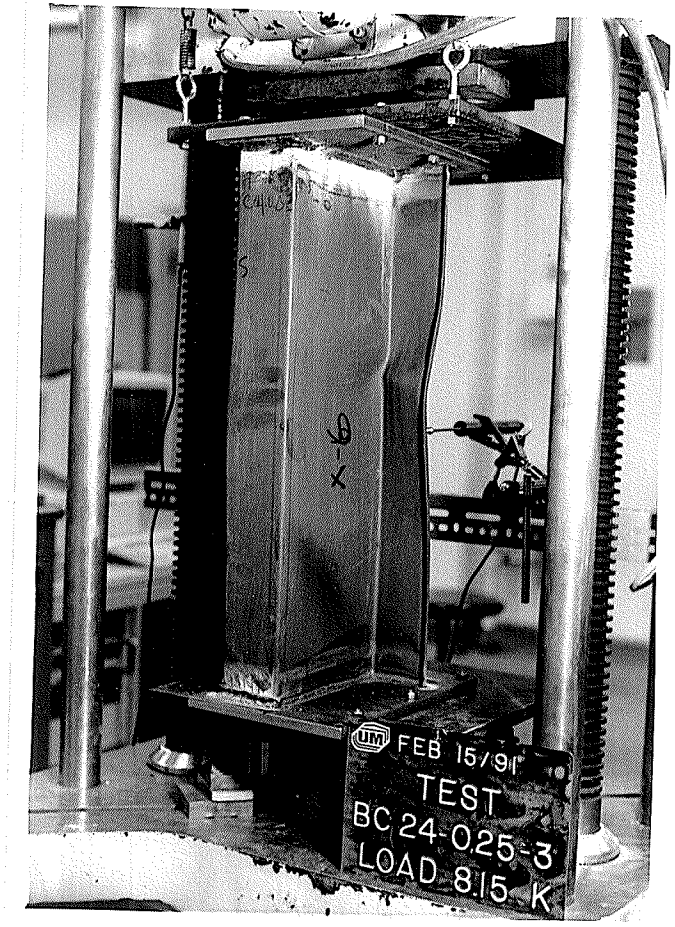

(a) Beam-Column Specimen with Edge Stiffeners

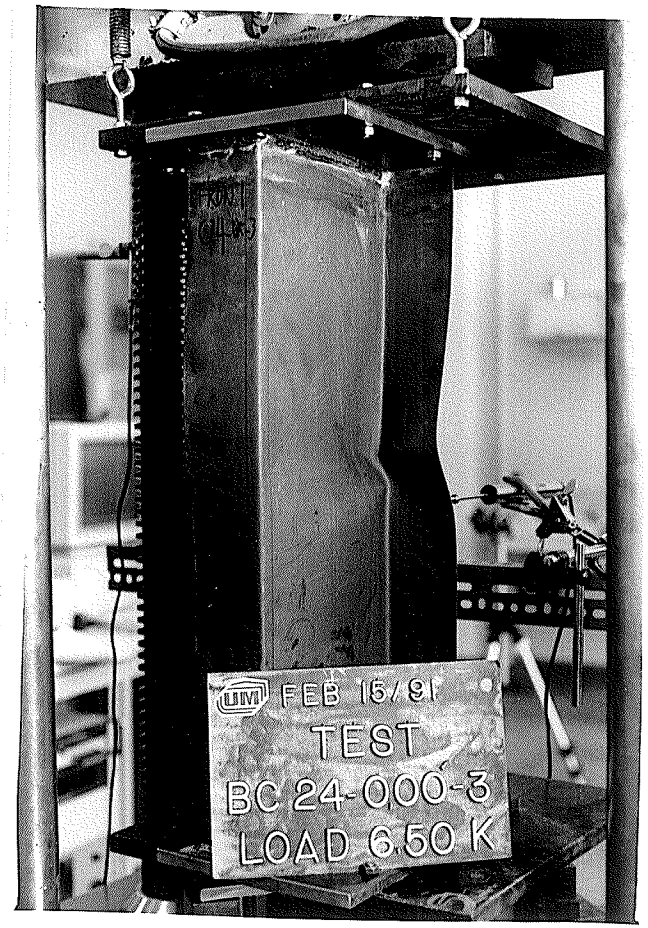

(b) Beam-Column Specimen without Edge Stiffeners

Figure 6.4 Typical Post-Test Z-Section Beam-Column Specimens with and without Edge Stiffeners

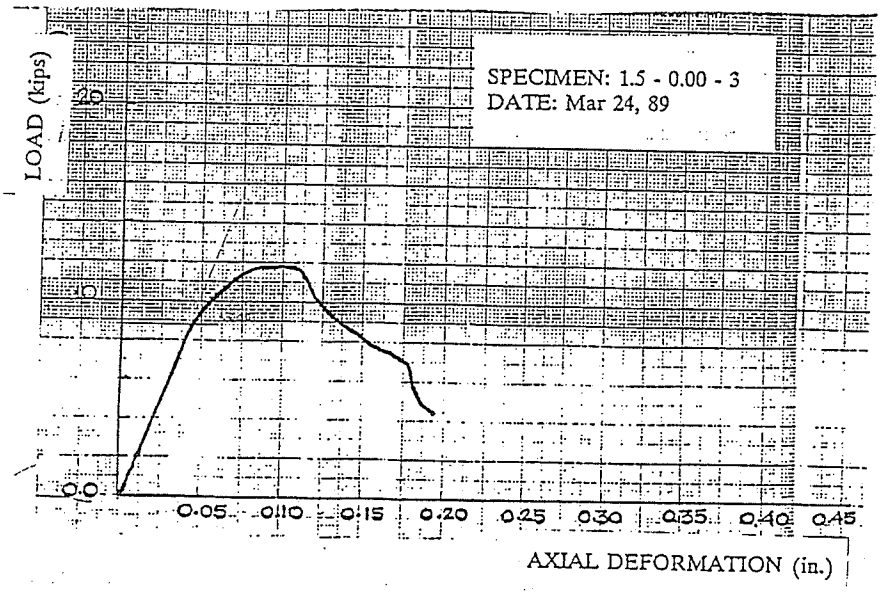

Figure 6.5 Typical X-Y Plot of Axial Load Versus Axial Deformation for Column Specimens without Edge Stiffeners

TABLE 6.1 Experimental and Analytical Results for the 18 inch Column Specimens with 1.50 inch Flat Width of Flanges

Specimen (1)	δ (in.) (2)	P_{Test} (kips) (3)	P_{AISI} (kips) (4)	P_{CSA} (kips) (5)	P_{Theory} (kips) (6)	$\frac{P_{Test}}{P_{AISI}}$ (7)	$\frac{P_{Test}}{P_{CSA}}$ (8)	$\frac{P_{Test}}{P_{Theory}}$ (9)
1.5-0.00-1[a]	0.08	11.90	8.60	8.69	11.90	1.38	1.37	1.00
1.5-0.00-2[a]	0.08	11.05	8.05	8.13	11.15	1.37	1.36	0.99
1.5-0.00-3[a]	0.10	11.90	7.86	7.75	10.63	1.55	1.54	1.12
1.5-0.25-1	0.12	18.90	21.03	24.53	18.65	0.90	0.77	1.01
1.5-0.25-2	0.10	17.45	20.63	23.90	18.25	0.85	0.73	0.96
1.5-0.25-3	0.13	19.30	20.30	23.51	18.01	0.95	0.82	1.07
1.5-0.50-1	0.09	17.90	24.10	26.86	19.28	0.74	0.67	0.93
1.5-0.50-2	0.13	19.90	24.21	26.92	19.33	0.82	0.74	1.03
1.5-0.50-3	0.13	15.25	23.96	26.72	19.23	0.64	0.57	0.79
1.5-0.75-1	0.13	18.10	23.24	25.80	18.83	0.78	0.70	0.96
1.5-0.75-2	0.11	19.80	23.38	26.00	18.88	0.85	0.76	1.05
1.5-0.75-3	0.13	20.87	24.07	26.90	19.45	0.87	0.78	1.07
1.5-1.00-1	0.14	20.90	22.83	24.80	18.82	0.92	0.84	1.11
1.5-1.00-2	0.12	19.30	22.86	24.78	18.79	0.84	0.78	1.03
1.5-1.00-3	0.13	18.25	22.76	24.70	18.78	0.80	0.74	0.97

[a] Curved portion at the flange-edge stiffener junction not included

TABLE 6.2 Experimental and Analytical Results for the 18 inch Column Specimens with 2.00 inch Flat Width of Flanges

Specimen (1)	δ (in.) (2)	P_{Test} (kips) (3)	P_{AISI} (kips) (4)	P_{CSA} (kips) (5)	P_{Theory} (kips) (6)	$\frac{P_{Test}}{P_{AISI}}$ (7)	$\frac{P_{Test}}{P_{CSA}}$ (8)	$\frac{P_{Test}}{P_{Theory}}$ (9)
2.0-0.00-1[a]	0.08	11.20	5.21	5.26	7.43	2.15	2.13	1.51
2.0-0.00-2[a]	0.08	11.85	4.95	4.99	7.06	2.40	2.37	1.68
2.0-0.00-3[a]	0.10	11.90	4.93	4.98	7.03	2.41	2.39	1.69
2.0-0.25-1	0.10	17.48	20.61	23.89	15.51	0.85	0.73	1.13
2.0-0.25-2	0.10	17.70	21.10	24.42	16.06	0.84	0.72	1.10
2.0-0.25-3	0.12	16.49	21.11	24.57	16.17	0.78	0.67	1.02
2.0-0.50-1	0.11	17.60	23.51	27.49	18.37	0.75	0.64	0.96
2.0-0.50-2	0.10	15.10	23.64	27.58	18.48	0.64	0.55	0.82
2.0-0.50-3	0.14	20.05	23.35	27.37	18.32	0.86	0.73	1.09
2.0-0.75-1	0.14	16.00	25.48	28.23	19.12	0.63	0.57	0.84
2.0-0.75-2	0.12	20.08	25.47	28.20	19.14	0.79	0.71	1.05
2.0-0.75-3	0.10	18.70	25.53	28.31	19.08	0.73	0.66	0.98
2.0-1.00-1	0.14	18.15	24.92	27.21	19.36	0.73	0.67	0.94
2.0-1.00-2	0.10	17.35	24.17	26.23	18.72	0.72	0.66	0.93
2.0-1.00-3	0.13	19.40	25.73	28.18	20.03	0.75	0.69	0.97

[a] Curved portion at the flange-edge stiffener junction not included

TABLE 6.3 Experimental and Analytical Results for the 18 inch Column Specimens with 2.50 inch Flat Width of Flanges

Specimen (1)	δ (in.) (2)	P_{Test} (kips) (3)	P_{AISI} (kips) (4)	P_{CSA} (kips) (5)	P_{Theory} (kips) (6)	$\frac{P_{Test}}{P_{AISI}}$ (7)	$\frac{P_{Test}}{P_{CSA}}$ (8)	$\frac{P_{Test}}{P_{Theory}}$ (9)
2.5-0.00-1[a]	0.09	12.05	3.76	3.79	5.50	3.21	3.18	2.19
2.5-0.00-2[a]	0.09	12.45	3.76	3.80	5.50	3.31	3.28	2.26
2.5-0.00-3[a]	0.10	12.20	3.69	3.72	5.41	3.31	3.28	2.25
2.5-0.25-1	0.10	15.80	21.45	24.48	13.18	0.74	0.65	1.20
2.5-0.25-2	0.11	17.60	21.02	23.98	12.91	0.84	0.73	1.36
2.5-0.25-3	0.14	19.80	21.39	24.48	13.25	0.93	0.81	1.49
2.5-0.50-1	0.10	16.40	23.03	26.61	15.23	0.71	0.62	1.08
2.5-0.50-2	0.13	19.10	23.86	27.64	16.10	0.80	0.69	1.19
2.5-0.50-3	0.12	18.65	23.72	27.50	15.92	0.79	0.68	1.17
2.5-0.75-1	0.13	18.60	26.93	29.65	18.13	0.69	0.63	1.03
2.5-0.75-2	0.13	20.00	27.70	30.67	18.70	0.72	0.65	1.07
2.5-0.75-3	0.14	19.10	27.70	30.67	18.70	0.69	0.62	1.02
2.5-1.00-1	0.13	19.00	25.78	27.94	18.47	0.74	0.68	1.03
2.5-1.00-2	0.12	18.89	26.51	28.84	19.19	0.71	0.65	0.98
2.5-1.00-3	0.15	18.00	25.80	28.03	18.58	0.70	0.64	0.97

[a] Curved portion at the flange-edge stiffener junction not included

TABLE 6.4 Experimental and Analytical Results for the 24 inch Column Specimens

Specimen (1)	δ (in.) (2)	P_{Test} (kips) (3)	P_{AISI} (kips) (4)	P_{CSA} (kips) (5)	P_{Theory} (kips) (6)	$\frac{P_{Test}}{P_{AISI}}$ (7)	$\frac{P_{Test}}{P_{CSA}}$ (8)	$\frac{P_{Test}}{P_{Theory}}$ (9)
2.7-0.00-1[a]	0.13	12.40	3.83	14.37	5.28	3.24	3.21	2.35
2.7-0.00-2[a]	0.12	10.60	3.86	14.20	5.32	2.75	2.72	1.99
2.7-0.00-1[b]	0.12	13.05	13.59	14.01	6.60	0.96	0.93	1.98
2.7-0.00-2[b]	0.13	11.15	13.91	14.33	6.93	0.80	0.78	1.61
2.7-0.15-1	0.14	12.80	14.75	15.55	7.45	0.87	0.82	1.72
2.7-0.15-2	0.13	12.35	14.93	15.80	7.59	0.83	0.78	1.63
2.7-0.25-1	0.15	15.20	17.09	19.13	9.95	0.89	0.79	1.53
2.7-0.25-2	0.14	15.80	17.23	19.32	9.90	0.92	0.82	1.60
2.7-0.50-1	0.16	18.90	19.85	23.14	13.40	0.95	0.82	1.41
2.7-0.50-2	0.14	18.25	19.82	23.12	13.27	0.92	0.79	1.38
2.7-0.75-1	0.15	20.56	23.92	26.65	16.06	0.86	0.77	1.28
2.7-0.75-2	0.16	20.40	24.11	26.72	16.10	0.85	0.76	1.27
2.7-1.00-1	0.16	20.70	23.84	26.04	17.65	0.87	0.79	1.17
2.7-1.00-2	0.17	20.85	23.84	26.04	17.66	0.87	0.80	1.18
2.7-1.25-1	0.15	23.10	23.95	25.97	19.26	0.96	0.89	1.20
2.7-1.25-2	0.16	21.25	23.99	26.03	19.21	0.89	0.82	1.11
2.7-1.50-1	0.17	23.40	23.39	25.12	19.32	1.00	0.93	1.21
2.7-1.50-2	0.17	21.90	23.45	25.19	19.33	0.93	0.87	1.13
2.7-2.00-1	0.18	23.30	21.06	22.14	17.38	1.11	1.05	1.34
2.7-2.00-2	0.17	20.90	20.85	21.89	17.23	1.00	0.95	1.21

[a] Curved portion at the flange-edge stiffener junction not included
[b] Curved portion at the flange-edge stiffener junction included

TABLE 6.5 Experimental and Analytical Results for the 48 inch Column Specimens

Specimen	δ	P_{Test}	P_{AISI}	P_{CSA}	P_{Theory}	$\frac{P_{Test}}{P_{AISI}}$	$\frac{P_{Test}}{P_{CSA}}$	$\frac{P_{Test}}{P_{Theory}}$
	(in.)	(kips)	(kips)	(kips)	(kips)			
(1)	(2)	(3)	(4)	(5)	(6)	(7)	(8)	(9)
2.7-0.00-1[a]	0.15	11.50	3.88	13.18	5.36	2.96	2.93	2.15
2.7-0.00-2[a]	0.17	12.70	3.87	13.35	5.34	3.28	3.25	2.38
2.7-0.00-1[b]	0.15	12.55	14.36	15.09	8.52	0.87	0.83	1.47
2.7-0.00-2[b]	0.18	11.65	14.38	15.10	8.49	0.81	0.77	1.37
2.7-0.15-1	0.16	12.90	14.35	15.01	8.61	0.90	0.86	1.50
2.7-0.15-2	0.15	12.70	14.21	14.86	8.40	0.89	0.85	1.51
2.7-0.25-1	0.14	13.70	15.77	17.10	9.99	0.87	0.80	1.37
2.7-0.25-2	0.15	14.30	15.66	16.92	9.80	0.91	0.85	1.46
2.7-0.50-1	0.18	19.40	19.34	22.26	14.36	1.00	0.87	1.35
2.7-0.50-2	0.18	16.90	18.90	21.71	13.63	0.89	0.78	1.24
2.7-0.75-1	0.21	20.95	22.12	24.48	16.33	0.95	0.86	1.28
2.7-0.75-2	0.17	20.80	22.61	25.58	16.63	0.92	0.81	1.25
2.7-1.00-1	0.17	21.45	22.46	24.44	17.68	0.95	0.88	1.21
2.7-1.00-2	0.18	19.60	22.48	24.48	17.57	0.87	0.80	1.12
2.7-1.25-1	0.20	20.55	22.16	23.82	18.60	0.93	0.86	1.11
2.7-1.25-2	0.21	22.30	22.31	23.97	18.60	1.00	0.93	1.20
2.7-1.50-1	0.20	20.75	22.50	24.04	19.35	0.92	0.86	1.07
2.7-1.50-2	0.22	21.45	22.59	24.11	19.33	0.95	0.89	1.11
2.7-2.00-1	0.21	21.75	20.31	21.22	17.38	1.07	1.02	1.25
2.7-2.00-2	0.22	22.55	20.32	21.19	17.20	1.11	1.06	1.31

[a] Curved portion at the flange-edge stiffener junction not included
[b] Curved portion at the flange-edge stiffener junction included

TABLE 6.6 Experimental and Analytical Results for the 54 inch Beam Specimens

Specimen (1)	δ (in.) (2)	M_{Test} (kips) in. (3)	M_{AISI} (kips) in. (4)	M_{CSA} (kips) in. (5)	M_{Theory} (kips) in. (6)	$\frac{M_{Test}}{M_{AISI}}$ (7)	$\frac{M_{Test}}{M_{CSA}}$ (8)	$\frac{M_{Test}}{M_{Theory}}$ (9)
2.7-0.00-1[a]	0.39	52.02	9.65	9.62	38.69	5.39	5.41	1.34
2.7-0.00-2[a]	0.42	53.79	10.02	10.00	40.05	5.37	5.38	1.34
2.7-0.00-1[b]	0.41	54.76	62.68	62.43	42.17	0.87	0.88	1.30
2.7-0.00-2[b]	0.41	53.79	63.00	63.19	41.04	0.85	0.85	1.31
2.7-0.15-1	0.43	54.06	62.32	62.49	39.89	0.87	0.87	1.36
2.7-0.15-2	0.43	53.08	64.17	64.44	40.83	0.83	0.82	1.30
2.7-0.25-1	0.46	54.06	68.49	70.91	41.81	0.79	0.76	1.29
2.7-0.25-2	0.47	57.60	68.69	70.45	43.82	0.84	0.82	1.31
2.7-0.50-1	0.43	58.22	80.29	85.85	45.44	0.73	0.68	1.28
2.7-0.50-2	0.45	58.75	81.83	87.52	45.45	0.72	0.67	1.29
2.7-0.75-1	0.45	62.11	92.99	97.87	46.96	0.67	0.63	1.32
2.7-0.75-2	0.44	58.57	92.17	97.28	46.88	0.64	0.60	1.25
2.7-1.00-1	0.39	63.08	94.20	95.62	47.11	0.67	0.66	1.34
2.7-1.00-2	0.45	60.34	91.45	92.30	45.57	0.66	0.65	1.32
2.7-1.25-1	0.39	61.40	92.37	92.91	47.64	0.66	0.66	1.29
2.7-1.25-2	0.44	64.50	89.53	90.02	45.76	0.72	0.72	1.41
2.7-1.50-1	0.42	62.37	86.84	87.13	46.74	0.72	0.72	1.33
2.7-1.50-2	0.41	63.79	88.64	89.09	48.00	0.72	0.72	1.33
2.7-2.00-1	0.38	61.05	77.46	97.30	45.63	0.79	0.63	1.34
2.7-2.00-2	0.42	63.08	79.69	79.57	47.07	0.79	0.79	1.34

[a] Curved portion at the flange-edge stiffener junction not included
[b] Curved portion at the flange-edge stiffener junction included

TABLE 6.7 Experimental and Analytical Results for the 24 inch Beam-Column Specimens

Specimen	δ	P_{Test}	P_{AISI}	P_{CSA}	P_{Theory}		$\frac{P_{Test}}{P_{AISI}}$	$\frac{P_{Test}}{P_{CSA}}$	$\frac{P_{Test}}{P_{Theory}}$	
					Eq. 3.48	Eq. 3.51			Eq. 3.48	Eq. 3.51
	(in.)	(kips)	(kips)	(kips)	(kips)	(kips)				
(1)	(2)	(3)	(4)	(5)	(6)	(7)	(8)	(9)	(10)	(11)
2.7-0.00-3[a]	0.10	6.50	1.46	1.46	3.43	4.64	4.46	4.45	1.89	1.40
2.7-0.00-3[b]	0.10	7.00	7.17	7.20	4.33	6.06	0.98	0.97	1.62	1.15
2.7-0.15-3	0.10	7.95	7.84	8.08	4.71	6.64	0.98	0.95	1.62	1.15
2.7-0.25-3	0.10	8.15	8.54	9.09	5.14	7.26	0.95	0.90	1.59	1.12
2.7-0.50-3	0.10	8.90	10.02	11.18	6.12	8.61	0.89	0.80	1.45	1.03
2.7-0.75-3	0.11	9.25	11.94	13.00	6.97	9.73	0.77	0.71	1.33	0.95
2.7-1.00-3	0.12	9.35	12.46	12.96	7.30	10.09	0.79	0.76	1.35	0.98
2.7-1.25-3	0.11	9.00	12.39	12.51	7.47	10.31	0.73	0.72	1.20	0.87
2.7-1.50-3	0.10	9.05	12.17	12.01	7.49	10.33	0.74	0.75	1.21	0.88

[a] Curved portion at the flange-edge stiffener junction not included
[b] Curved portion at the flange-edge stiffener junction included

TABLE 6.8 Experimental and Analytical Results for the 48 inch Beam-Column Specimens

Specimen	δ	P_{Test}	P_{AISI}	P_{CSA}	P_{Theory}		$\frac{P_{Test}}{P_{AISI}}$	$\frac{P_{Test}}{P_{CSA}}$	$\frac{P_{Test}}{P_{Theory}}$	
					Eq. 3.48	Eq. 3.51			Eq. 3.48	Eq. 3.51
	(in.)	(kips)	(kips)	(kips)	(kips)	(kips)				
(1)	(2)	(3)	(4)	(5)	(6)	(7)	(8)	(9)	(10)	(11)
2.7-0.00-3[a]	0.11	6.62	1.42	1.42	3.40	4.57	4.68	4.67	1.95	1.45
2.7-0.00-3[b]	0.10	6.80	7.43	7.33	4.62	6.52	0.92	0.93	1.47	1.04
2.7-0.15-3	0.10	7.65	7.42	7.30	4.65	6.56	1.03	1.05	1.65	1.17
2.7-0.25-3	0.14	7.82	8.07	8.21	5.07	7.16	0.97	0.95	1.54	1.09
2.7-0.50-3	0.17	9.36	9.85	10.45	6.11	8.60	0.97	0.90	1.53	1.09
2.7-0.75-3	0.17	9.32	11.54	12.34	6.95	9.70	0.81	0.76	1.34	0.96
2.7-1.00-3	0.18	9.70	11.93	12.29	7.26	10.06	0.81	0.79	1.34	0.96
2.7-1.25-3	0.18	9.90	11.93	11.98	7.44	10.27	0.83	0.83	1.33	0.96
2.7-1.50-3	0.18	9.62	11.78	11.56	7.44	10.26	0.82	0.83	1.29	0.94

[a] Curved portion at the flange-edge stiffener junction not included
[b] Curved portion at the flange-edge stiffener junction included

6.2 ANALYTICAL RESULTS

The North American design specifications (AISI, 1989 and CSA, 1989) were used to determine the load-carrying capacity of Z-sections and the results were compared to the experimental ones. The relevant AISI Specification (AISI, 1989) and the Canadian Standard (CSA, 1989) design provisions were discussed in Chapter 2. To predict the capacity of the specimens using the AISI Specification (1989) and CSA Standard (1989), all safety factors were removed from the calculations. The average cross sectional dimensions, given in Tables B.1 to B.8, were used in all calculations. As determined from the tension coupon tests, a yield strength of 52.07 ksi was used for the 18 inch specimens, while a 47.03 ksi was used for the 24, 48, and 54 inch specimens. Detailed calculations for the strength of typical column, beam, and beam-column sections are given in Appendix D using the AISI Specification (1989) and CSA Standard (1989), while they are given in Appendix E using the theoretical models.

The ratios between the experimental and analytical results, for each series of specimens, are shown in Figures 6.6 to 6.15 as functions of the overall width of edge stiffener. Figures 6.6, 6.7, and 6.8 refer to the 18 inch column specimens with nominal flange flat widths of 1.5, 2.0, and 2.5 inches, respectively, while Figures 6.9 and 6.10 refer to the 24 and 48 inch column specimens, respectively. The effect of the overall edge stiffener width on the bending capacity of beam specimens is shown in Figure 6.11. Figures 6.12 to 6.15 show the effect of the edge stiffener on the load-carrying capacity of the 24 and 48 inch beam-column specimens.

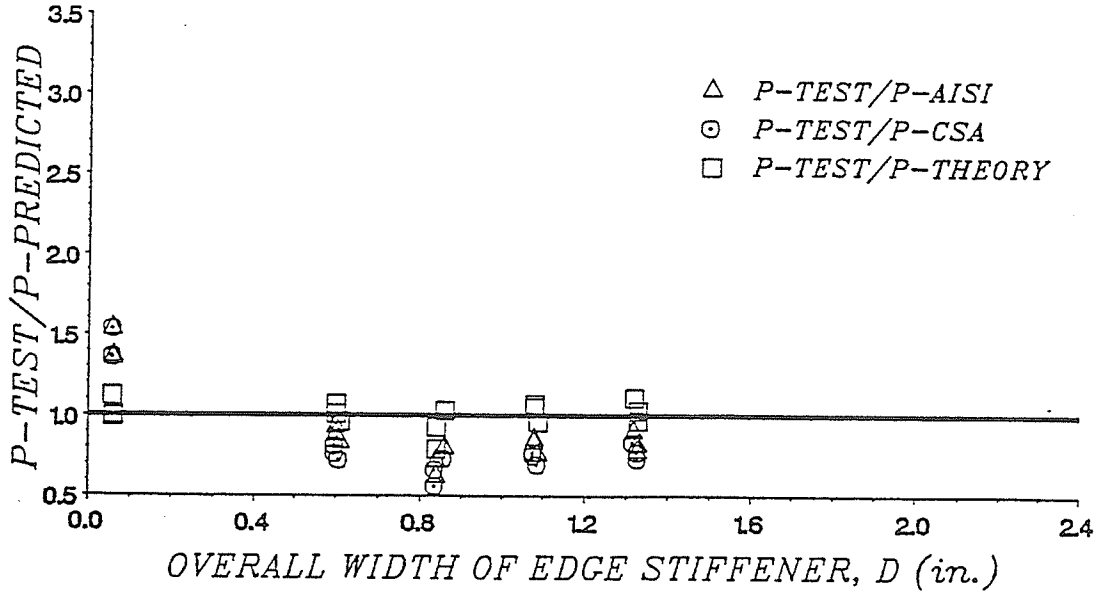

Figure 6.6 Analytical Load Ratios for the 18 inch Column Specimens with 1.5 inch Flat Width of Flanges

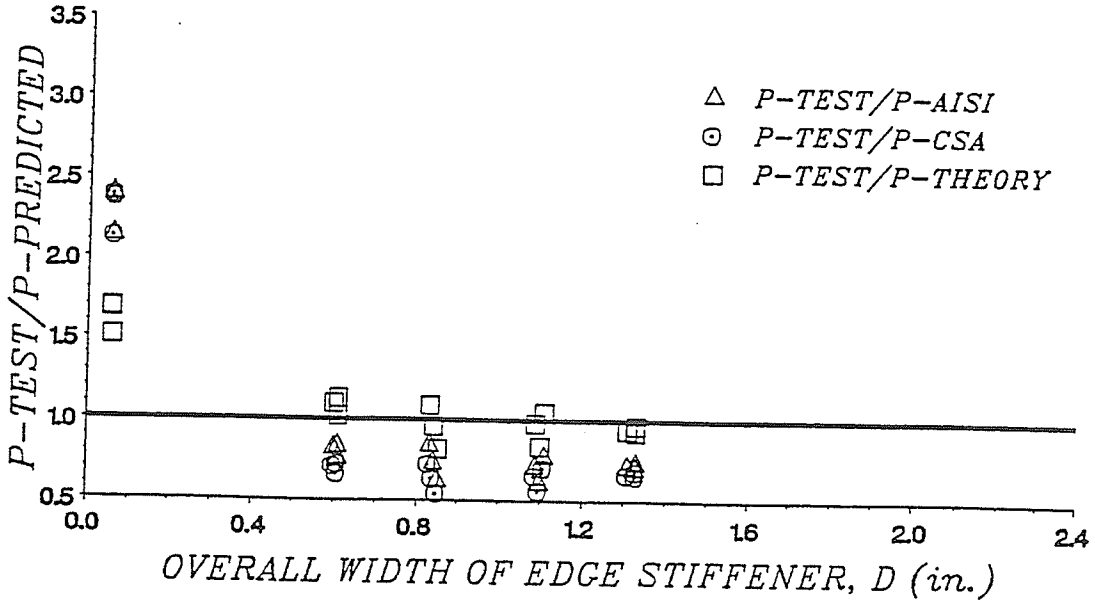

Figure 6.7 Analytical Load Ratios for the 18 inch Column Specimens with 2.0 inch Flat Width of Flanges

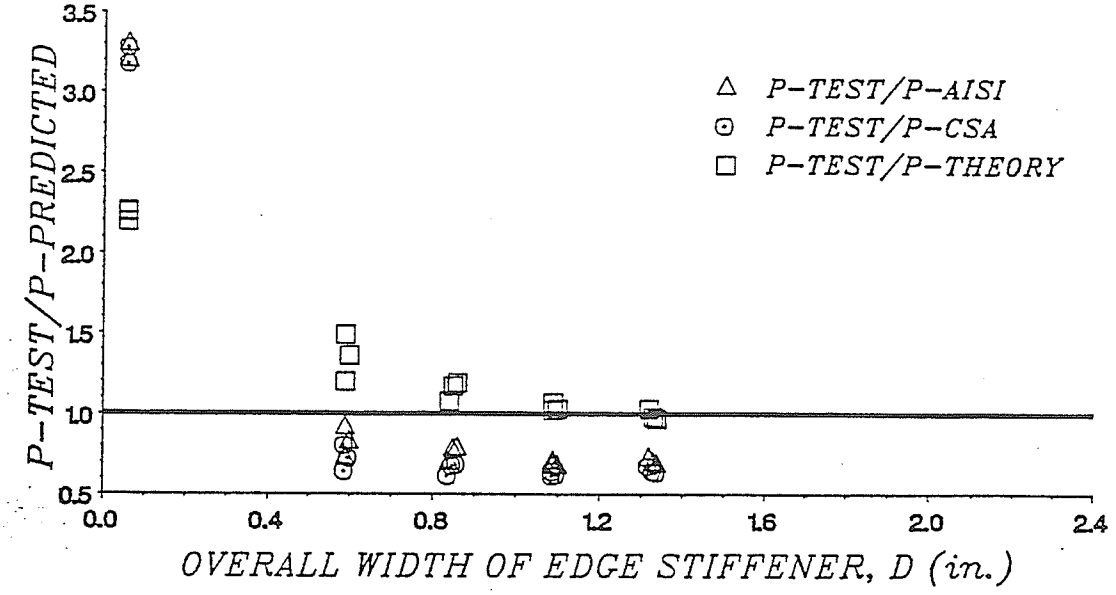

Figure 6.8 Analytical Load Ratios for the 18 inch Column Specimens with 2.5 inch Flat Width of Flanges

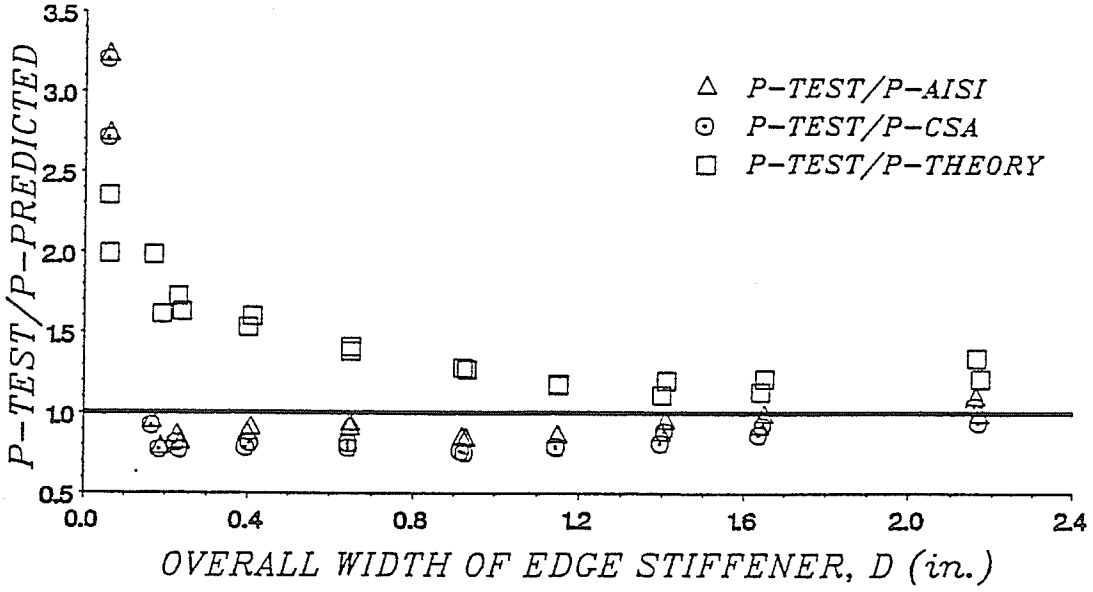

Figure 6.9 Analytical Load Ratios for the 24 inch Column Specimens

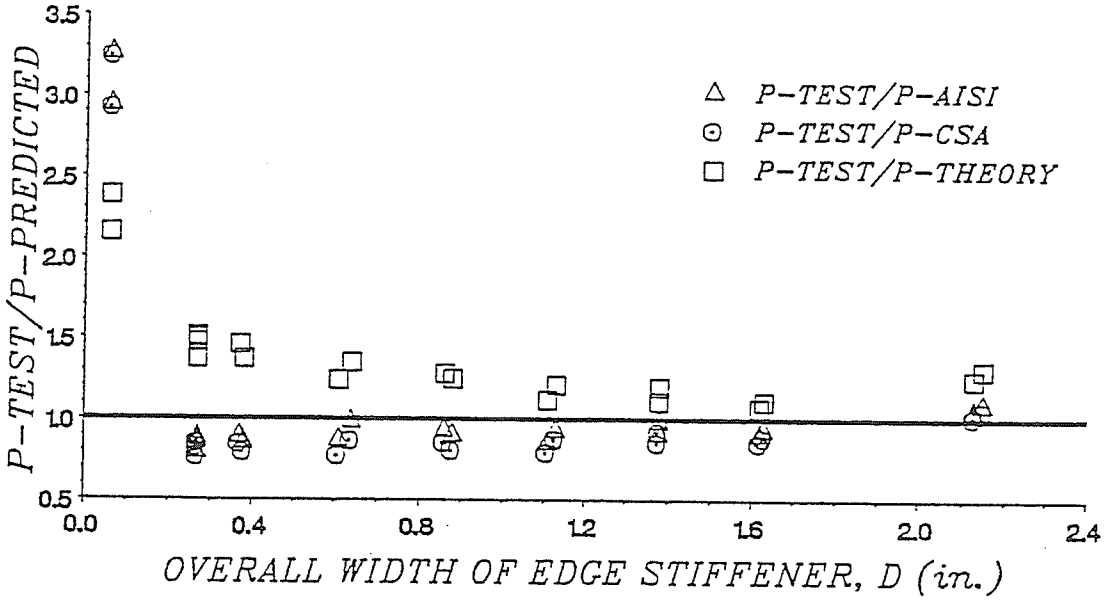

Figure 6.10 Analytical Load Ratios for the 48 inch Column Specimens

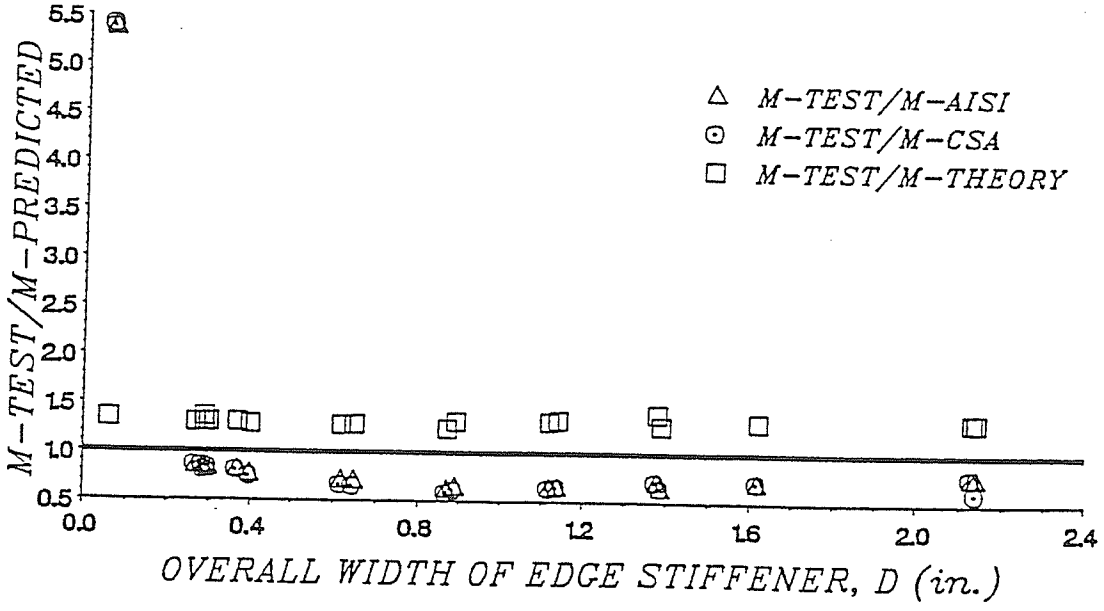

Figure 6.11 Analytical Load Ratios for the 54 inch Beam Specimens

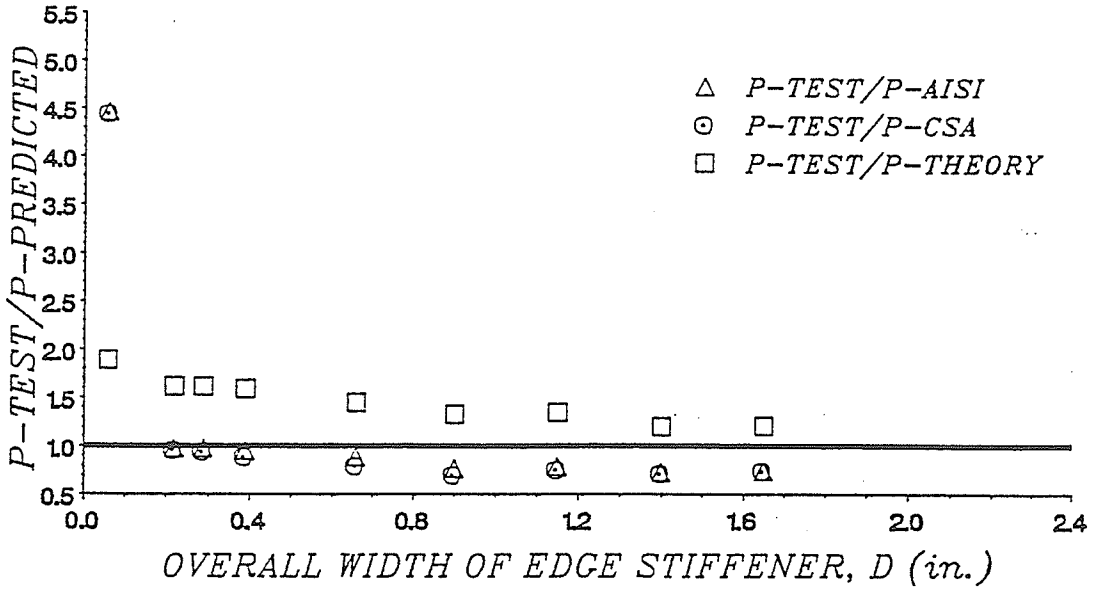

Figure 6.12 Analytical Load Ratios for the 24 inch Beam-Column Specimens (Theoretical Equation 3.48)

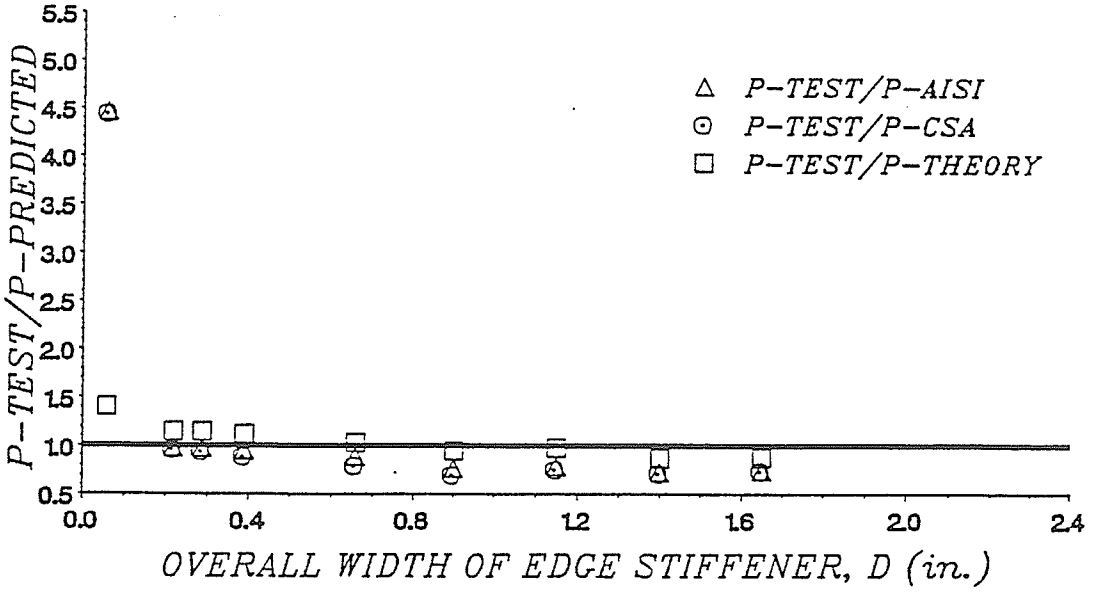

Figure 6.13 Analytical Load Ratios for the 24 inch Beam-Column Specimens (Theoretical Equation 3.51)

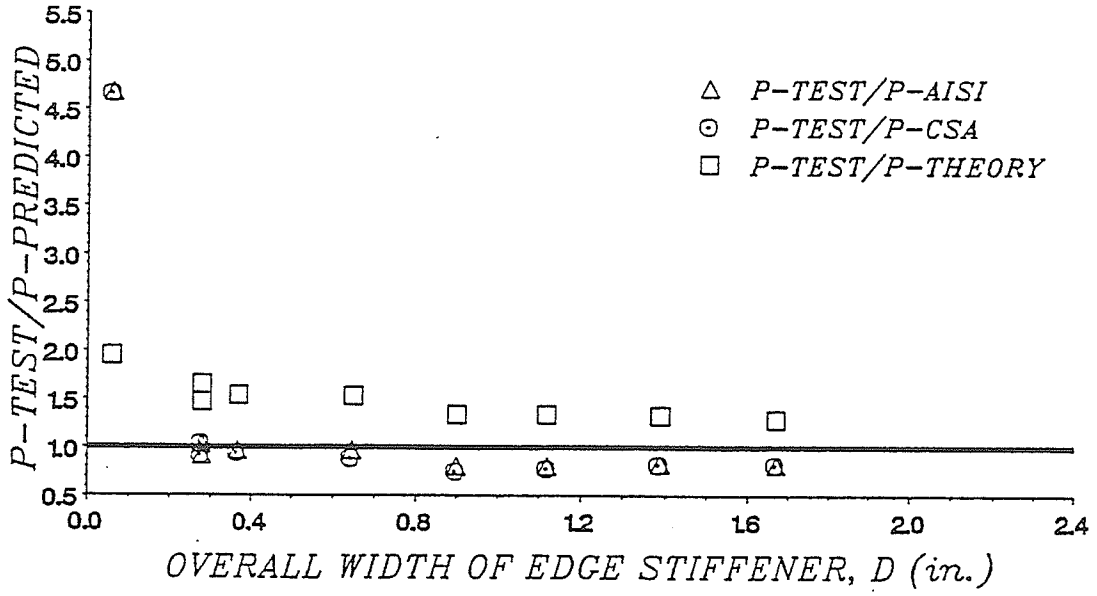

Figure 6.14 Analytical Load Ratios for the 48 inch Beam-Column Specimens (Theoretical Equation 3.48)

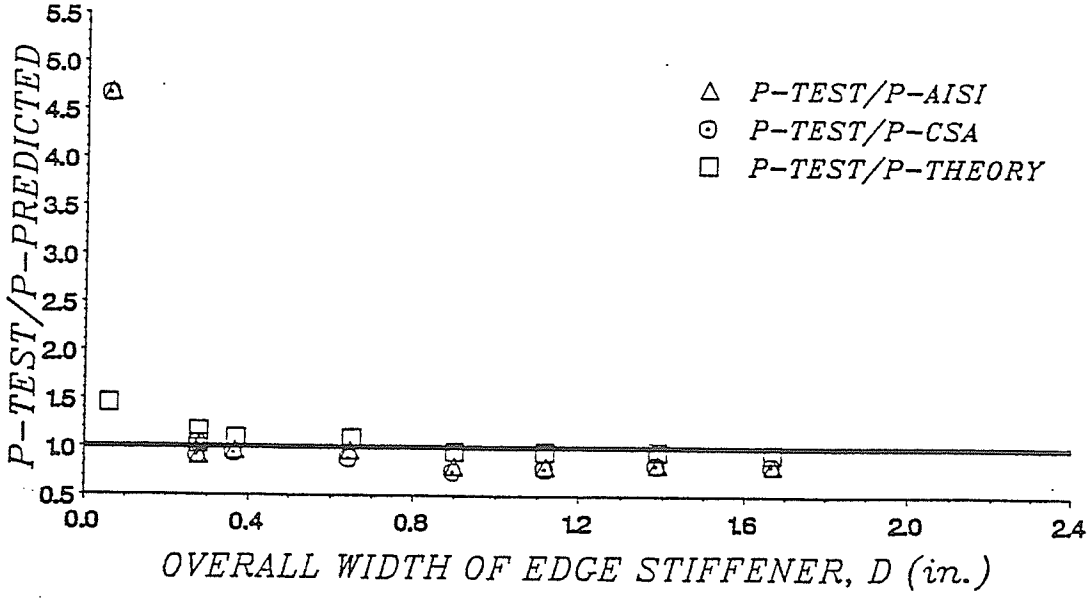

Figure 6.15 Analytical Load Ratios for the 48 inch Beam-Column Specimens (Theoretical Equation 3.51)

The experimental results along with the analytical results are also shown as functions of the overall width of edge stiffener in Figures 6.16 to 6.25. In these figures, the nominal cross section dimensions of the Z-section specimens and the specified yield strength of material (50 ksi) were employed in constructing the analytical curves.

According to the analytical curves for those sections without edge stiffeners, where the flanges were classified by the AISI Specification (1989) and CSA Standard (1989) as unstiffened elements, the critical stress was limited to the local buckling stress of the compression flanges. Thus, the capacity of the members was computed on the basis of the local buckling stress of the compression flanges and either the unreduced cross section for compression members or the unreduced elastic section modulus for bending members. The computed capacity of members was therefore lower than the experimental capacity. The difference between the methods used to compute the capacities of sections with edge stiffeners and sections without edge stiffeners also resulted in the discontinuity shown in the AISI and CSA curves of Figures 6.16 to 6.25.

To evaluate the analytical results, the average and standard deviation of the ratios between the analytical results and the experimental results were used. Since a small number of specimens for each series tests was conducted, the standard deviation tends to be larger than it would normally be expected. A brief discussion of the comparison between the experimental and analytical results is given in the following sections.

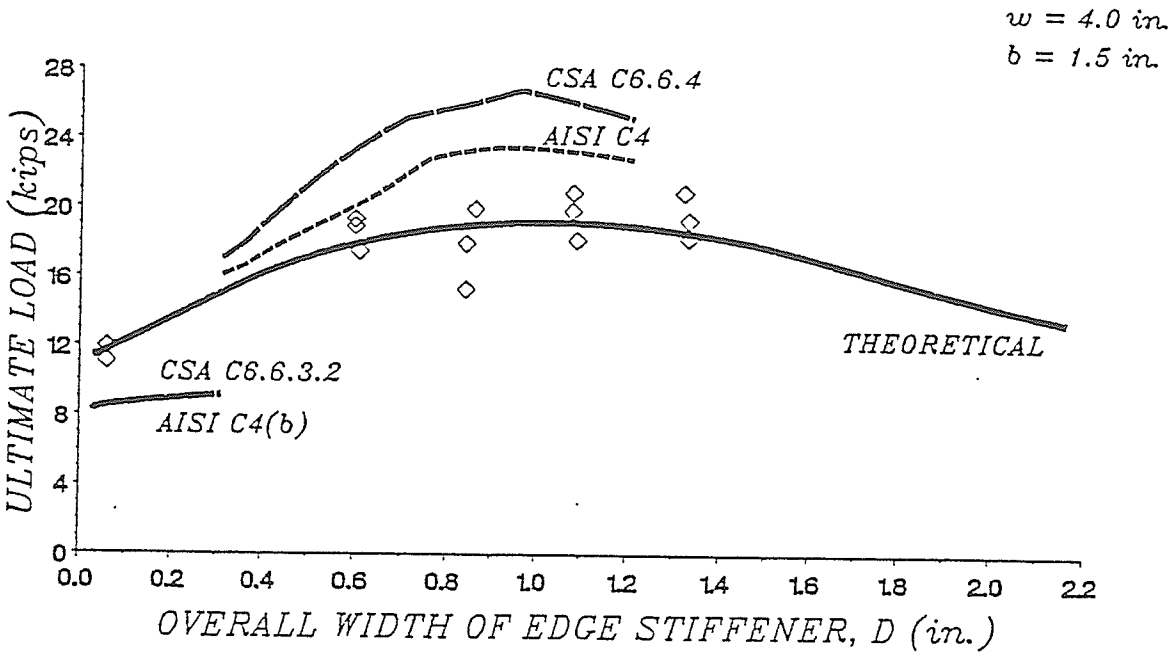

Figure 6.16 Experimental and Analytical Loads for the 18 inch Column Specimens with 1.5 inch Flat Width of Flanges

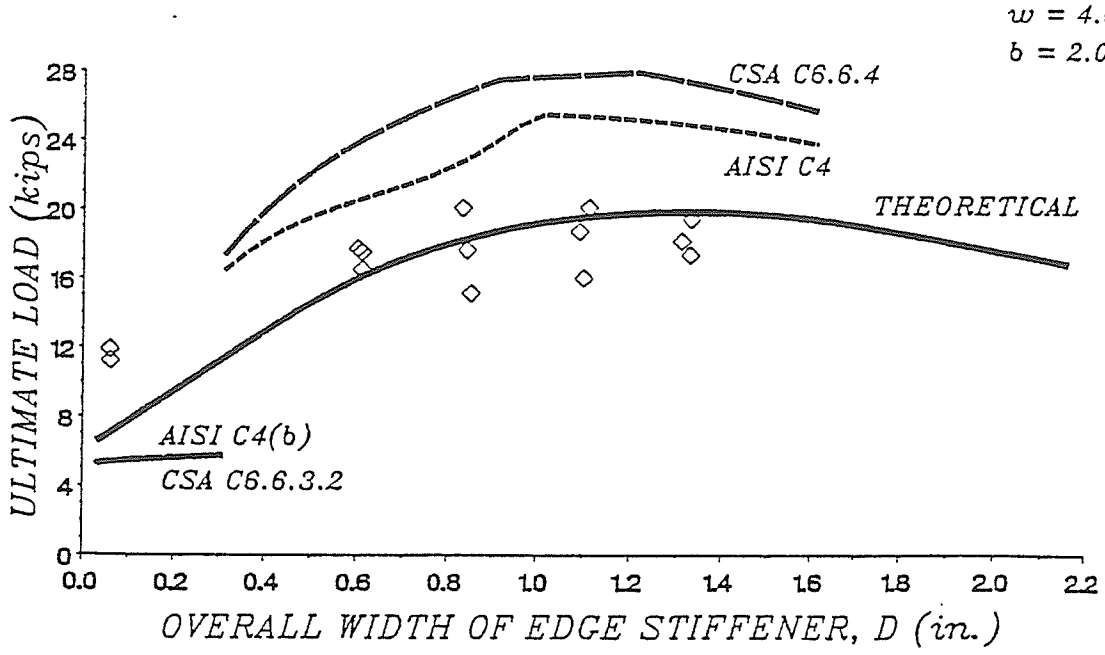

Figure 6.17 Experimental and Analytical Loads for the 18 inch Column Specimens with 2.0 inch Flat Width of Flanges

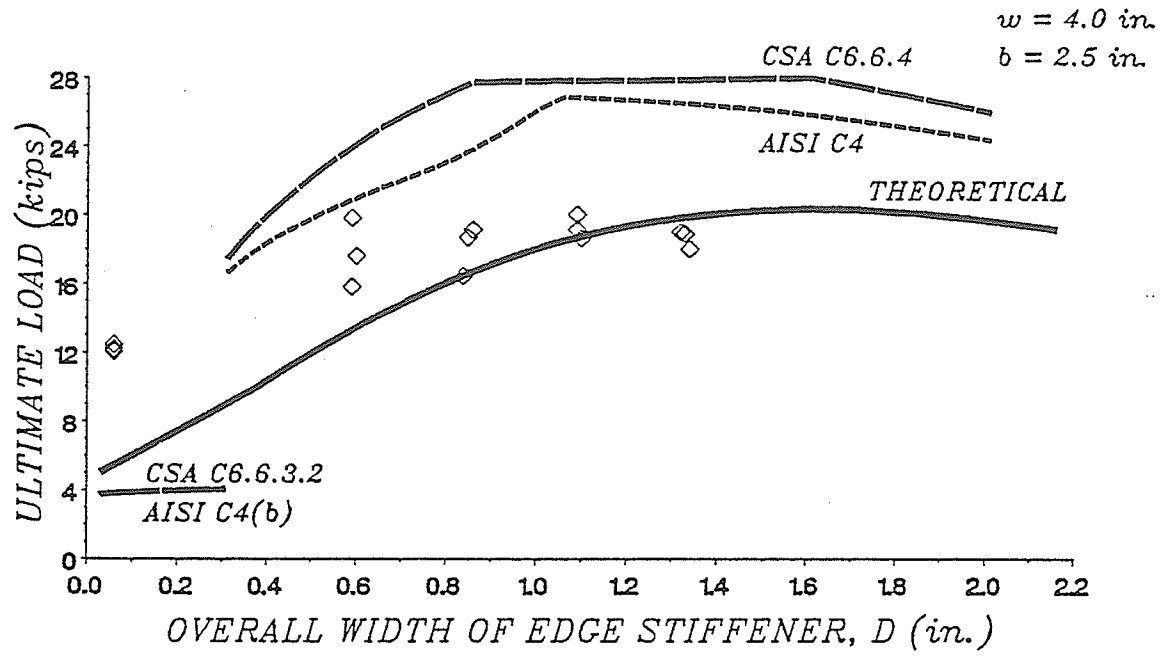

Figure 6.18 Experimental and Analytical Loads for the 18 inch Column Specimens with 2.5 inch Flat Width of Flanges

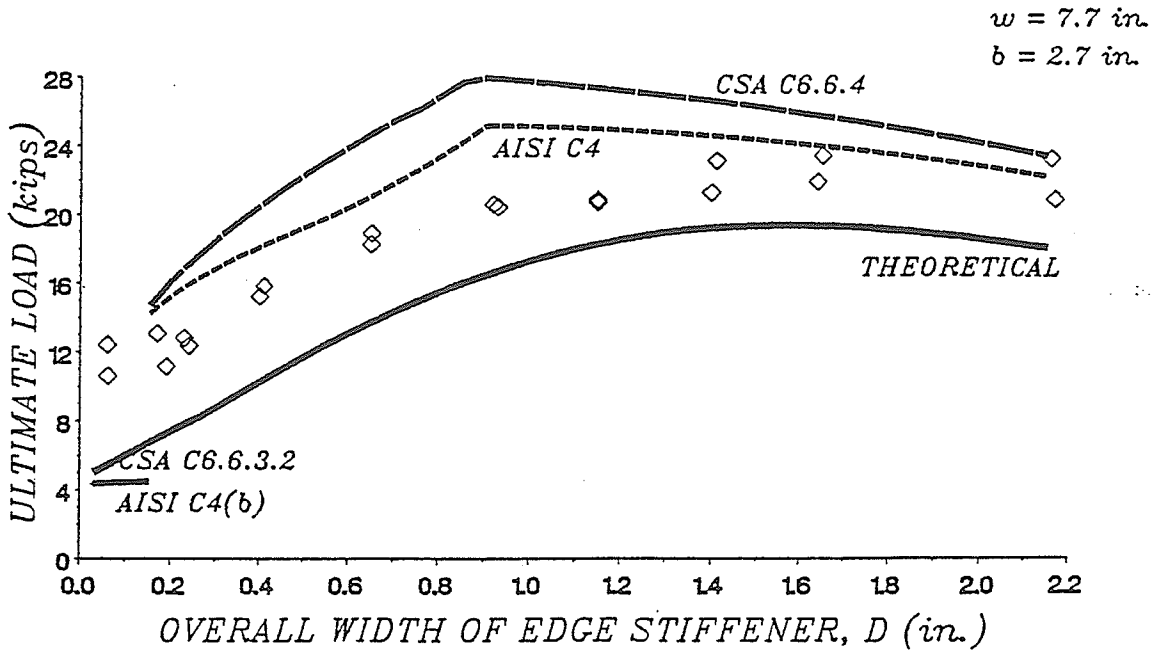

Figure 6.19 Experimental and Analytical Loads for the 24 inch Column Specimens

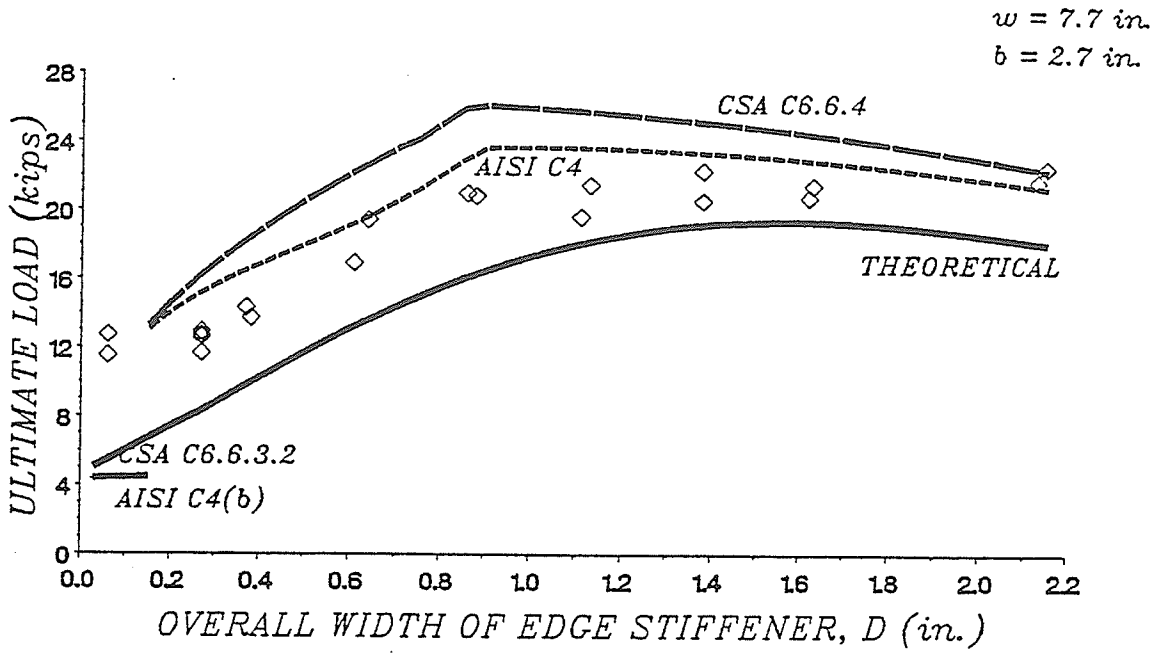

Figure 6.20 Experimental and Analytical Loads for the 48 inch Column Specimens

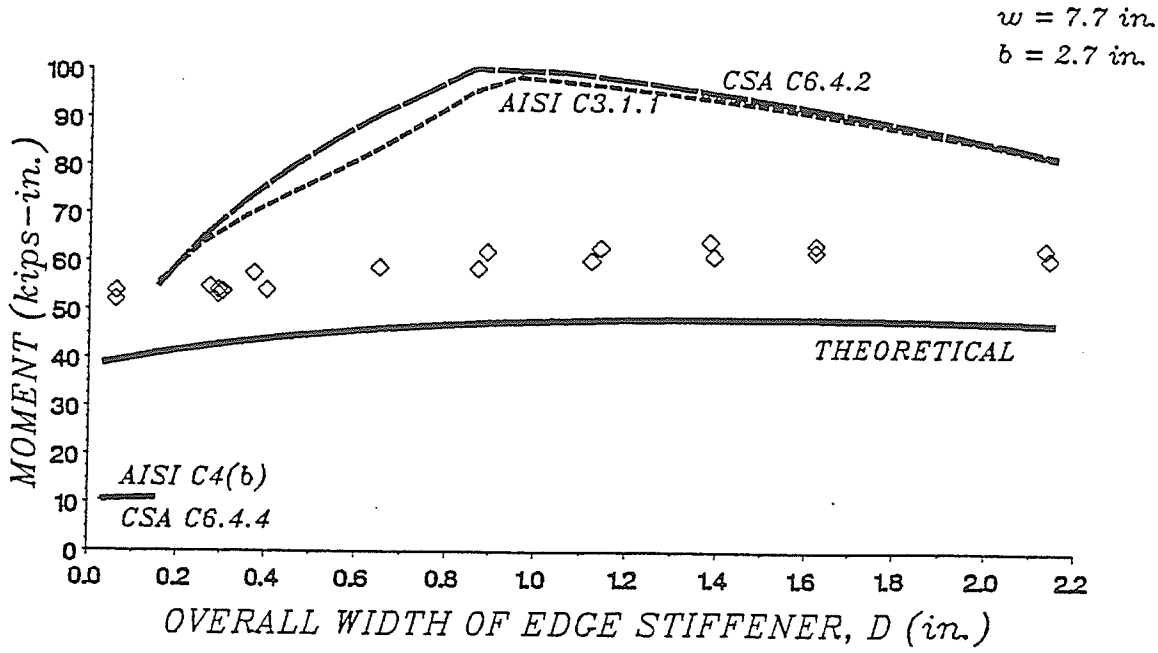

Figure 6.21 Experimental and Analytical Loads for the 54 inch Beam Specimens

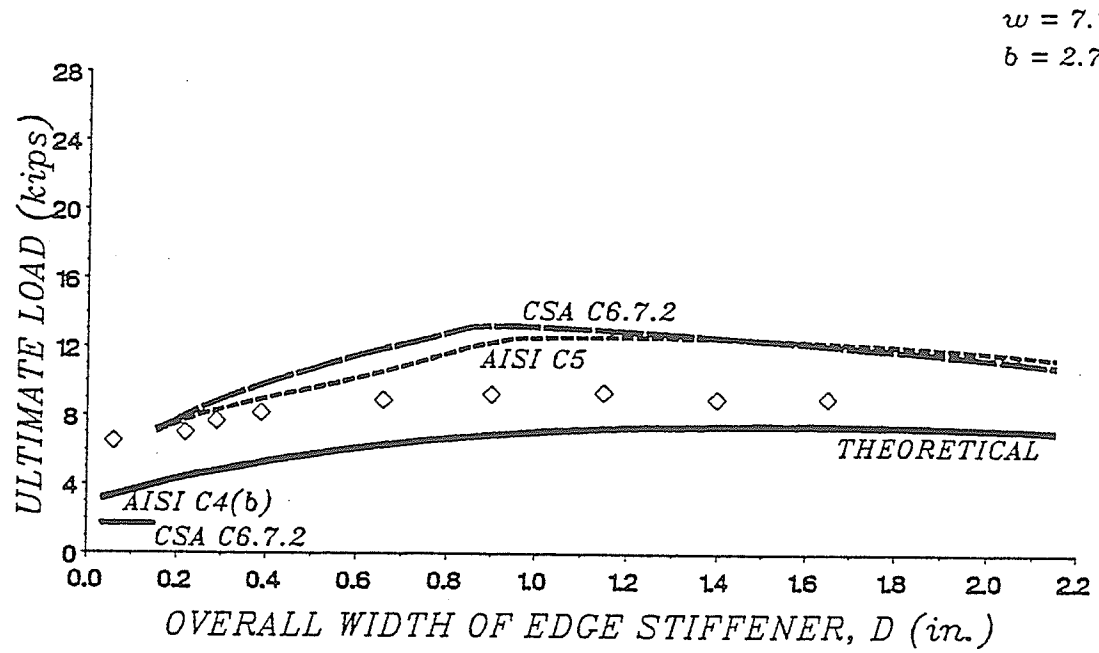

Figure 6.22 Experimental and Analytical Loads for the 24 inch Beam-Column Specimens (Theoretical Equation 3.48)

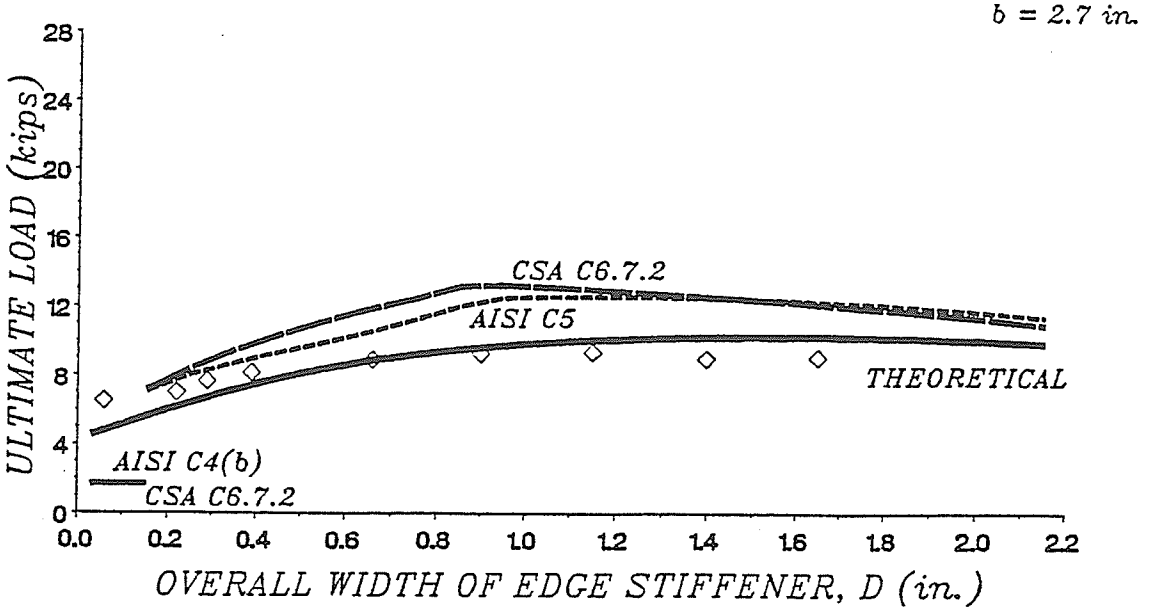

Figure 6.23 Experimental and Analytical Loads for the 24 inch Beam-Column Specimens (Theoretical Equation 3.51)

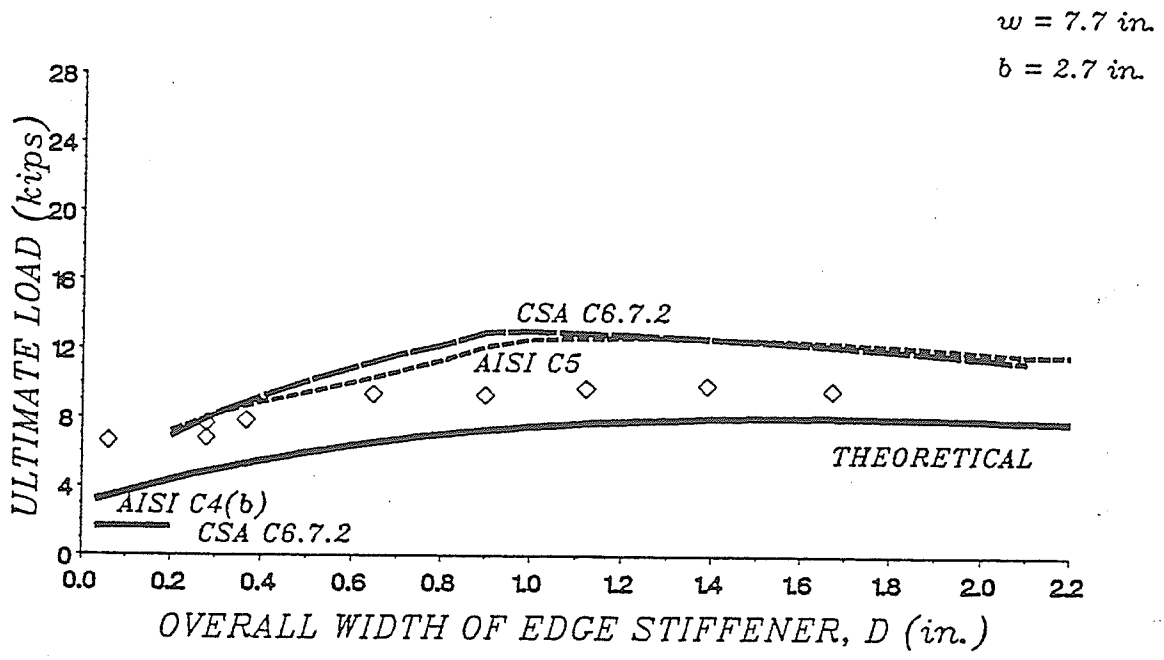

Figure 6.24 Experimental and Analytical Loads for the 48 inch Beam-Column Specimens (Theoretical Equation 3.48)

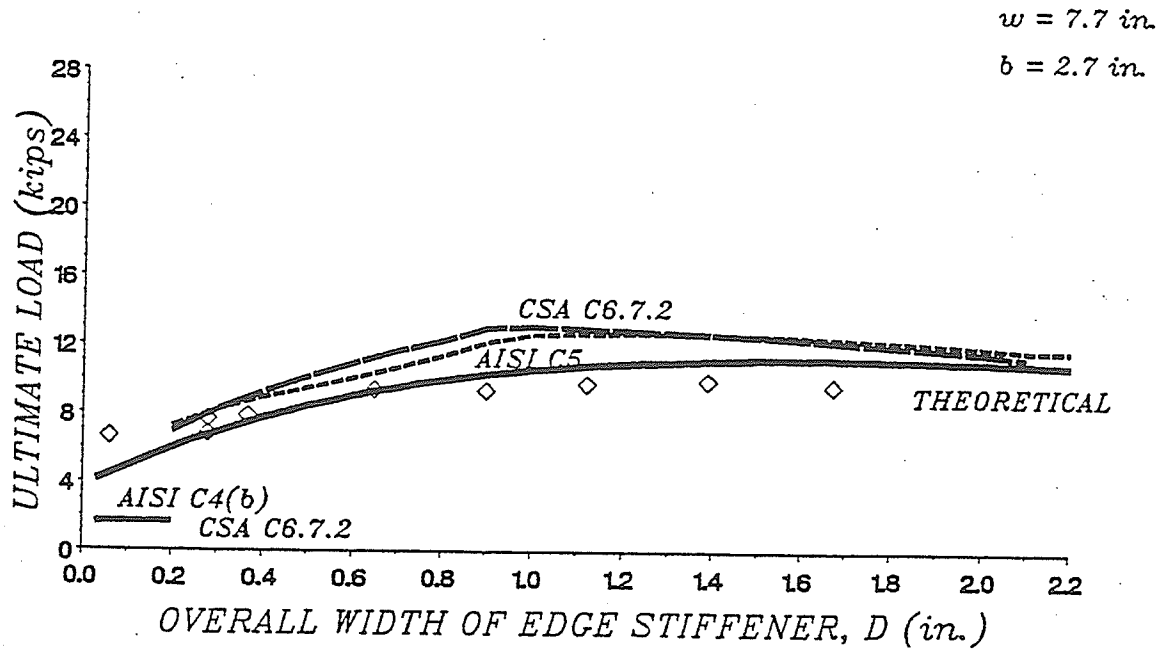

Figure 6.25 Experimental and Analytical Loads for the 48 inch Beam-Column Specimens (Theoretical Equation 3.51)

6.2.1 AISI Specification (1989)

In the case of column specimens, Tables 6.1 to 6.5 show that the predicted loads computed according to the AISI Specification (1989) for sections without edge stiffeners were much lower than the experimental results. However, for sections with edge stiffeners, the ratios between the experimental and predicted results were found to be less than 1.0, indicating a degree of unconservatism in the Specification.

For the 18 inch column specimens with a flange width of 1.50 inches, the ratio between the experimental and predicted results (AISI, 1989) ranged from 1.37 to 1.55 for specimens without edge stiffeners, while for the sections with edge stiffeners the ratio ranged from 0.64 to 0.95 (ave = 0.83; std dev = 0.084). Similarly, for the sections with 2.00 inch flanges the ratio ranged from 2.15 to 2.41 for the sections without edge stiffeners and from 0.63 to 0.86 for the sections with edge stiffeners (ave = 0.76; std dev = 0.074). For the sections with 2.50 inch flanges, the ratio for the sections without edge stiffeners ranged from 3.21 to 3.31, while for the sections with edge stiffeners the ratio ranged from 0.69 to 0.93 (ave = 0.76; std dev = 0.073).

The results of the 18 inch column specimens indicate that the predicted loads for the sections without edge stiffeners were very conservative. The predicted loads varied from 30% to 73% of the experimental loads. On the other hand, the results for the sections with edge stiffeners were unconservative and the predicted loads varied from 105% to 159% of the experimental loads.

For the 24 inch column specimens, the ratio of the experimental and predicted results, for the sections without edge stiffeners, ranged from 2.75 to 3.24, while for the sections with edge stiffeners the ratio ranged from 0.80 to 1.11 (ave = 0.92, std dev = 0.074). For the 48 inch column specimens, the ratio for the sections without edge stiffeners ranged from 2.96 to 3.28, while for the sections with edge stiffeners the ratio ranged from 0.81 to 1.11 (ave = 0.93, std dev = 0.074).

In summary, the AISI Specification (1989) underestimated the load-carrying capacity of the column specimens without edge stiffeners by an amount ranging from 27% to 70% of the experimental results, while it overestimated the load-carrying capacity of the column specimens with edge stiffeners by an amount ranging from -10% to 59% of the experimental results.

In the case of beam specimens, the ratios between the experimental and predicted results obtained from the AISI Specification (1989) are shown in Figure 6.11 as a function of the overall width of edge stiffener. In this figure, the ratios for those specimens with edge stiffeners are less than 1.0, indicating that the Specification overestimated their capacity. The ratio between the experimental and predicted results, for the sections without edge stiffeners, ranged from 5.37 to 5.39, while for the sections with edge stiffeners the ratio ranged from 0.64 to 0.87 (ave = 0.75; std dev = 0.078). In this case, the Specification (AISI, 1989) underestimated the bending capacity of the beam specimens without edge stiffeners by as much as 81% of the experimental results, while it overestimated the capacity of the specimens with edge stiffeners by an amount ranging from 15% to 56% of the

experimental results.

In the case of beam-column specimens, Tables 6.7 and 6.8 show that the predicted loads (AISI, 1989) for sections without edge stiffeners were much lower than those sections with edge stiffeners and were very conservative when compared with the experimental loads. However, for sections with edge stiffeners, the predicted loads were higher than the experimental results, indicating a degree of unconservatism in the Specification.

For the 24 inch beam-column specimens, the ratio between the experimental and predicted result was 4.46 for the specimen without edge stiffeners, while for the specimens with edge stiffeners the ratio ranged from 0.73 to 0.98 (ave = 0.85; std dev = 0.108). For the 48 inch beam-column specimens, the ratio for the section without edge stiffeners was 4.68, while for the sections with edge stiffeners the ratio ranged from 0.81 to 1.03 (ave = 0.90; std dev = 0.088).

Equation C4-5 (AISI, 1989) considers the local buckling capacity of the unstiffened elements of the sections as the load-carrying capacity that the sections can carry. Ignoring the restriction imposed by Equation C4-5 and taking into account the post-buckling capacity of the sections, the ratio between the experimental and predicted results, for the 24 inch beam-column specimens, ranged from 0.73 to 1.04 (ave = 0.87; std dev = 0.119) and for the 48 inch beam-column specimens the ratio ranged from 0.81 to 1.11 (ave = 0.92; std dev = 0.109). Therefore, the elimination of Equation C4-5 in the Specification gives a better representation of the capacity of these sections.

In summary, the AISI Specification (1989) underestimated the load-carrying capacity of the beam-column specimens without edge stiffeners by approximately 79% of the experimental results, while it overestimated the load-carrying capacity of the beam-column specimens with edge stiffeners by an amount ranging from -3% to 37% of the experimental results.

6.2.2 CSA Standard (1989)

In the case of column specimens, the predicted loads (CSA, 1989) given in Tables 6.1 to 6.5 for sections without edge stiffeners were much lower than the experimental loads. However, for sections with edge stiffeners, the predicted loads were higher than the experimental loads, indicating a degree of unconservatism in the Standard.

For the 18 inch column specimens with a flange width of 1.50 inches, the ratio between the experimental and predicted results, for the sections without edge stiffeners, ranged from 1.36 to 1.54, while for the sections with edge stiffeners the ratio ranged from 0.57 to 0.84 (ave = 0.74; std dev = 0.072). Similarly, for the sections with 2.00 inch flanges, the ratio ranged from 2.13 to 2.39 for the sections without edge stiffeners and from 0.55 to 0.73 for the sections with edge stiffeners (ave = 0.67; std dev = 0.058). For the sections with 2.50 inch flanges, the ratio for the sections without edge stiffeners ranged from 3.18 to 3.28, while that for the sections with edge stiffeners ranged from 0.62 to 0.81 (ave = 0.67; std dev = 0.054).

The results indicate that the predicted loads for the sections without edge stiffeners were very conservative. The predicted loads varied from 30% to 74% of the experimental loads. On the other hand, the results for the sections with edge stiffeners were unconservative and the predicted loads varied from 119% to 182% of the experimental loads.

For the 24 inch column specimens, the ratio between the experimental and predicted results, for the sections without edge stiffeners, ranged from 2.72 to 3.21, while for the sections with edge stiffeners the ratio ranged from 0.76 to 1.05 (ave = 0.84; std dev = 0.079). For the 48 inch column specimens, the ratio for the sections without edge stiffeners ranged from 2.93 to 3.25, while for the sections with edge stiffeners the ratio ranged from 0.77 to 1.06 (ave = 0.87; std dev = 0.075).

In summary, the CSA Standard (1989) underestimated the load-carrying capacity of the column specimens without edge stiffeners by an amount ranging from 26% to 70% of the experimental results, while it overestimated the load-carrying capacity of the column specimens with edge stiffeners by an amount ranging from -6% to 82% of the experimental results.

In the case of beam specimens, the ratio between the experimental and predicted results, for the sections without edge stiffeners, ranged from 5.38 to 5.41, while for the sections with edge stiffeners the ratio ranged from 0.60 to 0.88 (ave = 0.73; std dev = 0.090). In this case, the CSA Standard (1989) underestimated the bending capacity of the beam specimens without edge stiffeners by as much as 82% of the experimental results, while it overestimated the capacity of the sections with

edge stiffeners by an amount ranging from 14% to 67% of the experimental results.

In the case of beam-column specimens, Tables 6.7 and 6.8 show that the predicted loads (CSA, 1989) for sections without edge stiffeners were much lower than the experimental loads. However, for the sections with edge stiffeners, the predicted loads were higher than the experimental results, indicating a degree of unconservatism in the Standard.

One 24 inch and one 48 inch beam-column specimens without edge stiffeners were tested. The ratios between the experimental and predicted results were 4.45 and 4.67, respectively. The remaining specimens had edge stiffeners, the ratio ranged from 0.71 to 0.97 (ave = 0.82; std dev = 0.105) for the 24 inch specimens and from 0.76 to 1.05 (ave = 0.88; std dev = 0.096) for the 48 inch specimens.

Clause 6.6.3.2 of CSA Standard (1989) considers the local buckling capacity of unstiffened elements of sections as the load-carrying capacity of these sections. Ignoring the restriction imposed by Clause 6.6.3.2 and taking into account the post-buckling strength of the sections, the ratio between the experimental and predicted results, for the 24 inch beam-column specimens, ranged from 0.71 to 1.03 (ave = 0.84; std dev = 0.120), while for the 48 inch beam-column specimens the ratio ranged from 0.76 to 1.15 (ave = 0.91; std dev = 0.127).

In summary, the CSA Standard (1989) underestimated the load-carrying capacity of the beam-column specimens without edge stiffeners by approximately 79% of the experimental results, while it overestimated the load-carrying capacity of the beam-column specimens with edge stiffeners by an amount ranging from -5%

to 41% of the experimental results.

6.2.3 Theoretical Models

For the 18 inch column specimens with a flange width of 1.50 inches, the ratio between the experimental and theoretical results ranged from 0.79 to 1.12 (ave = 1.01; std dev = 0.082). for the sections with 2.00 inch flanges, the ratio ranged from 0.82 to 1.69 (ave = 1.11; std dev = 0.282), while for sections with 2.50 inch flanges the ratio ranged from 0.97 to 2.26 (ave = 1.35; std dev = 0.477). In the case of the 24 inch column specimens, the ratio ranged from 1.11 to 2.35 (ave = 1.47; std dev = 0.338), while for the 48 inch column specimens the ratio ranged from 1.07 to 2.38 (ave = 1.39; std dev = 0.331).

In summary, the theoretical model for columns yield results which ranged from 42% to 127% of the experimental results. On the average, the theoretical values were 78% of the experimental results. The results indicate that, in general, the predicted loads are in good agreement with the experimental loads and, in most cases, are conservative.

In the case of beam specimens, a comparison between the experimental and theoretical results indicate that the values predicted by the simplified theoretical model (Equation 3.32) were as much as 29% lower than the experimental results. The ratio between the experimental and theoretical results ranged from 1.25 to 1.41 (ave = 1.32; std dev = 0.034). The simplified theoretical model resulted in bending capacities which ranged from 71% to 80% of the experimental results. The results

indicate that the predicted bending capacities are in good agreement with the experimental bending capacities, in all cases, are conservative.

In the case of beam-column specimens, the experimental results were compared to the predicted results obtained from the interaction Equations 3.48 and 3.51. The ratio between the experimental and theoretical results, for the 24 inch specimens, ranged from 1.20 to 1.89 (ave = 1.47; std dev = 0.227) when Equation 3.46 was used. For the 48 inch specimens, the ratio ranged from 1.29 to 1.95 (ave = 1.49; std dev = 0.210) when the same equation was used. Using Equation 3.51, the ratio ranged from 0.87 to 1.40 (ave = 1.06; std dev = 0.167) for the 24 inch specimens, and from 0.94 to 1.45 (ave = 1.07; std dev = 0.162) for the 48 inch specimens. Thus, Equation 3.51 gave much better approximations of the member capacity than Equation 3.48.

Equation 3.48 estimated the load-carrying capacity of the specimens to be in the range of 51% to 83% of the experimental loads, while Equation 3.51 estimated the load-carrying capacity of the specimens to be in the range of 69% to 115% of the experimental loads. On the average, the theoretical values obtained through Equations 3.48 and 3.51 were 67% and 94% of the experimental values, respectively.

It should be noted that the theoretical models do not limit the maximum ratios of D/b_f and d/t which is the case with the design specifications. Also, the theoretical models do not differentiate between sections with edge stiffeners and section without edge stiffeners. Thus, in Figures 6.16 to 6.25 the discontinuity in the theoretical curve between unstiffened and stiffened flange sections observed in the

design guideline predictions does not exist.

6.2.4 ANSYS Analysis

As described in Chapter 4, the ANSY results in somewhat lower than that measured during testing. This could be attributed to the fact that the ANSYS program does not account for any post-buckling capacity and also due to the type of support conditions assumed in the models. The ANSYS analysis, however, proved to be a function of the type of computer facility. The higher capacity of computer the shorter time is required.

CHAPTER 7

CONCLUSIONS AND RECOMMENDATIONS

7.1 CONCLUSIONS

On the basis of the findings from this research, a number of conclusions were drawn as follows:

1) Observations made during the testing of the specimens indicated that the failure mode of the sections was by distortional buckling of the flange-edge stiffener component.

2) Design specifications (AISI, 1989 and CSA, 1989) underestimated the load-carrying capacity of the sections tested without edge stiffeners, while they overestimated the load-carrying capacity of the sections with edge stiffeners. The amounts by which these specifications overestimated the capacity of the sections tested are shown in Table 7.1. The AISI Specification (1989), in general, produced more conservative results than the CSA Standard (1989).

3) The design specifications (AISI, 1989 and CSA, 1989) limit the ratios of D/b_f and d/t. A limited number of specimens which exceeded these limits were tested. The results indicated that the design guidelines are also applicable beyond these limits.

4) In general, the theoretical models yielded conservative results for the load-carrying capacity of Z-sections, as shown in Table 7.1.

TABLE 7.1 Comparison Between Analytical and Experimental Results

SPECIMEN / ANALYSIS	COLUMNS (%)	BEAMS (%)	BEAM-COLUMNS (%)
AISI	17	33	15
CSA	44	37	29
ANSYS	-18	-1	-36
THEORY	-22*	-24**	-33***, -6****

* EQ. 3.26
** EQ. 3.32
*** EQ. 3.48
**** EQ. 3.51

5) The theoretical models for column, beam, and beam-column provide a more realistic representation of member behaviour for those sections where local buckling of the web preceded distortional buckling of the flange-edge stiffener component.

6) For beam-column tests, the quadratic Equation 3.51 gave a better correlation with the experimental results as compared to the ones obtained from the linear Equation 6.48.

7) Results for column, beam, and beam-column specimens obtained through the ANSYS finite element analysis program were conservative, as shown in Table 7.1. The ANSYS analysis gave good results for the limited number of cold-formed steel sections checked in this study.

7.2 RECOMMENDATIONS

Based on the findings from the present study, it was recommended that:

1) The specifications (AISI, 1989 and CSA, 1989) for the design of cold-formed steel structural members be revised to reflect the member behaviour more realistically. For the case of sections with partially stiffened flanges, it is questionable whether any significant post-buckling capacity is developed. It is, thus, recommended that distortional buckling of the compression portion be used as the basis for determining the capacity of cold-formed sections. However, in the case of beams and beam-columns, further experimental investigation is recommended to

justify the proposed simplified theoretical models.

2) The limitation in the design guidelines for the maximum ratios of D/b_f and d/t should be reviewed and modified.

3) The treatment of Z-sections with unstiffened flange predicted in accordance with specifications should be reviewed.

4) The effect of sloping edge stiffeners on the distortional buckling strength of cold-formed sections should be examined.

5) The use of the ANSYS program as an analytical tool for Z-sections should be further explored.

REFERENCES

American Iron and Steel Institute, (1980), "The Design and Fabrication of Cold-Formed Steel Structures," N.W., Washington, D.C.

American Iron and Steel Institute, (1980), "Specification for the Design of Cold-Formed Steel Structural Members," N.W., Washington, D.C.

American Iron and Steel Institute, (1983), "Cold-Formed Steel Design Manual," N.W., Washington, D.C.

American Iron and Steel Institute, (1986), "Specification for the Design of Cold-Formed Steel Structural Members," Part I of Cold-Formed Steel Design Manual, N.W., Washington, D.C.

American Iron and Steel Institute, (1989), "Specification for the Design of Cold-Formed Steel Structural Members," Part I of Cold-Formed Steel Design Manual, N.W., Washington, D.C.

American Society for Testing and Materials, (1985), "ASTM E 8M-85 Standard Methods for Tension Testing of Metallic Materials", Philadelphia.

American Society for Testing and Materials, (1991), "ASTM A607-90a Standard Specification for Steel, Sheet and Strip, High-Strength, Low-Alloy, Columbium or Vanadium, or Both, Hot-Rolled and Cold-Rolled," Philadelphia.

Canadian Sheet Steel Building Institute, (1982), "Standard for Steel Building Systems," Publication 38.4-82, Ontario, Canada.

Canadian Standard Association, (1980), "Cold-Formed Steel Structural Members," CAN/CSA-S136-M80 Structural Design, Rexdale (Toronto), Ontario, Canada.

Canadian Standard Association, (1984), "Cold-Formed Steel Structural Members," CAN/CSA-S136-M84 Structural Design, Rexdale (Toronto), Ontario, Canada.

Canadian Standard Association, (1989), "Cold-Formed Steel Structural Members," CAN/CSA-S136-M89 Structural Design, Rexdale (Toronto), Ontario, Canada.

Charnvarnichborikarn, P., and Polyzois, D., (1990), "Experimental and Analytical Investigation of Cold-Formed Z-Section Steel Members in Compression," Research Report, Department of Civil Engineering, The University of Manitoba, Winnipeg, Manitoba, Canada.

Charnvarnichborikarn, P., and Polyzois, D., (1991), "New Approach for Cold-Formed Steel Z-Section Columns," The 13th Canadian Congress of Applied Mechanics, CANCAM'91, June 2-6, pp. 338-339.

Charnvarnichborikarn, P., and Polyzois, D., (1991), "Experimental and Analytical Investigation of Cold-Formed Z-Section Steel Members in Flexure," Research Report, Department of Civil Engineering, The University of Manitoba, Winnipeg, Manitoba, Canada.

Charnvarnichborikarn, P., and Polyzois, D., (1991), "Buckling Behaviour and Design of Cold-Formed Steel Z-Section Beams," The 13th Canadian Congress of Applied Mechanics, CANCAM'91, June 2-6, pp. 340-341.

Charnvarnichborikarn, P., and Polyzois, D., (1991), "Experimental and Analytical Investigation of Cold-formed Steel Z-Section Beam-Columns," Research Report, Department of Civil Engineering, The University of Manitoba, Winnipeg, Manitoba, Canada.

Cohen, J.M., and Pekoz, T., (1986), "Local Buckling of Plate Elements," Proceeding of the Sessions of Structural Congress, ASCE, pp. 235-244.

Desmond, T.P., (1978), "The Behaviour and Strength of Thin-Walled Compression Elements with Longitudinal Stiffeners," Research Report No. 369, Department of Structural Engineering, Cornell University, Ithaca, New York.

Goodier, J.N., (1941), "The Buckling of Compressed Bars by Torsion and Flexure" Bulletin 27, Cornell University, Engineering Experimental Station, Ithaca, N.Y.

Haussler, R., (1964), "Strength of Elastically Stabilized Beams," Journal of the Structural Division, Proceeding of the American Society of Civil Engineers, ASCE, Vol. 90, No. ST3, pp. 219-264.

Johnston, B.G., ed., (1976), "Structural Stability Research Council," Guide to Stability Design Criteria for Metal Structures, 3rd ed., John Wiley & Sons, Inc., New York.

Lars, H., (1986), "Elastically Braced Light Gauge Beams with Open Sections," Proceeding, thin-Walled Metal Structures in Building, IABSE Colloquium, Stockholm, Vol. 49, pp. 27-34.

Lau, C.W. and Hancock, G.J., (1987), "Distortional Buckling Formulas for Channel Columns," Journal of Structural Engineering, Vol. 113, No. 5, pp. 1063-1078.

Le, Q.P., Polyzois, D., and Charnvarnichborikarn, P., (1990), "Behaviour of Cold-Formed Steel Members in Compression," Research Report, Department of Civil Engineering, The University of Manitoba, Winnipeg, Manitoba, Canada.

Marsh, C., (1985), "Influence of Lips on Flanges and Angles," Unpublished Technical Note of Canadian Standard Association (CSA), Canada.

Martens, K.J.L., Polyzois, D., and Charnvarnichborikarn, P., (1989), "The Buckling of Cold-Formed Steel Columns," Research Report, Department of Civil Engineering, The University of Manitoba, Winnipeg, Manitoba, Canada.

Mulligan, G.P., and Pekoz, T.B., (1983), "Local Buckled Thin-Walled Columns," journal of the Structural Division, ASCE, Vol. 110, No. ST11, pp. 2635-2654.

Pekoz, T.B., (1983), "Diaphragm-Braced Thin-Walled Channel and Z-Section Beams," Chapter 6, Beams and Beam-Columns Stability and Strength, Edited by Narayanan, R., Applied Science Publishers Ltd., U.S.A., pp. 161-184.

Pekoz, T.B., (1986), "Development of A Unified Approach to the Design of Cold-Formed Steel Members," American Iron and Steel Institute, Report SG-86-4, N.W., Washington, D.C.

Polyzois, D., and Charnvarnichborikarn, P., (1990), "Web-Flange Interaction in Cold-Formed Steel Z-Section Columns," Submitted to Journal of Structural Engineering, ASCE.

Polyzois, D., and Charnvarnichborikarn, P., (1991), "Failure of Cold-Formed Steel Z-Section Beams by Localized Buckling of Web-Flange Interaction," Paper to be submitted to "An International Journal of Thin-Walled Structural Engineering".

Purnadi, R.W. Ir., (1990), "Experimental and Analytical Study of Cold-Formed Z-Section Steel Members Under Axial Loading," Ph.D. Dissertation, University of Texas at Austin, August.

Rosner, C.N., Polyzois, D., and Charnvarnichborikarn, P., (1989), "An Experimental Investigation on the Behaviour of Cold-Formed Steel Columns," Research Report, Department of Civil Engineering, The University of Manitoba, Winnipeg, Manitoba, Canada.

Sudharmapal, A.R., (1988), "Behaviour of Cold-Formed Z-Section Members in Compression," M.S. Thesis, The University of Texas at Austin.

Swanson Analysis System, Inc., (1990), "ANSYS Program Technical Description of Capabilities," Johnson Road, P.O. Box 65, Houston, P.A., 15342-0065.

Timoshenko, S.P., and Gere, J.M., (1961), "Theory of Elastic Stability," McGraw-Hill Book Co., New York.

Vlasov, V.Z., (1961), "Thin-Walled Elastic Beams," 2nd ed., National Science Foundations and Department of Commerce, Washington, D.C., (By the Israel Program for Scientific Translations, Jerusalem).

Weng, C.C., and Pekoz, T.B., (1990), "Compression Tests of Cold-Formed Steel Columns," Journal of Structural Engineering, ASCE, Vol. 116, No.5, pp. 1230-1246.

Wilkstrom, P., (1971), "Z and C Purlins Connected with Corrugated Steel Sheeting," Proceeding of the First Specialty Conference on Cold-Formed Steel Structures, University of Missouri-Rolla, St. Louis, Missouri, U.S.A., August 19-20, pp. 136-139.

Winter, G., (1959), "Strength of Thin Steel Compression Flanges," Transactions, American Society of Civil Engineers (ASCE), Paper No. 2305, pp. 527-554.

Yu, W.W., (1991), "Cold-Formed Steel Design," Wiley-Interscience, New York, N.Y.

APPENDIX A

DEFINITIONS

To review the structural behaviour of thin elements, It is necessary to become familiar with the terms generally used in the design of cold-formed steel structural members and used particularly in this dissertation. Some of the following definitions of general terms are based on the AISI Specification (1989) and the CSA Standard (1989).

1) **Cold-Formed Steel Structural Members.** Cold-formed steel structural members are shapes which are manufactured by press-braking blanks sheared from sheets, cut lengths of coils or plates, or by cold-roll forming. The forming operations are performed at ambient room temperature that is manifest without addition of heat.

2) **Thickness.** A thickness used in the calculation of sectional properties and the design of cold-formed sections should be the thickness of base steel. Any thickness of coating material should be deducted from the overall thickness of steel. In the AISI Specification (1989) it is specified that the uncoated minimum thickness of the cold-formed product, as delivered to the job site, shall not, at any location, be less than 95% of the thickness, used in the design. An exception is at bends, such as corners, where the thickness may be less due to cold-forming effects. However, the thinning is usually on the order of 1 to 3% and can be ignored in calculating sectional properties.

3) **Unstiffened Compression Element.** An unstiffened compression element is a flat compression element that is stiffened at only one edge parallel to the direction of stress.

4) **Stiffened or Partially Stiffened Compression Element.** A stiffened or partially stiffened compression element is a flat compression element (i.e., a plane compression flange of a flexural member or a plane web of a compression member) of which both edges parallel to the direction of stress are stiffened by a stiffening means such as web elements, flanges, edge stiffeners or the like.

5) **Flat Width.** A flat width is the width of the straight portion of the element and does not include the bent portion of the section. For unstiffened flanges, the flat width is the width of the flat projection of the flanges, measured from the end of the bend adjacent to the web to the free edge of the flanges. The flat width of a stiffened element is the width between the adjacent stiffening means, exclusive of bends.

6) **Overall Width of Edge Stiffener.** A overall width of edge stiffener consists of the width of the straight portion of the edge stiffener and the bent portion at the flange-edge stiffener junction of the sections.

7) **Flat-Width Ratio.** A flat-width is the ratio of the flat width to the thickness, a flat-width-to-thickness ratio. It should be realized that in cold-formed steel design, unstiffened compression elements with b/t ratio exceeding 30 and stiffened compression elements with b/t ratio exceeding 250 may develop noticeable deformation under design loads without detriment to load-carrying capacity.

8) **Effective Design Width.** An effective design width is a reduced design width for computing sectional properties of flexural and compression members when the b/t ratio of a stiffened compression element exceeds the limitation (AISI, 1989

and CSA, 1989). This effective design width is also a concept which facilitates taking account of local buckling and post-buckling strength for compression elements.

9) **Effective Width Ratio.** An effective width ratio is the ratio of the effective width to the thickness of an element, determined in accordance with the AISI Specification (1989) and the CSA Standard (1989).

10) **Effective Cross Sectional Area.** A cross sectional area calculated using the effective widths of compressive elements in accordance with the design guidelines.

11) **Point-Symmetric Section.** A point-symmetric section is a section symmetrical about a point (centroid of sections). A Z-section having equal flanges is a point-symmetric section.

12) **Torsional-Flexural Buckling.** A torsional-flexural buckling is a mode of buckling in which compression members can bend and twist simultaneously. This type of buckling mode is critical, in particular when the shear centre of the section does not coincide with the centroid.

13) **Stress.** In the AISI Specification (1989), the term "Stress" means force per unit area and is expressed in ksi, whereas it is expressed in MPa in the CSA Standard (1989).

14) **Yield Point.** In ASTM Specification (1985), the terms "Yield Point" or "Yield Strength" are often used for steels having different stress-strain characteristics.

15) **Virgin Steel and its properties.** Virgin steel refers to steel received from the producer or warehouse before being cold-worked as a result of fabricating operations. Virgin steel properties are mechanical properties (yield point, tensile strength, and elongation) of the steel.

APPENDIX B

DIMENSIONS AND PROPERTIES OF SPECIMENS

TABLE B.1 Average Cross Sectional Dimensions of the 18 inch Column Specimens with 1.5 inch Flat Width of Flanges

Specimen	L(in.)	θ(°)	w(in.)	b_f(in.)	c(in.)	r(in.)	t(in.)	D(in.)
1.5-0.00-1[a]	18.03	-	4.03	1.50	-	0.28	0.060	0.06
1.5-0.00-2[a]	18.03	-	3.99	1.51	-	0.28	0.059	0.06
1.5-0.00-3[a]	18.00	-	4.02	1.51	-	0.28	0.058	0.06
1.5-0.25-1	18.00	90.5	3.96	1.50	0.29	0.28	0.060	0.60
1.5-0.25-2	18.03	90.0	3.97	1.50	0.29	0.29	0.059	0.61
1.5-0.25-3	18.02	90.0	3.98	1.52	0.28	0.28	0.059	0.59
1.5-0.50-1	18.00	89.8	3.97	1.50	0.52	0.29	0.059	0.84
1.5-0.50-2	18.00	89.8	3.98	1.51	0.54	0.29	0.059	0.86
1.5-0.50-3	18.02	89.8	3.97	1.50	0.53	0.28	0.059	0.84
1.5-0.75-1	18.03	89.8	3.98	1.50	0.78	0.28	0.058	1.09
1.5-0.75-2	18.00	89.8	3.99	1.52	0.77	0.28	0.058	1.08
1.5-0.75-3	18.02	90.3	3.96	1.50	0.76	0.29	0.059	1.08
1.5-1.00-1	18.02	90.0	3.97	1.51	1.01	0.28	0.059	1.32
1.5-1.00-2	18.00	90.0	3.99	1.50	1.01	0.29	0.059	1.33
1.5-1.00-3	18.02	90.3	4.00	1.51	1.02	0.28	0.059	1.33

[a] Curved portion at the flange-edge stiffener junction not included

TABLE B.2 Average Cross Sectional Dimensions of the 18 inch Column Specimns with 2.0 inch Flat Width of Flanges

Specimen	L(in.)	θ(°)	w(in.)	b_f(in.)	c(in.)	r(in.)	t(in.)	D(in.)
2.0-0.00-1[a]	18.00	-	4.04	2.00	-	0.29	0.059	0.06
2.0-0.00-2[a]	18.02	-	4.04	2.00	-	0.29	0.058	0.06
2.0-0.00-3[a]	18.02	-	4.07	2.00	-	0.27	0.058	0.06
2.0-0.25-1	18.02	89.0	4.01	2.00	0.30	0.28	0.058	0.61
2.0-0.25-2	18.02	89.5	3.96	1.99	0.28	0.29	0.059	0.60
2.0-0.25-3	18.02	89.0	3.98	1.99	0.30	0.28	0.059	0.61
2.0-0.50-1	18.00	90.3	3.95	2.01	0.53	0.28	0.059	0.84
2.0-0.50-2	18.00	89.8	3.97	2.00	0.54	0.28	0.059	0.85
2.0-0.50-3	18.00	90.3	3.93	2.00	0.52	0.28	0.059	0.83
2.0-0.75-1	18.02	90.3	3.99	1.98	0.78	0.29	0.058	1.10
2.0-0.75-2	18.02	90.0	3.99	1.98	0.79	0.29	0.058	1.10
2.0-0.75-3	18.02	89.8	3.99	1.99	0.77	0.29	0.058	1.09
2.0-1.00-1	18.02	90.0	4.00	2.00	1.00	0.28	0.058	1.31
2.0-1.00-2	18.03	89.8	3.98	2.00	1.02	0.28	0.057	1.33
2.0-1.00-3	18.02	89.8	3.97	2.00	1.01	0.29	0.059	1.33

[a] Curved portion at the flange-edge stiffener junction not included

TABLE B.3 Average Cross Sectional Dimensions of the 18 inch Column Specimns with 2.5 inch Flat Width of Flanges

Specimen	L(in.)	θ(°)	w(in.)	b_f(in.)	c(in.)	r(in.)	t(in.)	D(in.)
2.5-0.00-1[a]	18.03	-	4.06	2.48	-	0.29	0.059	0.06
2.5-0.00-2[a]	18.03	-	4.07	2.48	-	0.29	0.059	0.06
2.5-0.00-3[a]	18.03	-	4.03	2.50	-	0.28	0.059	0.06
2.5-0.25-1	18.03	89.5	3.96	2.52	0.27	0.29	0.059	0.59
2.5-0.25-2	18.03	89.0	3.99	2.50	0.28	0.29	0.058	0.60
2.5-0.25-3	18.03	90.0	4.02	2.50	0.28	0.28	0.059	0.59
2.5-0.50-1	18.02	89.5	3.96	2.51	0.53	0.28	0.057	0.84
2.5-0.50-2	18.02	89.0	3.94	2.49	0.54	0.29	0.058	0.86
2.5-0.50-3	18.02	89.5	3.95	2.51	0.54	0.28	0.058	0.85
2.5-0.75-1	18.02	89.8	3.93	2.49	0.78	0.29	0.058	1.10
2.5-0.75-2	18.02	90.5	3.97	2.49	0.77	0.29	0.059	1.09
2.5-0.75-3	18.02	89.8	3.97	2.49	0.77	0.29	0.059	1.09
2.5-1.00-1	18.02	89.5	3.95	2.52	1.01	0.28	0.057	1.32
2.5-1.00-2	18.02	89.8	3.96	2.52	1.02	0.28	0.058	1.33
2.5-1.00-3	18.02	89.5	3.96	2.51	1.02	0.29	0.057	1.34

[a] Curved portion at the flange-edge stiffener junction not included

TABLE B.4 Average Cross Sectional Dimensions of the 24 inch Column Specimens

Specimen	L(in.)	θ(°)	w(in.)	b_f(in.)	c(in.)	r(in.)	t(in.)	D(in.)
2.7-0.00-1[a]	23.99	-	7.70	2.83	-	0.16	0.058	0.06
2.7-0.00-2[a]	23.99	-	7.69	2.81	-	0.15	0.058	0.06
2.7-0.00-1[b]	24.02	90.0	7.72	2.75	0.00	0.14	0.058	0.17
2.7-0.00-2[b]	24.00	90.0	7.60	2.70	0.00	0.16	0.058	0.19
2.7-0.15-1	24.00	90.0	7.65	2.68	0.05	0.15	0.058	0.23
2.7-0.15-2	24.00	90.0	7.67	2.68	0.06	0.15	0.058	0.24
2.7-0.25-1	24.00	90.0	7.62	2.65	0.22	0.15	0.058	0.40
2.7-0.25-2	24.01	90.0	7.67	2.70	0.23	0.15	0.058	0.41
2.7-0.50-1	24.02	90.0	7.68	2.64	0.47	0.15	0.058	0.65
2.7-0.50-2	24.00	90.0	7.64	2.67	0.48	0.14	0.058	0.65
2.7-0.75-1	24.00	90.0	7.67	2.66	0.72	0.17	0.058	0.92
2.7-0.75-2	23.99	90.0	7.66	2.67	0.73	0.17	0.058	0.93
2.7-1.00-1	24.00	90.0	7.72	2.66	0.96	0.16	0.058	1.15
2.7-1.00-2	24.00	90.0	7.73	2.66	0.96	0.16	0.058	1.15
2.7-1.25-1	24.02	90.0	7.78	2.65	1.23	0.15	0.059	1.41
2.7-1.25-2	24.01	90.0	7.64	2.66	1.22	0.15	0.059	1.40
2.7-1.50-1	24.01	90.0	7.66	2.65	1.47	0.15	0.059	1.65
2.7-1.50-2	24.01	90.0	7.65	2.66	1.46	0.15	0.059	1.64
2.7-2.00-1	24.02	90.0	7.60	2.67	1.98	0.15	0.058	2.16
2.7-2.00-2	24.01	90.0	7.67	2.63	1.99	0.15	0.058	2.17

[a] Curved portion at the flange-edge stiffener junction not included
[b] Curved portion at the flange-edge stiffener junction included

TABLE B.5 Average Cross Sectional Dimensions of the 48 inch Column Specimens

Specimen	L(in.)	θ(°)	w(in.)	b_f(in.)	c(in.)	r(in.)	t(in.)	D(in.)
2.7-0.00-1[a]	48.03	-	7.75	2.81	-	0.16	0.058	0.06
2.7-0.00-2[a]	48.00	-	7.66	2.81	-	0.17	0.058	0.06
2.7-0.00-1[b]	48.03	90.0	7.56	2.57	0.08	0.16	0.058	0.27
2.7-0.00-2[b]	48.00	91.9	7.61	2.58	0.08	0.16	0.058	0.27
2.7-0.15-1	48.03	90.0	7.58	2.55	0.07	0.17	0.058	0.27
2.7-0.15-2	48.00	92.8	7.61	2.57	0.07	0.17	0.058	0.27
2.7-0.25-1	48.01	88.3	7.60	2.57	0.17	0.18	0.058	0.38
2.7-0.25-2	48.03	87.3	7.62	2.58	0.16	0.18	0.058	0.37
2.7-0.50-1	48.01	89.9	7.54	2.56	0.44	0.17	0.059	0.64
2.7-0.50-2	48.00	89.5	7.59	2.61	0.41	0.17	0.059	0.61
2.7-0.75-1	48.01	89.9	7.63	2.62	0.67	0.16	0.059	0.86
2.7-0.75-2	48.03	90.3	7.62	2.61	0.69	0.16	0.059	0.88
2.7-1.00-1	48.03	90.0	7.64	2.62	0.94	0.16	0.058	1.13
2.7-1.00-2	47.99	90.6	7.64	2.62	0.92	0.16	0.058	1.11
2.7-1.25-1	48.03	90.5	7.64	2.60	1.19	0.16	0.058	1.38
2.7-1.25-2	48.00	90.5	7.64	2.60	1.19	0.16	0.058	1.38
2.7-1.50-1	48.02	90.1	7.64	2.63	1.43	0.16	0.059	1.62
2.7-1.50-2	48.00	90.6	7.61	2.62	1.44	0.16	0.059	1.63
2.7-2.00-1	48.03	90.3	7.63	2.62	1.94	0.16	0.058	2.13
2.7-2.00-2	47.97	90.6	7.61	2.57	1.94	0.18	0.058	2.15

[a] Curved portion at the flange-edge stiffener junction not included
[b] Curved portion at the flange-edge stiffener junction included

TABLE B.6 Average Cross Sectional Dimensions of the 54 inch Beam Specimens

Specimen	L(in.)	θ(°)	w(in.)	b_f(in.)	c(in.)	r(in.)	t(in.)	D(in.)
2.7-0.00-1[a]	54.06	-	7.67	2.79	-	0.17	0.058	0.06
2.7-0.00-2[a]	54.03	-	7.65	2.80	-	0.16	0.059	0.06
2.7-0.00-1[b]	53.98	90.0	7.62	2.60	0.07	0.17	0.059	0.27
2.7-0.00-2[b]	54.00	90.0	7.64	2.58	0.09	0.18	0.058	0.30
2.7-0.15-1	54.03	89.3	7.65	2.54	0.09	0.17	0.058	0.29
2.7-0.15-2	54.00	89.9	7.64	2.53	0.10	0.16	0.059	0.29
2.7-0.25-1	54.02	89.9	7.66	2.58	0.20	0.17	0.058	0.40
2.7-0.25-2	54.03	91.9	7.60	2.62	0.17	0.17	0.059	0.37
2.7-0.50-1	54.02	90.3	7.63	2.59	0.42	0.17	0.059	0.62
2.7-0.50-2	54.02	90.8	7.64	2.58	0.45	0.17	0.059	0.65
2.7-0.75-1	54.03	90.8	7.61	2.57	0.68	0.18	0.059	0.89
2.7-0.75-2	53.97	90.8	7.62	2.59	0.67	0.17	0.059	0.87
2.7-1.00-1	54.03	91.0	7.64	2.58	0.95	0.16	0.059	1.14
2.7-1.00-2	54.03	90.5	7.60	2.58	0.93	0.16	0.058	1.12
2.7-1.25-1	54.09	90.4	7.63	2.57	1.19	0.17	0.059	1.39
2.7-1.25-2	54.03	91.3	7.63	2.56	1.18	0.17	0.058	1.38
2.7-1.50-1	54.03	90.3	7.63	2.61	1.42	0.17	0.058	1.62
2.7-1.50-2	54.00	90.0	7.66	2.63	1.44	0.15	0.059	1.62
2.7-2.00-1	54.00	90.5	7.63	2.62	1.95	0.16	0.058	2.14
2.7-2.00-2	54.03	90.4	7.64	2.63	1.95	0.15	0.059	2.14

[a] Curved portion at the flange-edge stiffener junction not included
[b] Curved portion at the flange-edge stiffener junction included

TABLE B.7 Average Cross Sectional Dimensions of the 24 inch Beam-Column Specimens

Specimen	L(in.)	θ(°)	w(in.)	b_f(in.)	c(in.)	r(in.)	t(in.)	D(in.)
2.7-0.00-3[a]	23.99	-	7.72	2.85	-	0.17	0.058	0.06
2.7-0.00-3[b]	24.01	90.0	7.66	2.61	0.00	0.18	0.058	0.28
2.7-0.15-3	24.00	90.0	7.66	2.56	0.08	0.18	0.058	0.28
2.7-0.25-3	24.01	90.0	7.64	2.61	0.18	0.18	0.058	0.37
2.7-0.50-3	23.99	90.0	7.66	2.60	0.46	0.17	0.058	0.65
2.7-0.75-3	23.99	90.0	7.67	2.65	0.70	0.17	0.059	0.90
2.7-1.00-3	24.00	90.0	7.72	2.57	0.93	0.19	0.059	1.12
2.7-1.25-3	24.01	90.0	7.71	2.61	1.19	0.18	0.059	1.39
2.7-1.50-3	24.01	90.0	7.66	2.61	1.44	0.18	0.059	1.67

[a] Curved portion at the flange-edge stiffener junction not included
[b] Curved portion at the flange-edge stiffener junction included

TABLE B.8 Average Cross Sectional Dimensions of the 48 inch Beam-Column Specimens

Specimen	L(in.)	θ(°)	w(in.)	b_f(in.)	c(in.)	r(in.)	t(in.)	D(in.)
2.7-0.00-3[a]	48.00	-	7.57	2.87	-	0.17	0.058	0.06
2.7-0.00-3[b]	48.00	90.0	7.61	2.57	0.08	0.17	0.058	0.22
2.7-0.15-3	48.02	90.0	7.61	2.54	0.08	0.17	0.058	0.29
2.7-0.25-3	48.01	89.5	7.59	2.56	0.16	0.18	0.058	0.39
2.7-0.50-3	48.01	89.5	7.62	2.58	0.44	0.18	0.058	0.66
2.7-0.75-3	48.00	90.3	7.57	2.62	0.70	0.17	0.059	0.90
2.7-1.00-3	48.02	90.5	7.62	2.61	0.92	0.17	0.059	1.15
2.7-1.25-3	48.01	90.0	7.60	2.62	1.19	0.17	0.059	1.40
2.7-1.50-3	48.02	90.4	7.61	2.62	1.47	0.17	0.059	1.65

[a] Curved portion at the flange-edge stiffener junction not included
[b] Curved portion at the flange-edge stiffener junction included

TABLE B.9 Calculated Cross Sectional Properties of the 18 inch Column Specimens with 1.5 inch Flat Width of Flanges

Specimen	A(in²)	Ixx(in⁴)	Iyy(in⁴)	Ixy(in⁴)	α (°)	Iup(in⁴)	Ivp(in⁴)	r_u(in.)	r_v(in.)	J(in⁴)	C_w(in⁶)
1.5-0.00-1[a]	0.53	1.78	0.43	0.66	-22.2	2.05	0.16	1.97	0.55	0.001	1.44
1.5-0.00-2[a]	0.52	1.73	0.43	0.65	-22.6	2.00	0.16	1.96	0.55	0.001	1.41
1.5-0.00-3[a]	0.51	1.73	0.42	0.65	-22.4	1.99	0.15	1.97	0.55	0.001	1.40
1.5-0.25-1	0.56	1.84	0.58	0.78	-25.6	2.22	0.20	1.99	0.60	0.001	1.97
1.5-0.25-2	0.55	1.85	0.58	0.79	-25.7	2.23	0.20	2.01	0.61	0.001	2.02
1.5-0.25-3	0.55	1.84	0.58	0.78	-25.6	2.21	0.20	2.00	0.60	0.001	1.97
1.5-0.50-1	0.58	1.91	0.70	0.88	-27.7	2.38	0.24	2.02	0.64	0.001	2.55
1.5-0.50-2	0.58	1.94	0.72	0.90	-27.9	2.41	0.24	2.03	0.65	0.001	2.64
1.5-0.50-3	0.58	1.89	0.69	0.87	-27.6	2.34	0.23	2.01	0.64	0.001	2.48
1.5-0.75-1	0.60	1.92	0.80	0.93	-29.5	2.45	0.27	2.02	0.67	0.001	3.08
1.5-0.75-2	0.60	1.94	0.81	0.95	-29.6	2.48	0.27	2.03	0.68	0.001	3.14
1.5-0.75-3	0.61	1.96	0.82	0.96	-29.7	2.50	0.28	2.03	0.68	0.001	3.17
1.5-1.00-1	0.64	1.98	0.94	1.01	-31.4	2.60	0.32	2.02	0.71	0.001	3.82
1.5-1.00-2	0.64	2.02	0.95	1.03	-31.3	2.65	0.32	2.04	0.71	0.001	3.95
1.5-1.00-3	0.64	2.01	0.94	1.03	-31.2	2.63	0.32	2.03	0.71	0.001	3.90

[a] Curved portion at the flange-edge stiffener junction not included

TABLE B.10 Calculated Cross Sectional Properties of the 18 inch Column Specimens with 2.0 inch Flat Width of Flanges

Specimen	A(in²)	Ixx(in⁴)	Iyy(in⁴)	Ixy(in⁴)	α (°)	Iup(in⁴)	Ivp(in⁴)	r_u(in.)	r_v(in.)	J(in⁴)	C_w(in⁶)
2.0-0.00-1[a]	0.58	2.11	0.80	1.01	-28.6	2.66	0.25	2.14	0.66	0.001	2.56
2.0-0.00-2[a]	0.57	2.07	0.79	0.99	-28.6	2.61	0.25	2.14	0.66	0.001	2.52
2.0-0.00-3[a]	0.57	2.04	0.75	0.95	-28.0	2.54	0.24	2.12	0.65	0.001	2.38
2.0-0.25-1	0.60	2.13	1.00	1.13	-31.6	2.83	0.30	2.17	0.71	0.001	3.27
2.0-0.25-2	0.61	2.13	1.01	1.14	-31.9	2.84	0.30	2.16	0.70	0.001	3.26
2.0-0.25-3	0.61	2.13	1.00	1.13	-31.8	2.83	0.30	2.16	0.70	0.001	3.25
2.0-0.50-1	0.64	2.18	1.20	1.25	-34.4	3.03	0.35	2.18	0.74	0.001	4.04
2.0-0.50-2	0.64	2.19	1.20	1.25	-34.1	3.04	0.35	2.18	0.74	0.001	4.08
2.0-0.50-3	0.63	2.15	1.18	1.23	-34.3	2.99	0.34	2.17	0.74	0.001	3.94
2.0-0.75-1	0.66	2.25	1.36	1.34	-35.9	3.21	0.40	2.21	0.78	0.001	5.05
2.0-0.75-2	0.66	2.25	1.37	1.34	-36.0	3.22	0.40	2.21	0.78	0.001	5.10
2.0-0.75-3	0.65	2.22	1.34	1.32	-35.8	3.17	0.39	2.20	0.77	0.001	4.90
2.0-1.00-1	0.68	2.27	1.53	1.41	-37.6	3.35	0.45	2.22	0.81	0.001	5.96
2.0-1.00-2	0.67	2.21	1.52	1.38	-37.9	3.29	0.44	2.21	0.81	0.001	5.90
2.0-1.00-3	0.70	2.31	1.60	1.45	-38.1	3.44	0.46	2.22	0.81	0.001	6.22

[a] Curved portion at the flange-edge stiffener junction not included

TABLE B.11 Calculated Cross Sectional Properties of the 18 inch Column Specimens with 2.5 inch Flat Width of Flanges

Specimen	A(in²)	Ixx(in⁴)	Iyy(in⁴)	Ixy(in⁴)	α (°)	Iup(in⁴)	Ivp(in⁴)	r_u(in.)	r_v(in.)	J(in⁴)	C_w(in⁶)
2.5-0.00-1[a]	0.64	2.43	1.31	1.40	-34.1	3.38	0.36	2.30	0.75	0.001	4.00
2.5-0.00-2[a]	0.64	2.44	1.31	1.41	-34.0	3.39	0.36	2.30	0.75	0.001	4.02
2.5-0.00-3[a]	0.64	2.38	1.30	1.38	-34.4	3.32	0.35	2.28	0.75	0.001	3.88
2.5-0.25-1	0.67	2.45	1.59	1.59	-38.0	3.69	0.42	2.35	0.79	0.001	5.04
2.5-0.25-2	0.66	2.44	1.56	1.56	-37.6	3.64	0.41	2.35	0.79	0.001	5.00
2.5-0.25-3	0.67	2.48	1.57	1.57	-37.2	3.67	0.42	2.34	0.79	0.001	5.00
2.5-0.50-1	0.67	2.40	1.64	1.64	-40.1	3.79	0.45	2.37	0.82	0.001	5.88
2.5-0.50-2	0.69	2.45	1.68	1.68	-40.3	3.87	0.47	2.38	0.82	0.001	6.06
2.5-0.50-3	0.69	2.44	1.67	1.67	-40.3	3.85	0.46	2.37	0.82	0.001	6.00
2.5-0.75-1	0.71	2.48	1.79	1.79	-42.3	4.11	0.52	2.40	0.86	0.001	7.34
2.5-0.75-2	0.73	2.57	1.83	1.83	-41.9	4.21	0.53	2.41	0.86	0.001	7.54
2.5-0.75-3	0.73	2.57	1.83	1.83	-41.9	4.21	0.53	2.41	0.86	0.001	7.54
2.5-1.00-1	0.73	2.48	1.85	1.85	-44.2	4.28	0.57	2.42	0.89	0.001	8.63
2.5-1.00-2	0.74	2.54	1.89	1.89	-44.2	4.37	0.59	2.43	0.89	0.001	8.89
2.5-1.00-3	0.73	2.52	1.88	1.88	-44.2	4.34	0.58	2.44	0.89	0.001	8.91

[a] Curved portion at the flange-edge stiffener junction not included

TABLE B.12 Calculated Cross sectional Properties of the 24 inch Column Specimens

Specimen	A(in²)	Ixx(in⁴)	Iyy(in⁴)	Ixy(in⁴)	α (°)	Ixp(in⁴)	Iyp(in⁴)	r_x(in.)	r_y(in.)	J(in⁴)	C_w(in⁶)
2.7-0.00-1[a]	0.83	8.40	1.31	2.44	-17.3	9.15	0.56	3.31	0.82	0.001	14.02
2.7-0.00-2[a]	0.83	8.25	1.26	2.36	-17.0	8.97	0.54	3.29	0.81	0.001	13.38
2.7-0.00-1[b]	0.82	8.12	1.16	2.24	-16.4	8.78	0.50	3.28	0.78	0.001	12.46
2.7-0.00-2[b]	0.81	7.92	1.16	2.22	-16.6	8.58	0.50	3.25	0.78	0.001	12.19
2.7-0.15-1	0.82	8.00	1.16	2.23	-16.5	8.66	0.50	3.26	0.78	0.001	12.35
2.7-0.15-2	0.82	8.06	1.17	2.24	-16.5	8.73	0.51	3.27	0.79	0.001	12.53
2.7-0.25-1	0.83	8.14	1.30	2.39	-17.5	8.89	0.55	3.27	0.81	0.001	13.77
2.7-0.25-2	0.84	8.37	1.37	2.49	-17.7	9.17	0.58	3.30	0.83	0.001	14.69
2.7-0.50-1	0.86	8.62	1.54	2.69	-18.6	9.53	0.63	3.33	0.86	0.001	16.83
2.7-0.50-2	0.86	8.51	1.56	2.69	-18.9	9.43	0.64	3.31	0.86	0.001	16.73
2.7-0.75-1	0.90	9.11	1.90	3.09	-20.3	10.25	0.75	3.38	0.91	0.001	21.29
2.7-0.75-2	0.90	9.11	1.92	3.11	-20.5	10.27	0.76	3.38	0.92	0.001	21.54
2.7-1.00-1	0.93	9.41	2.11	3.31	-21.1	10.69	0.83	3.40	0.94	0.001	24.46
2.7-1.00-1	0.93	9.43	2.11	3.32	-21.1	10.71	0.83	3.40	0.94	0.001	24.53
2.7-1.25-1	0.97	9.88	2.36	3.59	-21.9	11.32	0.92	3.41	0.97	0.001	28.63
2.7-1.25-2	0.96	9.49	2.37	3.53	-22.4	10.95	0.91	3.37	0.97	0.001	27.65
2.7-1.50-1	0.99	9.71	2.61	3.74	-23.2	11.32	1.00	3.38	1.00	0.001	31.58
2.7-1.50-2	0.99	9.70	2.62	3.75	-23.3	11.31	1.00	3.37	1.00	0.001	31.57
2.7-2.00-1	1.03	9.67	3.13	4.05	-25.5	11.61	1.19	3.35	1.07	0.001	39.86
2.7-2.00-2	1.04	9.81	3.04	4.02	-24.9	11.68	1.17	3.36	1.06	0.001	39.58

[a] Curved portion at the flange-edge stiffener junction not included
[b] Curved portion at the flange-edge stiffener junction included

TABLE B.13 Calculated Cross Sectional Properties of the 48 inch Column Specimens

Specimen (1)	A(in²) (2)	Ixx(in⁴) (3)	Iyy(in⁴) (4)	Ixy(in⁴) (5)	α (°) (6)	Ixp(in⁴) (7)	Iyp(in⁴) (8)	r_x(in.) (9)	r_y(in.) (10)	J(in⁴) (11)	C_w(in⁶) (12)
2.7-0.00-1[a]	0.83	8.48	1.29	2.42	-17.0	9.22	0.55	3.33	0.81	0.001	13.98
2.7-0.00-2[a]	0.83	8.35	1.32	2.44	-17.4	9.11	0.56	3.31	0.82	0.001	14.00
2.7-0.00-1[b]	0.81	7.81	1.13	2.16	-16.5	8.45	0.49	3.23	0.78	0.001	11.86
2.7-0.00-2[b]	0.81	7.94	1.14	2.19	-16.4	8.58	0.49	3.25	0.78	0.001	12.14
2.7-0.15-1	0.81	7.88	1.12	2.17	-16.4	8.52	0.48	3.24	0.77	0.001	11.95
2.7-0.15-2	0.81	7.90	1.12	2.17	-16.3	8.54	0.48	3.25	0.77	0.001	11.93
2.7-0.25-1	0.82	8.12	1.24	2.33	-17.1	8.84	0.53	3.27	0.80	0.001	13.33
2.7-0.25-2	0.83	8.17	1.24	2.34	-17.0	8.89	0.53	3.28	0.80	0.001	13.41
2.7-0.50-1	0.87	8.57	1.56	2.70	-18.8	9.49	0.64	3.30	0.86	0.001	16.76
2.7-0.50-2	0.87	8.66	1.56	2.72	-18.7	9.58	0.64	3.32	0.86	0.001	16.87
2.7-0.75-1	0.90	8.94	1.77	2.96	-19.8	10.00	0.71	3.34	0.89	0.001	19.60
2.7-0.75-2	0.90	9.00	1.82	3.00	-20.0	10.09	0.73	3.35	0.90	0.001	20.16
2.7-1.00-1	0.91	9.10	2.02	3.19	-21.0	10.32	0.79	3.36	0.93	0.001	22.96
2.7-1.00-1	0.91	9.08	2.00	3.17	-20.9	10.29	0.79	3.36	0.93	0.001	22.68
2.7-1.25-1	0.94	9.28	2.23	3.39	-21.9	10.64	0.87	3.36	0.96	0.001	26.19
2.7-1.25-2	0.94	9.37	2.27	3.44	-22.0	10.76	0.88	3.37	0.97	0.001	26.82
2.7-1.50-1	0.99	9.68	2.57	3.71	-23.1	11.26	0.99	3.37	1.00	0.001	31.04
2.7-1.50-2	0.99	9.66	2.61	3.74	-23.3	11.27	1.00	3.37	1.00	0.001	31.47
2.7-2.00-1	1.03	9.74	3.02	3.99	-25.0	11.60	1.16	3.36	1.06	0.001	38.91
2.7-2.00-2	1.03	9.75	3.01	3.99	-24.9	11.60	1.16	3.36	1.06	0.001	39.08

[a] Curved portion at the flange-edge stiffener junction not included
[b] Curved portion at the flange-edge stiffener junction included

TABLE B.14 Calculated Cross Sectional Properties of the 54 inch Beam Specimens

Specimen	A(in.^{2})	I_{xx}(in.^{4})	I_{yy}(in.^{4})	I_{xy}(in.^{4})	α (°)	I_{xp}(in.^{4})	I_{yp}(in.^{4})	r_x(in.)	r_y(in.)	J(in.^{4})	C_w(in.^{6})
2.7-0.00-1[a]	0.80	7.85	1.00	2.04	-15.4	8.41	0.44	3.24	0.74	0.001	10.88
2.7-0.00-2[a]	0.81	7.91	1.02	2.06	-15.5	8.48	0.45	3.23	0.75	0.001	10.95
2.7-0.00-1[b]	0.83	8.12	1.17	2.25	-16.5	8.79	0.50	3.26	0.78	0.001	12.50
2.7-0.00-2[b]	0.82	8.11	1.17	2.25	-16.5	8.78	0.51	3.27	0.79	0.001	12.71
2.7-0.15-1	0.81	7.97	1.10	2.16	-16.1	8.59	0.48	3.26	0.77	0.001	11.94
2.7-0.15-2	0.82	8.00	1.09	2.15	-16.0	8.62	0.48	3.24	0.76	0.001	11.79
2.7-0.25-1	0.83	8.24	1.25	2.36	-17.0	8.96	0.53	3.29	0.80	0.001	13.65
2.7-0.25-2	0.84	8.28	1.30	2.41	-17.3	9.03	0.55	3.28	0.81	0.001	13.84
2.7-0.50-1	0.87	8.65	1.51	2.67	-18.4	9.54	0.62	3.31	0.85	0.001	16.49
2.7-0.50-2	0.87	8.70	1.53	2.69	-18.5	9.60	0.63	3.32	0.85	0.001	16.78
2.7-0.75-1	0.90	8.98	1.78	2.97	-19.8	10.04	0.71	3.34	0.89	0.001	19.88
2.7-0.75-2	0.90	8.94	1.77	2.95	-19.7	10.00	0.71	3.34	0.89	0.001	19.61
2.7-1.00-1	0.93	9.19	1.99	3.18	-20.7	10.40	0.79	3.35	0.92	0.001	22.78
2.7-1.00-1	0.91	8.91	1.94	3.09	-20.8	10.08	0.76	3.34	0.92	0.001	21.90
2.7-1.25-1	0.96	9.44	2.25	3.43	-21.8	10.82	0.88	3.36	0.96	0.001	26.61
2.7-1.25-2	0.94	9.26	2.18	3.35	-21.7	10.59	0.85	3.36	0.95	0.001	25.76
2.7-1.50-1	0.97	9.52	2.52	3.65	-23.1	11.08	0.97	3.38	1.00	0.001	30.55
2.7-1.50-2	0.99	9.66	2.53	3.68	-23.0	11.21	0.98	3.37	0.99	0.001	30.67
2.7-2.00-1	1.03	9.74	3.02	3.99	-25.0	11.60	1.16	3.35	1.06	0.001	39.00
2.7-2.00-2	1.05	9.87	3.04	4.04	-24.9	11.75	1.17	3.35	1.06	0.001	39.18

[a] Curved portion at the flange-edge stiffener junction not included
[b] Curved portion at the flange-edge stiffener included

TABLE B.15 Calculated Cross Sectional Properties of the 24 inch Beam-Column Specimens

Specimen	A(in²)	I_{xx}(in⁴)	I_{yy}(in⁴)	I_{xy}(in⁴)	α (°)	I_{xp}(in⁴)	I_{yp}(in⁴)	r_x(in.)	r_y(in.)	J(in⁴)	C_w(in⁶)
2.7-0.00-3[a]	0.81	8.08	1.07	2.13	-15.7	8.68	0.47	3.27	0.76	0.001	11.65
2.7-0.00-3[b]	0.81	8.08	1.13	2.20	-16.2	8.72	0.49	3.27	0.78	0.001	12.23
2.7-0.15-3	0.82	8.10	1.14	2.22	-16.3	8.75	0.49	3.27	0.78	0.001	12.45
2.7-0.25-3	0.83	8.31	1.30	2.41	-17.3	9.06	0.55	3.30	0.81	0.001	14.07
2.7-0.50-3	0.86	8.65	1.54	2.70	-18.6	9.56	0.63	3.33	0.86	0.001	16.97
2.7-0.75-3	0.91	9.22	1.89	3.10	-20.1	10.36	0.75	3.37	0.91	0.001	21.24
2.7-1.00-3	0.94	9.63	2.07	3.32	-20.7	10.88	0.82	3.40	0.93	0.001	24.60
2.7-1.25-3	0.97	9.83	2.37	3.60	-22.0	11.28	0.92	3.41	0.97	0.001	28.70
2.7-1.50-3	1.00	9.87	2.63	3.79	-23.2	11.50	1.01	3.40	1.01	0.001	32.42

[a] Curved portion at the flange-edge stiffener junction not included
[b] Curved portion at the flange-edge stiffener junction included

TABLE B.16 Calculated Cross Sectional Properties of the 48 inch Beam-Column Specimens

Specimen	A(in²)	I_{xx}(in⁴)	I_{yy}(in⁴)	I_{xy}(in⁴)	α (°)	I_{xp}(in⁴)	I_{yp}(in⁴)	r_x(in.)	r_y(in.)	J(in⁴)	C_w(in⁶)
2.7-0.00-3[a]	0.80	7.77	1.09	2.12	-16.2	8.39	0.47	3.23	0.77	0.001	11.37
2.7-0.00-3[b]	0.81	7.92	1.13	2.18	-16.3	8.56	0.49	3.25	0.78	0.001	12.04
2.7-0.15-3	0.81	7.87	1.09	2.14	-16.1	8.48	0.48	3.24	0.77	0.001	11.72
2.7-0.25-3	0.82	8.06	1.22	2.30	-17.0	8.76	0.52	3.27	0.80	0.001	13.06
2.7-0.50-3	0.86	8.57	1.52	2.67	-18.6	9.47	0.63	3.32	0.85	0.001	16.69
2.7-0.75-3	0.90	8.90	1.84	3.01	-20.2	10.01	0.73	3.33	0.90	0.001	20.19
2.7-1.00-3	0.93	9.25	2.05	3.24	-21.0	10.50	0.80	3.36	0.93	0.001	23.35
2.7-1.25-3	0.96	9.45	2.35	3.51	-22.3	10.90	0.91	3.37	0.97	0.001	27.43
2.7-1.50-3	0.99	9.68	2.63	3.76	-23.4	11.31	1.01	3.37	1.01	0.001	31.95

[a] Curved portion at the flange-edge stiffener junction not included
[b] Curved portion at the flange-edge stiffener junction included

APPENDIX C

LOAD - AXIAL DEFORMATION PLOTS

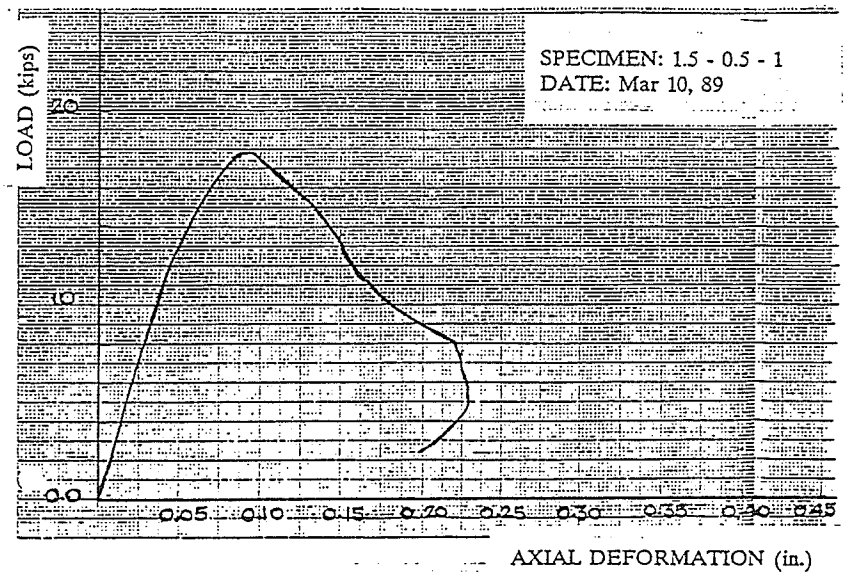

Figure C.1 Typical X-Y Plot of Axial Load Versus Axial Deformation for the 18 inch Column Specimens with 1.5 inch Flat Width of Flanges and 0.5 inch Flat Width of Edge Stiffeners

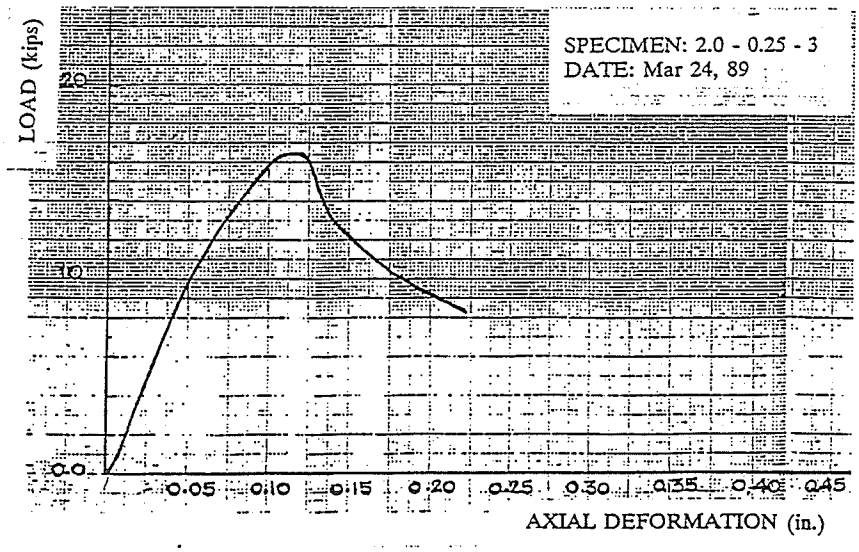

Figure C.2 Typical X-Y Plot of Axial Load Versus Axial Deformation for the 18 inch Column Specimens with 2.0 inch Flat Width of Flanges and 0.25 inch Flat Width of Edge Stiffeners

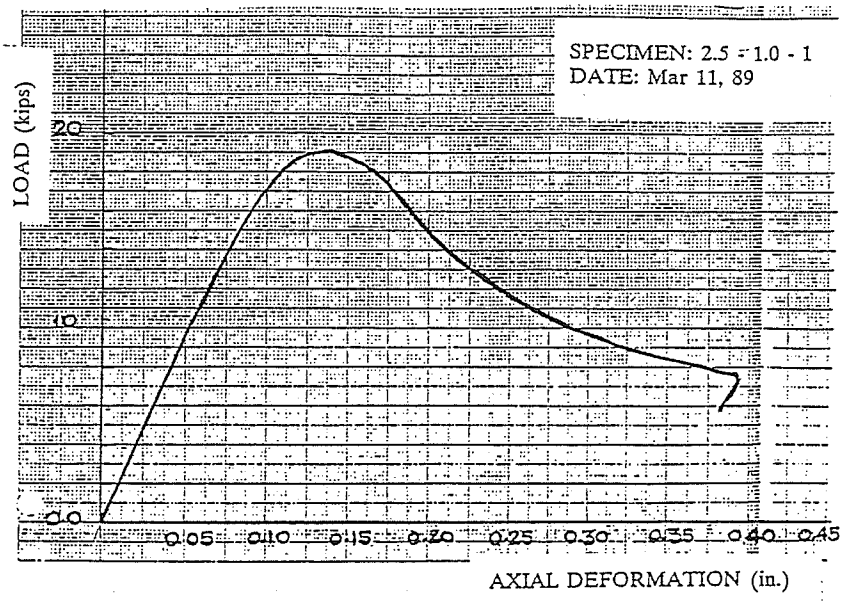

Figure C.3 Typical X-Y Plot of Axial Load Versus Axial Deformation for the 18 inch Column Specimens with 2.5 inch Flat Width of Flanges and 1.0 inch Flat Width of Edge Stiffeners

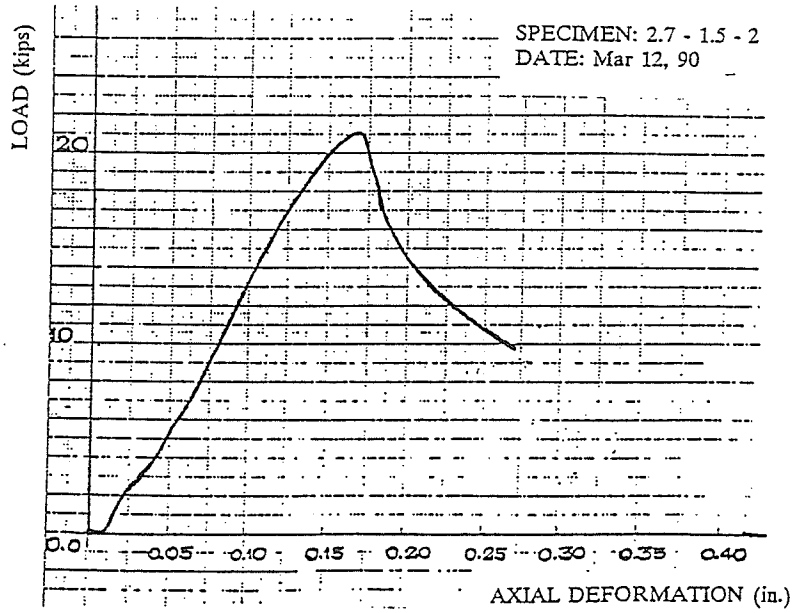

Figure C.4 Typical X-Y Plot of Axial Load Versus Axial Deformation for the 24 inch Column Specimens with 1.50 inch Flat Width of Edge Stiffeners

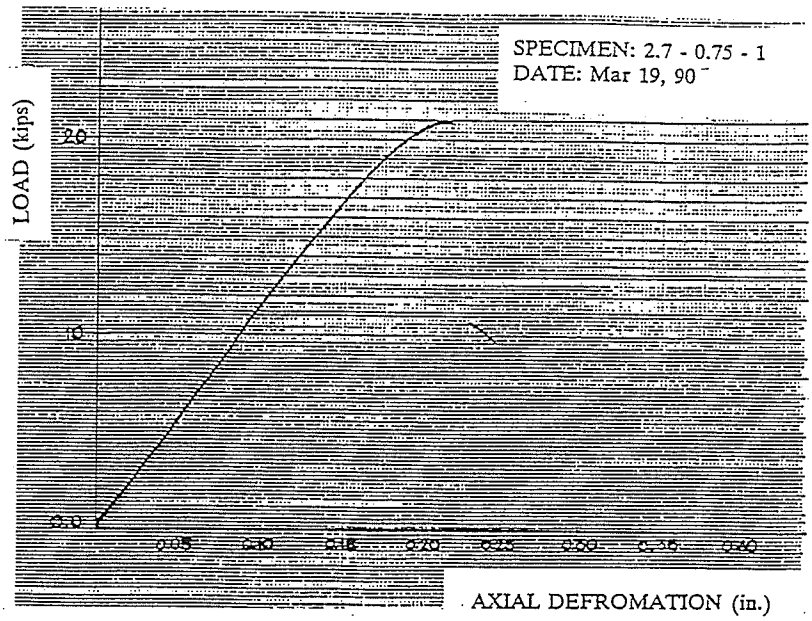

Figure C.5 Typical X-Y Plot of Axial Load Versus Axial Deformation for the 48 inch Column Specimens with 0.75 inch Flat Width of Edge Stiffeners

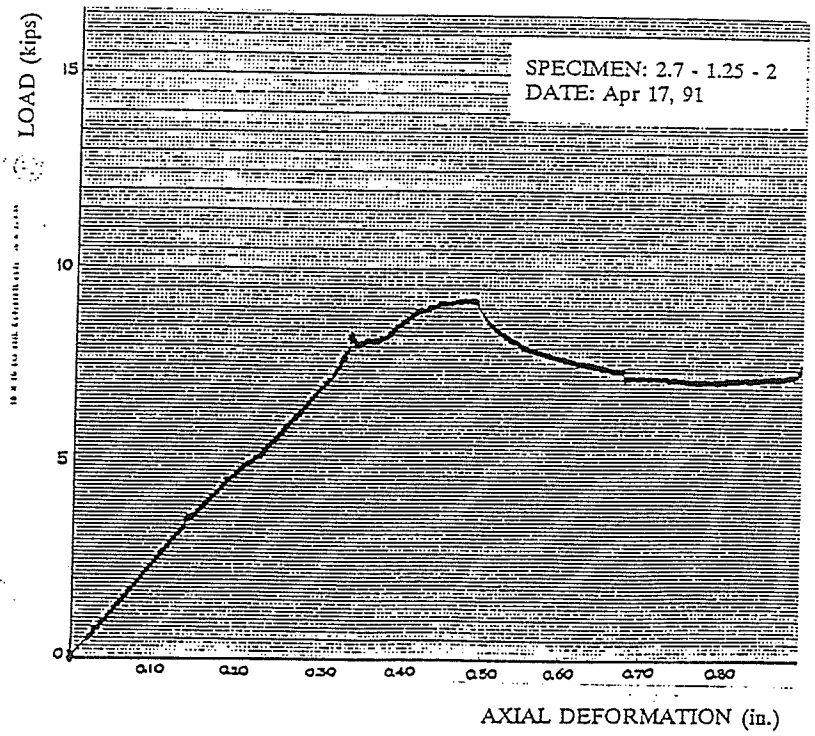

Figure C.6 Typical X-Y Plot of Axial Load Versus Vertical Deflection at Midspan for the 54 inch Beam Specimens with 2.50 inch Flat Width of Edge Stiffeners

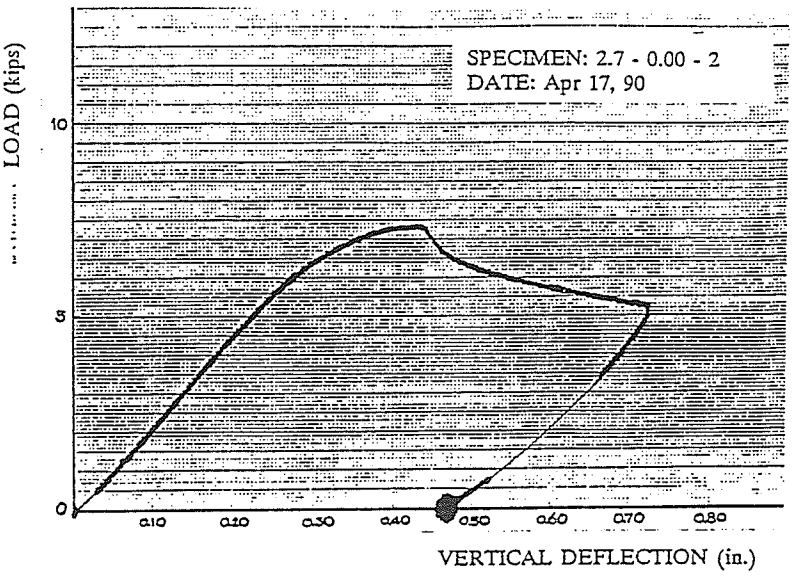

Figure C.7 Typical X-Y Plot of Axial Load Versus Vertical Deflection at Midspan for the 54 inch Beam Specimens without Edge Stiffeners

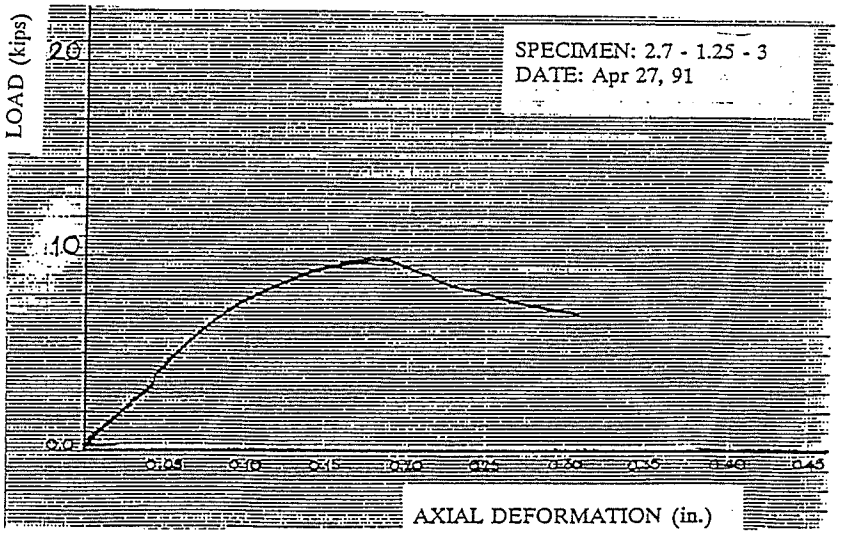

Figure C.8 Typical X-Y Plot of Axial Load Versus Axial Deformation for the 48 inch Beam-Column Specimens 1.25 inch Flat Width of Edge Stiffeners

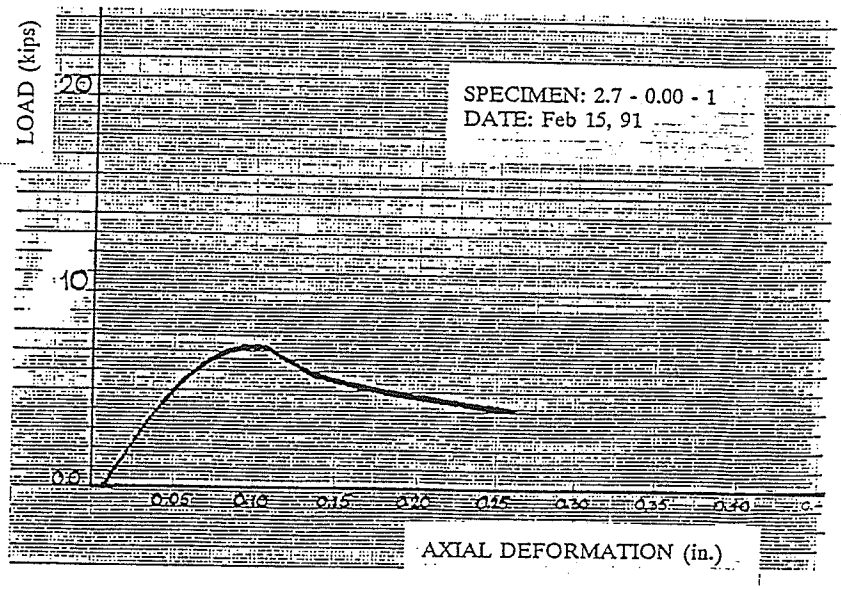

Figure C.9 Typical X-Y Plot of Axial Load Versus Axial Deformation for the 24 inch Beam-Column Specimens without Edge Stiffeners

APPENDIX D

MEMBER STRENGTH CALCULATED USING AISI AND CSA SPECIFICATIONS (1989)

In this Appendix, detailed calculations for the strength of typical column, beam, and beam-column sections based on the two design specifications are given. These detail calculations follow the listing of the relevant Clauses and Equations which are those used in the specifications.

D.1 AISI SPECIFICATION (1989)

D.1.1 COLUMNS

D.1.1.1 Unstiffened Flange Section of Column

An example of concentric loading, unstiffened flange section of column, using specimen 2.7-0.00-2[a], the length of specimen is 48.00 inches.

Section dimensions;

Total depth (H) = *8.06 in.*

Thickness (t) = *0.058 in.*

Flat width of web (w) = *7.66 in.*

Flat width of flange (b_f) = *2.81 in.*

Flat width of edge stiffener (c) = *0.00 in.*

Radius at element junction (r) = *0.17 in.*

Angle between flange and web (θ) = *90.00 degrees*

Gross section properties;

Area (A) = *0.83 $in.^2$*

Moment of Inertia about the geometric x-axis (I_{xx}) = *8.35 $in.^4$*

Moment of Inertia about the geometric y-axis (I_{yy}) = 1.32 $in.^4$

Product of Inertia (I_{xy}) = 2.44 $in.^4$

Moment of Inertia about the principal x-axis (I_{xp}) = 9.11 $in.^4$

Moment of Inertia about the principal y-axis (I_{yp}) = 0.56 $in.^4$

Warping constant of torsion (C_w) = 14.00 $in.^6$

St. Venant torsion constant (J) = 0.001 $in.^4$

Yield strength (F_y) = 47.03 *ksi*

Modulus of elasticity (E) = 29,500 *ksi*

Test Result;

P_{Test} = 12.70 kips

Critical Compressive Resistance; (Clause C4(b))

Local buckling capacity of unstiffened flange:

P_n = 3.27 kips

Load-Carrying Capacity; (Clause C4)

P_n = 3.27 kips

Therefore, P_{AISI} = 3.27 kips

Hence; P_{Test}/P_{AISI} = 3.28

D.1.1.2 Stiffened Flange Section of Column

An example of concentric loading, stiffened flange section of column, using specimen 2.7-0.75-1, the length of specimen is 24.00 inches.

Section dimensions;

Total depth (H) = *8.07 in.*

Thickness (t) = *0.058 in.*

Flat width of web (w) = *7.67 in.*

Flat width of flange (b_f) = *2.66 in.*

Flat width of stiffener (c) = *0.72 in.*

Radius at element junction (r) = *0.17 in.*

Angle between flange and web (θ) = *90.00 degrees*

Gross section properties;

Area (A) = *0.90* $in.^2$

Moment of Inertia about the geometric x-axis (I_{xx}) = *9.11* $in.^4$

Moment of Inertia about the geometric y-axis (I_{yy}) = *1.90* $in.^4$

Product of Inertia (I_{xy}) = *3.09* $in.^4$

Moment of Inertia about the principal x-axis (I_{xp}) = *10.25* $in.^4$

Moment of Inertia about the principal y-axis (I_{yp}) = *0.75* $in.^4$

Warping constant of torsion (C_w) = *21.29* $in.^6$

St. Venant torsion constant (J) = *0.001* $in.^4$

Yield strength (F_y) = *47.03 ksi*

Modulus of elasticity (E) = *29,500 ksi*

Test Result;

P_{Test} = 20.56 kips

Critical Stress; (Clause C4)

Elastic flexural buckling stress:

σ_{ex} = 5763.54 ksi

σ_{ey} = 423.02 ksi

Torsional buckling stress:

σ_t = 979.41 ksi

Therefore, F_e = 423.02 ksi

Since, $F_e > F_y/2$, F_n = 45.72 ksi

Effective Area; (Clause B2.1, B3.1 and B4.2)

A_e = 0.52 in.^{2}

Load-Carrying Capacity; (Clause C4)

P_n = 23.92 kips

Therefore, P_{AISI} = 23.92 kips

Hence; P_{Test}/P_{AISI} = 0.86

D.1.2 BEAMS

D.1.2.1 Unstiffened Flange Section of Beam

An example of pure bending, unstiffened flange section of beam, using specimen 2.7-0.00-1[a], the length of specimen is 54.06 inches.

Section dimensions;

Total depth (H) = *8.07 in.*

Thickness (t) = *0.058 in.*

Flat width of web (w) = *7.67 in.*

Flat width of flange (b_f) = *2.79 in.*

Flat width of stiffener (c) = *0.00 in.*

Radius at element junction (r) = *0.17 in.*

Angle between flange and web (θ) = *90.00 degrees*

Gross section properties;

Area (A) = *0.80* $in.^2$

Moment of Inertia about the geometric x-axis (I_{xx}) = *7.85* $in.^4$

Moment of Inertia about the geometric y-axis (I_{yy}) = *1.00* $in.^4$

Product of Inertia (I_{xy}) = *2.04* $in.^4$

Moment of Inertia about the principal x-axis (I_{xp}) = *8.41* $in.^4$

Moment of Inertia about the principal y-axis (I_{yp}) = *0.44* $in.^4$

Warping constant of torsion (C_w) = *10.88* $in.^6$

St. Venant torsion constant (J) = *0.001* $in.^4$

Yield strength (F_y) = *47.03 ksi*

Modulus of elasticity (E) = *29,500 ksi*

Test Result;

M_{Test} = 52.02 kips-in.

Critical Moment Resistance; (Clause C3.1)

Moment Resistance caused by local buckling of unstiffened flange:

M_n = 9.65 kips-in.

Bending Capacity; (Clause C3.1)

M_n = 9.65 kips-in.

Therefore, M_{AISI} = 9.65 kips-in.

Hence; M_{Test}/M_{AISI} = 5.39

D.1.2.2 Stiffened Flange Section of Beam

An example of pure bending, stiffened flange section of beam, using specimen 2.7-0.75-1, the length of specimen is 53.97 inches.

Section dimensions;

Total depth (H) = *8.02 in.*

Thickness (t) = *0.059 in.*

Flat width of web (w) = *7.62 in.*

Thickness (t) = *0.059 in.*

Flat width of flange (b_f) = *2.59 in.*

Flat width of stiffener (c) = *0.67 in.*

Radius at element junction (r) = *0.17 in.*

Angle between flange and web (θ) = *90.80 degrees*

Gross section properties;

Area (A) = *0.90* $in.^2$

Moment of Inertia about the geometric x-axis (I_{xx}) = *8.94* $in.^4$

Moment of Inertia about the geometric y-axis (I_{yy}) = *1.77* $in.^4$

Product of Inertia (I_{xy}) = *2.95* $in.^4$

Moment of Inertia about the principal x-axis (I_{xp}) = *10.00* $in.^4$

Moment of Inertia about the principal y-axis (I_{yp}) = *0.71* $in.^4$

Warping constant of torsion (C_w) = *19.61 in.*^{6}

St. Venant torsion constant (J) = *0.001 in.*^{4}

Yield strength (F_y) = *47.03 ksi*

Modulus of elasticity (E) = *29,500 ksi*

Test Result;

M_{Test} = 58.57 kips-in.

Critical Stress; (Clause C3.1.1)

Elastic yielding stress:

F_y = 47.03 ksi

Therefore, F_c = 47.03 ksi

Effective Section Modulus; (Clause B2.1, B2.3 and B3.2)

S_e = 1.96 in.^{3}

Bending Capacity; (Clause C3.1)

M_n = 92.17 kips-in.

Therefore, M_{AISI} = 92.17 kips-in.

Hence; M_{Test}/M_{AISI} = 0.64

D.1.3 BEAM-COLUMNS

D.1.3.1 Unstiffened Flange Section of Beam-Column

An example of eccentric loading, unstiffened flange section of beam-column, using specimen 2.7-0.00-3[a], the length of specimen including supports is 48.00 inches.

Section dimensions;

Total depth (H) = *7.97 in.*

Thickness (t) = *0.058 in.*

Flat width of web (w) = *7.57 in.*

Flat width of flange (b_f) = *2.87 in.*

Flat width of stiffener (c) = *0.00 in.*

Radius at element junction (r) = *0.17 in.*

Angle between flange and web (θ) = *90.00 degrees*

Gross section properties;

Area (A) = *0.80 $in.^2$*

Moment of Inertia about the geometric x-axis (I_{xx}) = *7.77 $in.^4$*

Moment of Inertia about the geometric y-axis (I_{yy}) = *1.09 $in.^4$*

Product of Inertia (I_{xy}) = *2.12 $in.^4$*

Moment of Inertia about the principal x-axis (I_{xp}) = *8.39 $in.^4$*

Moment of Inertia about the principal y-axis (I_{yp}) = *0.47 $in.^4$*

Warping constant of torsion (C_w) = *11.37 $in.^6$*

St. Venant torsion constant (J) = *0.001 $in.^4$*

Yield strength (F_y) = *47.03 ksi*

Modulus of elasticity (E) = *29,500 ksi*

Test Result;

P_{Test} = 6.62 kips

Critical Compressive Resistance; (Clause C4(b))

Local buckling capacity of unstiffened flange:

P_n = 3.72 kips

Compressive Load; (Clause C4)

P_n = 3.72 kips

Therefore, P_a = 3.72 kips

Bending Capacity; (Clause C3.1.2)

Bending capacity caused by local buckling of unstiffened flange:

M_n = 9.14 kips-in.

Therefore, M_{ax} = 9.14 kips-in.

Load-Carrying Capacity of Beam-Column; (Clause C5)

P = 1.11 kips

Therefore, P_{AISI} = 1.11 kips

Hence; P_{Test}/P_{AISI} = 5.96

D.1.3.2 Stiffened Flange Section of Beam-Column

An example of eccentric loading, stiffened flange section of beam-column, using specimen 2.7-0.75-3, the length of specimen including supports is 49.13 inches.

Section dimensions;

Total depth (H) = 7.96 in.

Thickness (t) = 0.059 in.

Flat width of web (w) = 7.57 in.

Flat width of flange (b_f) = *2.62 in.*

Flat width of stiffener (c) = *0.70 in.*

Radius at element junction (r) = *0.17 in.*

Angle between flange and web (θ) = *90.30 degrees*

Gross section properties;

Area (A) = *0.90 in.*^{2}

Moment of Inertia about the geometric x-axis (I_{xx}) = *8.90 in.*^{4}

Moment of Inertia about the geometric y-axis (I_{yy}) = *1.84 in.*^{4}

Product of Inertia (I_{xy}) = *3.01 in.*^{4}

Moment of Inertia about the principal x-axis (I_{xp}) = *10.01 in.*^{4}

Moment of Inertia about the principal y-axis (I_{yp}) = *0.73 in.*^{4}

Warping constant of torsion (C_w) = *20.19 in.*^{6}

St. Venant torsion constant (J) = *0.001 in.*^{4}

Yield strength (F_y) = *47.03 ksi*

Modulus of elasticity (E) = *29,500 ksi*

Test Result;

P_{Test} = 9.32 kips

Critical Compressive Stress; (Clause C4)

Elastic flexural buckling stress:

σ_{ex} = 1340.16 ksi

σ_{ey} = 97.99 ksi

Torsional buckling stress:

σ_t = 227.61 ksi

Therefore, F_e = 97.99 ksi

Since, $F_e > F_y/2$, F_n = 41.39 ksi

Effective Area; (Clause B2.1, B3.1 and B4.2)

A_e = 0.55 in.^{2}

Compressive Load; (Clause C4)

P_n = 22.72 kips

Therefore, P_a = 22.72 kips

Bending Capacity; (Clause C3.1.2)

Elastic yielding bending capacity:

M_y = 105.09 kips-in.

Elastic lateral bending capacity:

M_e = 463.96 kips-in.

Since, $M_e > 2.78*M_y$, M_c = 105.09 kips-in.

Effective modulus of section:

S_e = 1.98 in.^{3}

Therefore, M_{ax} = 105.09 kips-in.

Load-Carrying Capacity of Beam-Column; (Clause C5)

P = 11.54 kips

Therefore, P_{AISI} = 11.54 kips

Hence; P_{Test}/P_{AISI} = 0.81

D.2 CSA STANDARD (1989)

D.2.1 COLUMNS

D.2.1.1 Unstiffened Flange Section of Column

An example of concentric loading, unstiffened flange section of column, using specimen 2.7-0.00-2[a], the length of specimen is 1219.00 mm.

Section dimensions;

$$\text{Total depth } (H) = 204.72 \text{ mm}$$

$$\text{Thickness } (t) = 1.47 \text{ mm}$$

$$\text{Flat width of web } (w) = 194.56 \text{ mm}$$

$$\text{Flat width of flange } (b_f) = 71.37 \text{ mm}$$

$$\text{Flat width of stiffener } (c) = 0.00 \text{ mm}$$

$$\text{Radius at element junction } (r) = 4.32 \text{ mm}$$

$$\text{Angle between flange and web } (\theta) = 90.00 \text{ degrees}$$

Gross section properties;

$$\text{Area } (A) = 534.48 \text{ mm}^2$$

$$\text{Moment of Inertia about geometric x-axis } (I_{xx}) = 34.76 \times 10^5 \text{ mm}^4$$

$$\text{Moment of Inertia about geometric y-axis } (I_{yy}) = 5.49 \times 10^5 \text{ mm}^4$$

$$\text{Product of Inertia } (I_{xy}) = 10.16 \times 10^5 \text{ mm}^4$$

$$\text{Moment of Inertia about principal x-axis } (I_{xp}) = 37.92 \times 10^5 \text{ mm}^4$$

$$\text{Moment of Inertia about principal y-axis } (I_{yp}) = 2.33 \times 10^5 \text{ mm}^4$$

$$\text{Warping constant of torsion } (C_w) = 37.60 \times 10^8 \text{ mm}^6$$

$$\text{St. Venant torsion constant } (J) = 4.16 \times 10^2 \text{ mm}^4$$

Yield strength (F_y) = 324.04 MPa

Modulus of elasticity (E) = 203,000 MPa

Test Result;

P_{Test} = 56.52 kN

Critical Compressive Resistance; (Clause 6.6.3.2)

Local buckling capacity of unstiffened flange:

C_r = 17.36 kN

Load-Carrying Capacity; (Clause 6.6.1.3)

C_r = 17.36 kN

Therefore, P_{CSA} = 17.36 kN or 3.90 kips

Hence; P_{Test}/P_{CSA} = 3.25

D.2.1.2 Stiffened Flange Section of Column

An example of concentric loading, stiffened flange section of column, using specimen 2.7-0.75-1, the length of specimen is 610.00 mm.

Section dimensions;

Total depth (H) = 204.98 mm

Thickness (t) = 1.47 mm

Flat width of web (w) = 194.82 mm

Flat width of flange (b_f) = 67.56 mm

Flat width of stiffener (c) = 18.29 mm

Radius at element junction (r) = 4.32 mm

Angle between flange and web (θ) = 90.00 degrees

Gross section properties;

Area (A) = 580.64 mm^2

Moment of Inertia about the geometric x-axis (I_{xx}) = 37.92x10^5 mm^4

Moment of Inertia about the geometric y-axis (I_{yy}) = 7.91x10^5 mm^4

Product of Inertia (I_{xy}) = 12.86x10^5 mm^4

Moment of Inertia about the principal x-axis (I_{xp}) = 42.66x10^5 mm^4

Moment of Inertia about the principal y-axis (I_{yp}) = 3.12x10^5 mm^4

Warping constant of torsion (C_w) = 57.17x10^8 mm^6

St. Venant torsion constant (J) = 4.16x10^2 mm^4

Yield strength (F_y) = 324.04 MPa

Modulus of elasticity (E) = 203,000 MPa

Test Result;

P_{Test} = 91.49 kN or 20.56 kips

Critical Stress; (Clause 6.6.4)

Elastic flexural buckling stress:

F_{ex} = 33037.59 MPa

F_{ey} = 2424.84 MPa

Torsional buckling stress:

F_t = 5614.12 MPa

Therefore, F_e = 2424.84 MPa

F_p = 0.833*2424.84 = 2019.89 MPa

Since, $F_p > F_y/2$, F_a = 313.21 MPa

Effective Area; (Clause 5.6.2.1, 5.6.2.3 and 5.6.2.6)

A_e = 378.70 mm^2

Load-Carrying Capacity; (Clause 6.6.1.3)

C_r = 118.59 kN

Therefore, P_{CSA} = 118.59 kN or 26.65 kips

Hence; P_{Test}/P_{CSA} = 0.77

D.2.2 BEAMS

D.2.2.1 Unstiffened Flange Section of Beam

An example of pure bending, unstiffened flange section of beam, using specimen 2.7-0.00-1[a], the length of specimen is 1373.00 mm.

Section dimensions;

Total depth (H) = *204.98 mm*

Thickness (t) = *1.47 mm*

Flat width of web (w) = *194.82 mm*

Flat width of flange (b_f) = *70.87 mm*

Flat width of stiffener (c) = *0.00 mm*

Radius at element junction (r) = *4.32 mm*

Angle between flange and web (θ) = *90.00 degrees*

Gross section properties;

Area (A) = *516.13 mm^2*

Moment of Inertia about the geometric x-axis (I_{xx}) = 32.67×10^5 mm^4

Moment of Inertia about the geometric y-axis (I_{yy}) = 4.16×10^2 mm^4

Product of Inertia (I_{xy}) = 8.49×10^5 mm^4

Moment of Inertia about the principal x-axis (I_{xp}) = 35.01×10^5 mm^4

Moment of Inertia about the principal y-axis (I_{yp}) = 1.83×10^8 mm^4

Warping constant of torsion (C_w) = 29.22×10^8 mm^6

St. Venant torsion constant (J) = 4.16×10^2 mm^4

Yield stress (F_y) = 324.04 *MPa*

Modulus of elasticity (E) = 203,000 *MPa*

Test Result;

M_{Test} = 5.88 kN-m

Critical Moment Resistance; (Clause 6.4.4)

Moment resistance caused by local buckling of unstiffened flange:

M_r = 1.09 kN-m

Bending Capacity; (Clause 6.4.1.1)

M_r = 1.09 kN-m

Therefore, M_{CSA} = 1.09 kN-m or 9.62 kips-in.

Hence; M_{Test}/M_{CSA} = 5.41

D.2.2.2 Stiffened Flange Section of Beam

An example of pure bending, stiffened flange section of beam, using specimen 2.7-0.75-2, the length of specimen is 1370.84 mm.

Section dimensions;

Total depth (H) = 203.71 mm

Thickness (t) = 1.50 mm

Flat width of web (w) = 193.55 mm

Flat width of flange (b_f) = 65.79 mm

Flat width of stiffener (c) = 17.02 mm

Radius at element junction (r) = 4.32 mm

Angle between flange and web (θ) = 90.80 degrees

Gross section properties;

Area (A) = 587.64 mm^2

Moment of Inertia about the geometric x-axis (I_{xx}) = 37.21x10^5 mm^4

Moment of Inertia about the geometric y-axis (I_{yy}) = 7.37x10^5 mm^4

Product of Inertia (I_{xy}) = 12.28x10^5 mm^4

Moment of Inertia about the principal x-axis (I_{xp}) = 41.62x10^5 mm^4

Moment of Inertia about the principal y-axis (I_{yp}) = 2.96x10^5 mm^4

Warping constant of torsion (C_w) = 52.66x10^8 mm^6

St. Venant torsion constant (J) = 4.16x10^2 mm^4

Yield strength (F_y) = 324.04 MPa

Modulus of elasticity (E) = 203,000 MPa

Test Result;

M_{Test} = 6.62 kN-m

Critical Stress; (Clause 6.4.2.1)

Elastic yielding stress:

F_y = 324.04 MPa

Therefore, F_c = 324.04 MPa

Effective Section Modulus; (Clause 5.6.2)

S_e = 34049.29 mm^3

Bending Capacity; (Clause 6.4.1.1)

M_r = 11.03 kN-m

Therefore, M_{CSA} = 11.03 kN-m. or 97.28 kips-in.

Hence; M_{Test}/M_{CSA} = 0.60

D.2.3 BEAM-COLUMNS

D.2.3.1 Unstiffened Flange Section of Beam-Column

An example of eccentric loading, unstiffened flange section of beam-column, using specimen 2.7-0.00-3[a], the length of specimen included supports is 1219.00 mm.

Section dimensions;

Total depth (H) = *202.44 mm*

Thickness (t) = *1.47 mm*

Flat width of web (w) = *192.28 mm*

Flat width of flange (b_f) = *72.90 mm*

Flat width of stiffener (c) = *0.00 mm*

Radius at element junction (r) = *4.32 mm*

Angle between flange and web (θ) = 90.00 degrees

Gross section properties;

Area (A) = 516.13 mm^2

Moment of Inertia about the geometric x-axis (I_{xx}) = 32.34x10^5 mm^4

Moment of Inertia about the geometric y-axis (I_{yy}) = 4.54x10^5 mm^4

Product of Inertia (I_{xy}) = 8.82x10^5 mm^4

Moment of Inertia about the principal x-axis (I_{xp}) = 34.92x10^5 mm^4

Moment of Inertia about the principal y-axis (I_{yp}) = 1.96x10^5 mm^4

Warping constant of torsion (C_w) = 30.53x10^8 mm^6

St. Venant torsion constant (J) = 4.16x10^2 mm^4

Yield strength (F_y) = 324.04 MPa

Modulus of elasticity (E) = 203,000 MPa

Test Result;

P_{Test} = 29.46 kN

Critical Compressive Resistance; (Clause 6.6.3.2)

Local buckling capacity of unstiffened flange:

C_r = 16.05 kN

Compressive Load; (Clause 6.6.1.3)

C_r = 16.05 kN

Critical Moment Resistance; (Clause 6.4.4)

Moment resistance caused by local buckling of unstiffened flange:

M_r = 1.03 kN-m

Therefore, M_{rx} = 5.02 kN-m

Load-Carrying Capacity of Beam-Column; (Clause 6.7)

C_f = 6.31 kN

Therefore, P_{CSA} = 6.31 kN or 1.42 kips

Hence; P_{Test}/P_{CSA} = 4.67

D.2.3.2 Stiffened Flange Section of Beam-Column

An example of eccentric loading, stiffened flange section of beam-column, using specimen 2.7-0.75-3, the length of specimen included supports is 1247.78 mm.

Section dimensions;

Total depth (H) = *202.18 mm*

Thickness (t) = *1.50 mm*

Flat width of web (w) = *192.28 mm*

Flat width of flange (b_f) = *66.55 mm*

Flat width of stiffener (c) = *17.78 mm*

Radius at element junction (r) = *4.57 mm*

Angle between flange and web (θ) = *90.30 degrees*

Gross section properties;

Area (A) = *580.64 mm^2*

Moment of Inertia about the geometric x-axis (I_{xx}) = *37.04x10^5 mm^4*

Moment of Inertia about the geometric y-axis (I_{yy}) = *7.66x10^5 mm^4*

Product of Inertia (I_{xy}) = *12.53x10^5 mm^4*

Moment of Inertia about the principal x-axis (I_{xp}) = $41.66x10^5$ mm^4

Moment of Inertia about the principal y-axis (I_{yp}) = $3.04x10^5$ mm^4

Warping constant of torsion (C_w) = $54.22x10^8$ mm^6

St. Venant torsion constant (J) = $4.16x10^2$ mm^4

Yield strength (F_y) = *324.04 MPa*

Modulus of elasticity (E) = *203,000 MPa*

Test Result;

P_{Test} = 41.47 kN

Critical Compressive Stress; (Clause 6.6.4)

Elastic flexural buckling stress:

F_{ex} = 7682.00 MPa

F_{ey} = 561.69 MPa

Torsional buckling stress:

F_t = 1304.74 MPa

Therefore, F_e = 561.69 MPa

F_p = 0.833*561.69 = 467.89 MPa

Since, $F_p > F_y/2$, F_a = 277.31 MPa

Effective Area; (Clause 5.6.2)

A_e = 410.04 mm^2

Compressive Resistance; (Clause 6.6.1.3)

C_r = 113.70 kN

Therefore, P_{CSA} = 113.70 kN

Moment Resistance; (Clause 6.4.1.1)

Elastic yielding bending capacity:

M_y = 12.52 kN-m

Elastic lateral bending capacity:

M_r = 11.27 kN-m

Effective modulus of section:

S_e = 34615.93 mm^3

Therefore, M_{rx} = 10.66 kN-m

Load-Carrying Capacity of Beam-Column; (Clause 6.7)

C_f = 54.57 kN

Therefore, P_{CSA} = 54.57 kN or 12.34 kips

Hence; P_{Test}/P_{CSA} = 0.762

APPENDIX E

MEMBER STRENGTH CALCULATED USING THEORETICAL MODELS

In this Appendix, detailed calculations for the strength of typical column, beam, beam-column sections based on the thoretical models are given. These detail calculations follow the listing of the relevant sections which are those used in Chapter 3.

E.1 COLUMNS

E.1.1 Unstiffened Flange Section of Column

An example of concentric loading, unstiffened flange section of column, using specimen 2.7-0.00-2[a], the length of specimen is 48.00 inches.

Section dimensions;

Total depth (H) = *8.06 in.*

Thickness (t) = *0.058 in.*

Flat width of web (w) = *7.66 in.*

Flat width of flange (b_f) = *2.81 in.*

Flat width of stiffener (c) = *0.00 in.*

Radius at element junction (r) = *0.17 in.*

Angle between flange and web (θ) = *90.00 degrees*

Section properties of flange-edge stiffener component;

Area (A_d) = *0.18* $in.^2$

x-coordinate with respect to the centroid ($\overline{x}_d$) = *1.54 in.*

y-coordinate with respect to the centroid ($\overline{y}_d$) = *0.00 in.*

x-coordinate of the shear centre (x_{co}) = *1.54 in.*

y-coordinate of the shear centre (y_{co}) = *0.00 in.*

Moment of inertia about the geometric x-axis (I_{cx}) = *0.00014 in.*^{4}

Moment of inertia about the geometric y-axis (I_{cy}) = *0.13968 in.*^{4}

St. Venant torsion constant (J_c) = *0.00020 in.*^{4}

Gross section properties;

Area (A) = *0.83 in.*^{2}

Yield strength (F_y) = *47.03 ksi*

Modulus of elasticity (E) = *29,500 ksi*

Test Result;

P_{Test} = 12.70 kips

Critical Stress; (Chapter 3, 3.4.1)

Distortional buckling stress:

V = 3.14

N = 7.43

ψ = 0.00013

τ = 0.148

σ_{dcr} = 8.05 ksi

Since, $\sigma_{dcr} < F_y/2$, σ_{cr} = 8.05 ksi

Load-Carrying Capacity; (Chapter 3, 3.4.1)

P_{Theory} = 6.70 kips

Hence; P_{Test}/P_{Theory} = 1.90

E.1.2 Stiffened Flange Section of Column

An example of concentric loading, stiffened flange section of column, using specimen 2.7-0.75-1, the length of specimen is 24.00 inches.

Section dimensions;

Total depth (H) = *8.07 in.*

Thickness (t) = *0.058 in.*

Flat width of web (w) = *7.67 in.*

Flat width of flange (b_f) = *2.66 in.*

Flat width of stiffener (c) = *0.72 in.*

Radius at element junction (r) = *0.17 in.*

Angle between flange and web (θ) = *90.00 degrees*

Section properties of flange-edge stiffener component;

Area (A_d) = *0.21* $in.^2$

x-coordinate with respect to the centroid ($\overline{x}_c$) = *1.73 in.*

y-coordinate with respect to the centroid ($\overline{y}_c$) = *0.14 in.*

x-coordinate of the shear centre (x_{co}) = *2.79 in.*

y-coordinate of the shear centre (y_{co}) = *0.14 in.*

Moment of inertia about the geometric x-axis (I_{cx}) = *0.01116* $in.^4$

Moment of inertia about the geometric y-axis (I_{cy}) = *0.18293* $in.^4$

Product of inertia (I_{cxy}) = *0.02527* $in.^4$

St. Venant torsion constant (J_c) = *0.00024* $in.^4$

Gross section properties;

Area (A) = 0.89 in.²

Yield strength (F_y) = 47.03 ksi

Modulus of elasticity (E) = 29,500 ksi

Test Result;

P_{Test} = 20.56 kips

Critical Stress; (Chapter 3, 3.4.1)

Distortional buckling stress:

V = 3.92

N = 82.01

ψ = 0.00675

τ = 0.296

σ_{dcr} = 17.87 ksi

Since, $\sigma_{dcr} < F_y/2$, σ_{cr} = 17.87 ksi

Load-Carying Capacity; (Chapter 3, 3.4.1)

P_{THE} = 16.08 kips

Hence; P_{Test}/P_{Theory} = 1.28

E.2 BEAMS

E.2.1 Unstiffened Flange Section of Beam

An example of pure bending, unstiffened flange section of beam, using specimen 2.7-0.00-1[a], the length of specimen is 54.06 inches.

Section dimensions;

Total depth (H) = *8.07 in.*

Thickness (t) = *0.058 in.*

Flat width of web (w) = *7.67 in.*

Flat width of flange (b_f) = *2.79 in.*

Flat width of stiffener (c) = *0.00 in.*

Radius at element junction (r) = *0.00 in.*

Angle between flange and web (θ) = *90.00 degrees*

Section properties of equivalent column;

Area (A_d) = *0.24 $in.^2$*

Distance from neutral axis to the compressive fibre (d_c) = *3.80 in.*

x-coordinate of the shear centre (x_{co}) = *-1.031 in.*

y-coordinate of the shear centre (y_{co}) = *-0.205 in.*

x-coordinate of the elastic support (h_x) = *1.043 in.*

y-coordinate of the elastic support (h_y) = *7.630 in.*

Moment of inertia about the geometric x-axis (I_{cx}) = *0.03370 $in.^4$*

Moment of inertia about the geometric y-axis (I_{cy}) = *0.23630 $in.^4$*

Product of inertia (I_{cxy}) = *-0.0525 $in.^4$*

Warping constant of torsion (C_w) = *0.00000 $in.^6$*

St. Venant torsion constant (J_c) = *0.00027 $in.^4$*

Gross section properties;

Area (A) = *0.81 $in.^2$*

Elastic section modulus (S_x) = *1.9469 in.*^{3}

Yield strength (F_y) = *47.03 ksi*

Modulus of elasticity (E) = *29,500 ksi*

Elastic shear modulus (G) = *11346.15 ksi*

Distance from neutral axis to the centroid of flange (d) = *3.80 in.*

Test Result;

M_{Test} = 52.02 kips-in.

Critical Stress; (Chapter 3, 3.4.2)

Distortional buckling stress:

$\chi_1 = 2.195$

$\chi_2 = 0.000006$

$\chi_3 = -0.00060$

$\chi_4 = 14.512$

$k_\phi = 0.0603$

$\eta = 0.00065$

$\alpha_1 = 0.00438$

$\alpha_2 = 0.00016$

$\alpha_3 = 0.00000068$

$\sigma_e = 18.71$ ksi

$\sigma_{dcr} = 19.87$ ksi

Since, $\sigma_{dcr} < F_y/2$, $\sigma_{cr} = 19.87$ ksi

Bending Capacity; (Chapter 3, 3.4.2)

M_{Theory} = 38.69 kips-in.

Hence; M_{Test}/M_{Theory} = 1.34

E.2.2 Stiffened Flange Section of Beam

An example of pure bending, stiffened flange section of beam, using specimen 2.7-0.75-1, the length of specimen is 53.97 inches.

Section dimensions;

Total depth (H) = *8.02 in.*

Thickness (t) = *0.059 in.*

Flat width of web (w) = *7.62 in.*

Flat width of flange (b_f) = *2.59 in.*

Flat width of stiffener (c) = *0.67 in.*

Radius at element junction (r) = *0.17 in.*

Angle between flange and web (θ) = *90.80 degrees*

Section properties of equivalent column;

Area (A_d) = *0.29* $in.^2$

Distance from neutral axis to the compressive fibre (d_c) = *4.01 in.*

x-coordinate of the shear centre (x_{co}) = *-0.524 in.*

y-coordinate of the shear centre (y_{co}) = *-0.579 in.*

x-coordinate of the elastic support (h_x) = *-1.326 in.*

y-coordinate of the elastic support (h_y) = *7.544 in.*

Moment of inertia about the geometric x-axis (I_{cx}) = *0.03810 in.*^{4}

Moment of inertia about the geometric y-axis (I_{cy}) = *0.37060 in.*^{4}

Product of inertia (I_{cxy}) = *-0.03434 in.*^{4}

Warping constant of torsion (C_w) = *0.0385 in.*^{6}

St. Venant torsion constant (J_c) = *0.00034 in.*^{4}

Gross section properties;

Area (A) = *0.91 in.*^{2}

Elastic section modulus (S_x) = *2.2309 in.*^{3}

Yield strength (F_y) = *47.03 ksi*

Modulus of elasticity (E) = *29,500 ksi*

Elastic shear modulus (G) = *11346.15 ksi*

Distance from neutral axis to the centroid of flange (d) = *3.73 in.*

Test Result;

M_{Test} = 58.57 kips-in.

Critical Stress; (Chapter 3, 3.4.2)

Distortional buckling stress:

$\chi_1 = 3.163$

$\chi_2 = 0.0630$

$\chi_3 = -0.0268$

$\chi_4 = 24.078$

$k_\phi = 0.0561$

$\eta = 0.00052$

$\alpha_1 = 0.00403$

$\alpha_2 = 0.00021$

$\alpha_3 = 0.00000078$

$\sigma_c = 19.57$ ksi

$\sigma_{dcr} = 21.01$ ksi

Since, $\sigma_{dcr} < F_y/2$, $\sigma_{cr} = 21.01$ ksi

Bending Capacity; (Chapter 3, 3.4.2)

$M_{Theory} = 46.88$ kips-in.

Hence; $M_{Test}/M_{Theory} = 1.25$

E.3 BEAM-COLUMNS

E.3.1 Unstiffened Flange Section of Beam-Column

An example of eccentric loading, unstiffened flange section of beam-column, using specimen 2.7-0.00-3[a], the length of specimen included supports is 48.00 inches.

Section dimensions;

Total depth (H) = 7.97 in.

Thickness (t) = 0.058 in.

Flat width of web (w) = 7.57 in.

Flat width of flange (b_f) = 2.87 in.

Flat width of stiffener (c) = 0.00 in.

Radius at element junction (r) = 0.00 in.

Angle between flange and web (θ) = 90.00 degrees

Section properties of flange-edge stiffener component;

Area (A_d) = 0.26 $in.^2$

x-coordinate of the shear centre (x_{co}) = -1.392 *in.*

y-coordinate of the shear centre (y_{co}) = -0.422 *in.*

x-coordinate of the elastic support (h_x) = 1.084 *in.*

y-coordinate of the elastic support (h_y) = 7.372 *in.*

Moment of inertia about the geometric x-axis (I_{cx}) = 0.03379 $in.^4$

Moment of inertia about the geometric y-axis (I_{cy}) = 0.26130 $in.^4$

Product of inertia (I_{cxy}) = -0.0549 $in.^4$

Warping constant of torsion (C_w) = 0.02471 $in.^6$

St. Venant torsion constant (J_c) = 0.00031 $in.^4$

Gross section properties;

Area (A) = 0.80 $in.^2$

Elastic section modulus (S_x) = 1.9548 $in.^3$

Yield strength (F_y) = 47.03 *ksi*

Modulus of elasticity (E) = 29,500 *ksi*

Elastic shear modulus (G) = 11346.15 *ksi*

x coordinate of the eccentric loading (e_x) = 0.00 *in.*

y coordinate of the eccentric loading (e_y) = 4.00 *in.*

Test Result;

P_{Test} = 6.62 kips

Load-Carrying Capacity of Beam-Column; (Chapter 3, 3.4.3)

$$P_{Theory\ (Eq.3.48)} = 3.40 \text{ kips} \quad \text{or} \quad P_{Theory\ (Eq.3.51)} = 4.57 \text{ kips}$$

$$\text{Hence; } P_{Test}/P_{Theory\ (Eq.3.48)} = 1.95 \quad \text{or} \quad P_{Test}/P_{Theory\ (Eq.3.51)} = 1.45 \text{ kips}$$

E.3.2 Stiffened Flange Section of Beam-Column

An example of eccentric loading, stiffened flange section of beam-column, using specimen 2.7-0.75-3, the length of specimen included supports is 49.13 inches.

Section dimensions;

Total depth (H) = *7.96 in.*

Thickness (t) = *0.059 in.*

Flat width of web (w) = *7.57 in.*

Flat width of flange (b_f) = *2.62 in.*

Flat width of stiffener (c) = *0.70 in.*

Radius at element junction (r) = *0.15 in.*

Angle between flange and web (θ) = *90.30 degrees*

Section properties of flange-edge stiffener component;

Area (A_d) = *0.30 in.^{2}*

x-coordinate of the shear centre (x_{co}) = *-0.973 in.*

y-coordinate of the shear centre (y_{co}) = *-0.630 in.*

x-coordinate of the elastic support (h_x) = *1.353 in.*

y-coordinate of the elastic support (h_y) = *7.495 in.*

Moment of inertia about the geometric x-axis (I_{∞}) = *0.03890 in.^{4}*

Moment of inertia about the geometric y-axis (I_{cy}) = *0.39000 in.*^{4}

Product of inertia (I_{cxy}) = *-0.0320 in.*^{4}

Warping constant of torsion (C_w) = *0.05330 in.*^{6}

St. Venant torsion constant (J_c) = *0.00036 in.*^{4}

Gross section properties;

Area (A) = *0.92 in.*^{2}

Elastic section modulus (S_x) = *2.2739 in.*^{3}

Yield strength (F_y) = *47.03 ksi*

Modulus of elasticity (E) = *29,500 ksi*

Elastic shear modulus (G) = *11346.15 ksi*

x coordinate of the eccentric loading (e_x) = *0.00 in.*

y coordinate of the eccentric loading (e_y) = *4.00 in.*

Test Result;

P_{Test} = 9.32 kips

Load-Carrying capacity of Beam-Column; (Chapter 3, 3.4.3)

$P_{Theory\ (Eq.3.48)}$ = 6.95 kips or $P_{Theory\ (Eq.3.51)}$ = 9.70 kips

Hence; $P_{Test}/P_{Theory\ (Eq.3.48)}$ = 1.34 or $P_{Test}/P_{Theory\ (Eq.3.51)}$ = 0.96